Fall 2017

Holistic Approach in Microalgae Conversion to Bioproducts and Biofuels Through Flash Hydrolysis

Ali Teymouri
Old Dominion University, ateym001@odu.edu

HOLISTIC APPROACH IN MICROALGAE CONVERSION TO BIOPRODUCTS AND BIOFUELS THROUGH FLASH HYDROLYSIS

by

Ali Teymouri

B.S. May 2004, Islamic Azad University, Gachsaran, Iran
M.S. May 2008, Islamic Azad University, Shahroud, Iran

A Dissertation Submitted to the Faculty of
Old Dominion University in Partial Fulfillment of the
Requirements for the Degree of

DOCTOR OF PHILOSOPHY

CIVIL AND ENVIRONMENTAL ENGINEERING

OLD DOMINION UNIVERSITY
December 2017

Approved by:

_____
Sandeep Kumar (Director)

_____
Ben Stuart (Member)

_____
Gary Schafran (Member)

_____
James W. Lee (Member)

ABSTRACT

HOLISTIC APPROACH IN MICROALGAE CONVERSION TO BIOPRODUCTS AND BIOFUELS THROUGH FLASH HYDROLYSIS

Ali Teymouri

Old Dominion University, 2017

Director: Sandeep Kumar

In recent years, the demand for renewable energy, mainly biomass has increased. The U.S. Energy Information Administration reported that more than 13.3% of the total energy production in the first seven months of 2017 was produced from a biomass source. Among all biomass resources, microalgae has brought a lot of attention due to their numerous advantages such as higher growth rate and productivity compared with the conventional energy crops, higher energy conversion efficiency by photosynthesis, and less water requirement than terrestrial crops. However, its development is far behind industrial production. Several research efforts across the globe have been concerned with addressing the technical barriers in the commercialization of algae-based sustainable biorefineries. Nutrients cost and management have been highlighted as one of the most significant challenges in algae cultivation and downstream processing. Therefore, any technology advancement that can reduce the energy input to the process, any nutrients recycling that result in reduction of nutrients input or/and production of value-added bioproducts, will enhance the commercialization potential. This study has developed multiple viable pathways to effectively contribute to the algal based industries.

Chapter 1, includes an overall introduction through these approaches.

In Chapter 2, kinetics of peptides and arginine production from *Scenedesmus* sp. microalgae through flash hydrolysis (FH) were studied.

In chapter 3, the FH process on the *Nannochloropsis gaditana* as a high-ash marine algae was studied with focus on the biofuels intermediate (BI) characterization and the application of the hydrolysate as a nutrient source for algal cultivation.

In chapter 4, two pathways were developed to recover nutrients in the microalgae hydrolysate in the form of value-added bioproducts such as hydroxyapatite and dittmerite.

In chapter 5, the effect of reaction time on the phosphate removal from the algae hydrolysate and the chemistry of precipitates minerals were investigated.

In chapter 6, the effect of flash hydrolysis process on the lipid extractability of three algal species were investigated. In addition, biocrude yields and composition from hydrothermal liquefaction of raw and biofuels intermediates of *Chlorella vulgaris* were compared.

In chapter 7, several future works and research pathways were recommended by the author of this dissertation.

This dissertation is dedicated to my better half, Zeinab.

Editing formats of this dissertation are based on the American Chemical Society (chapters 2 and 5); the Elsevier publishing company (chapter 4 and 6); and the Wiley online library (chapter 3).

ACKNOWLEDGMENTS

There are many people who have contributed to the successful completion of this dissertation. I would like to express my sincere appreciation and gratitude to my major advisor Dr. Sandeep Kumar for his untiring guidance, advice, discussions, and support during my dissertation research; to my co-advisor Dr. Ben Stuart for his consistently solid and thoughtful advices; to my committee members Dr. Gary C. Schafran and Dr. James W. Lee for their valuable comments and suggestions; to the Department of Civil and Environmental Engineering for providing all the facilities and equipment required for my research over the last five years; to the current and former members of the Biomass Research Laboratory who helped me along the way with their friendship, help, advise, discussions, and solving problems together; to the Department of Chemistry and Biochemistry and Applied Research Center for their help with sample analysis and collaborative research; to my better half Zeinab for her love, encouragement, and support over the years of my dissertation work.

NOMENCLATURE

ACP	Amorphous calcium phosphate
AMP	Amorphous magnesium phosphate
AP	Atmospheric precipitation
AzCATI	Arizona Center for Algae Technology and Innovation
BBOT	2,5-bis (5-tert-butyl-benzoxazol-2-yl) thiophene
BGY	Billion gallon per year
BI	Biofuels intermediates
BRL	Biomass Research Laboratory
CAPEX	Capital expenditure
CDHA	Calcium deficient hydroxyapatite
CN	Cetane number
COD	Chemical oxygen demand
DHA	Docosahexaenoic acid
DI	Deionized
DOE	Department of Energy
DWAF	Dried weight ash-free basis
EA	Elemental analyzer
ECR	Energy conversion ratio
EDS	Energy dispersive spectroscopy
EISA	Energy Independence and Security Act
EPA	Environmental Protection Agency
EPA	Eicosapentaenoic acid
FAME	Fatty acid methyl ester

FD	Freeze dried
FFA	Free fatty acid
FH	Flash hydrolysis
FTIR	Fourier transform infrared spectroscopy
GC	Gas chromatograph
GC-FID	Gas chromatograph with flame ionization detector
GC-TCD	Gas chromatograph with thermal conductivity detector
GC-MS	Gas chromatograph with mass spectrometer
HAp	Hydroxyapatite
HHV	Higher heating value
HPLC	High performance liquid chromatograph
HTG	Hydrothermal gasification
HTL	Hydrothermal liquefaction
HTM	Hydrothermal mineralization
IC	Ion chromatography
ICDD	International center for diffraction data
IR	Infrared
IS	Internal standard
LCA	Life cycle assessment
MAP	Magnesium ammonium phosphate
Mmt	Million metric tons
ND	Not detected
NMR	Nuclear magnetic resonance spectroscopy
NREL	National Renewable Energy Laboratory

NSF	National Science Foundation
OCP	Octacalcium phosphate
OPEX	Operational expenditure
PUFA	Polyunsaturated fatty acid
RCD	Relative standard deviation
SEM	Scanning electron microscope
SNL	Sandia National Laboratory
TAG	Triacylglycerol
TC	Total carbon
TCP	Tricalcium phosphate
TEA	Techno-economic analysis
TGA	Thermogravimetric analysis
TMAH	Tetramethylammonium hydroxide
TN	Total nitrogen
TOC	Total organic carbon
TP	Total Phosphorus
WH	Whitlockite
XRD	X-ray diffraction
XRF	X-ray fluorescence

TABLE OF CONTENTS

LIST OF TABLES

Table Page

LIST OF FIGURES

Figure Page

CHAPTER 1

INTRODUCTION

1.1. Introduction

It has been reported that almost 87% of the world energy consumption in 2014 were solely relied on fossil fuels (Gençer & Agrawal, 2016). These resources are already being exploited and expected to being diminished in few years, while the demands for energy is drastically increasing. Therefore, societies are directed towards using alternative renewable energy sources such as wind, solar, hydropower, waves, geothermal, and biomass. Furthermore, the use of these renewable resources have less impact on the environment compared to the fossil fuels (Gollakota, Kishore, & Gu, 2017). Among all resources, biomass has a lot of interests. It has the potential to be converted to solid, liquid and gaseous fuels depending on the feedstock and the conversion technology. Comparing variety of biomass options, those that have no/less competition with food resources such as microalgae are under higher consideration. Utilizing algal biomass as energy source has lots of advantages including their capability in carbon dioxide fixation, adaptable growth condition, efficient photosynthesis process, high growth rate and productivity compared to terrestrial crops, occupying less land, and growth in different medias such as fresh water, wastewater, brackish water, and high saline (Ahmad, Yasin, Derek, & Lim, 2011; Chisti, 2007; Mata, Martins, & Caetano, 2010; Mutanda et al., 2011; Vonshak, 1990). There are more than 50,000 algal species on the planet. However, only few species were characterized and used in different applications. Algae absorb light, carbon dioxide, water, and inorganic salts such as iron, magnesium, phosphorus, nitrogen, and potassium to convert them to energy sources such

as lipids, carbohydrates, and proteins through photosynthesis process. Table 1 demonstrates a typical composition of the some common microalgae species (Becker, 2007a).

Table 1. Typical Composition of different microalgae (dry wt%).

Alga	**Protein**	**Carbohydrates**	**Lipids**
Anabaena cylindrica	43-56	25-30	4–7
Aphanizomenon flos-aquae	62	23	3
Chlamydomonas rheinhardii	48	17	21
Chlorella pyrenoidosa	57	26	2
Chlorella vulgaris	51-58	12-17	14-22
Dunaliella salina	57	32	6
Euglena gracilis	39–61	14–18	14–20
Porphyridium cruentum	28–39	40–57	9-14
Scenedesmus obliquus	50–56	10–17	12–14
Spirogyra sp.	6–20	33–64	11–21
Arthrospira maxima	60–71	13–16	6–7
Spirulina platensis	46–63	8–14	4–9
Synechococcus sp.	63	15	11

As can be seen, depending on the algae species, its composition may vary in a wide range. Microalgae species with higher lipid content are suitable feedstock for the production of renewable energy such as biodiesel, jet-fuel, biogasoline. However, those that have higher protein and carbohydrate fraction are excellent candidates for applications such as food supplements, human nutritional products, cosmetics, and animal feed (Slocombe & Benemann, 2016).

To utilize biomass for the above applications, multiple technologies have been suggested. However, they can all be classified under two main categories: biochemical and thermochemical conversions (Gollakota et al., 2017). Thermochemical processes are usually performed at higher temperature, pressure, and oxygen deprivation condition on various biomass feedstocks, aiming liquid fuel. Processes such as combustion, gasification, pyrolysis and liquefaction are under this category. Since life cycle analysis (LCA) have confirmed the dewatering stage as one of the most energy intensive processes in the algal-biofuel refineries (R. E. Davis et al., 2014; Handler, Shonnard, Kalnes, & Lupton, 2014), huge number of recent studies have focused on the hydrothermal processing of wet algal biomass to eliminate the costly dewatering step. Hydrothermal liquefaction (HTL) that can convert biomass to biocrude has gained the highest attention. The biocrude yield and its components substantially depend on the temperature and residence time (Patel, Guo, Izadpanah, Shah, & Hellgardt, 2016). A typical HTL process performed at 250–374 ºC, under pressures of 4–20 MPa (Tekin, Karagöz, & Bektaş, 2014). There are many ongoing studies to investigate the effect of HTL reaction parameters on the composition of the biocrude (Anastasakis & Ross, 2011; Eboibi, Lewis, Ashman, & Chinnasamy, 2014). At low temperatures, due to incomplete cell rupture, biocrude yield is low (Patel et al., 2016). Elevated temperatures and longer residence times, increases deoxygenation resulting in higher HHV of the biocrude (Saqib S. Toor et al., 2013). However, it reduces the mass of the aqueous phase due to gasification and raise nitrogen content in the biocrude (Patel et al., 2016). Although HTL process looks as a promising solution for algae processing, there are some drawbacks associated with this technology that decelerate its commercialization. Production of high amounts of NO_x emissions in the downstream processing originating from nitrogenous

compounds in proteins and chlorophyll content of microalgae is a serious challenge that this process needs to overcome (López Barreiro, Prins, Ronsse, & Brilman, 2013). In addition, the only way to develop an economically and environmentally sustainable algal derived biorefinaries is to recover nutrients mainly, phosphorus (Barbera, Teymouri, Bertucco, Stuart, & Kumar, 2017). Therefore, a comprehensive study needs to be conducted to address nutrients management in order to increase the potential for industrial scale algal biorefinaries. The overall goal of this dissertation is to address the above concerns by providing methods, techniques, and pathways to extract micro/macro-nutrients such as phosphorus and nitrogen from algal biomass and either recycle them for algal cultivation or producing value-added bioproducts. The lipid portion of microalgae can be further processed for biofuels or other desired lipid based bioproducts. This goal is in agreement with the novel integrated biorefinary concept that recently, proposed by the National Renewable Energy Laboratory (NREL) as the key for the commercialization of algal biofuels and bioproducts (Tao Dong, Eric P. Knoshaug, Ryan Davis, et al., 2016; Lieve M. L. Laurens et al., 2017).

Flash hydrolysis (FH) has been known as a sustainable continuous process that can utilize the wet algal biomass (microalgae slurry) at 280 ˚C and a very short residence time (10 s) to fractionate macronutrients such as nitrogen and phosphorus in the aqueous phase (hydrolysate), while preserving the lipids in the solid fraction known as biofuels intermediates (BI) (Jose Luis Garcia-Moscoso, Wassim Obeid, Sandeep Kumar, & Patrick G. Hatcher, 2013). Garcia et al. reported the presence of arginine as a free amino acid and peptides that were solubilized in the algae hydrolysate. However, the scope of the study was the overall capability of the FH method in nutrients extraction and lipids

preservation in the recovered BI. In chapter 2, the *Scenedesmus* sp. microalgae proteins hydrolysis to peptides and arginine were studied in detail. The FH process was optimized in order to reach the maximum amount of soluble peptides and arginine. Three reaction temperature (240, 280, and 320 ºC) and three residence time (6, 9, and 12 s) were selected and all products recovered after FH at the aforementioned conditions were fully characterized. A detailed kinetic study was performed to estimate the protein solubilization in the hydrolysate in the forms of peptides and arginine. L-arginine ($C_6H_{14}N_4O_2$) is commercially produced using specific strains of *Corynebacterium glutamicum* and used as a food supplement for both human and animal consumption (Utagawa, 2004). Providing marketable high value bioproducts would increase the overall efficiency of the production of algae based biorefineries and has the potential to reduce the cost of biofuel production from algal biomass.

In chapter 3 the viability of FH process was investigated through a high ash, lipid-rich *Nannochloropsis gaditana* marine algae. Detailed mass balance were conducted to evaluate the difference in the distribution of solid and liquid phase products of FH process. Since the algae was rich in lipids, biofuels intermediates were characterized to evaluate its quality for biofuels production. High-tech analytical techniques such as pyro-GC-MS were performed on both raw algae and the biofuels intermediates produced after FH process to track proteins, carbohydrates, and lipids alongside the process. Extent of nutrients removal from algal biomass to the hydrolysate were also measured. In accordance to main goal of this dissertation, the feasibility of direct recycling of the nutrients-rich hydrolysate for microalgae cultivation were investigated. The possibility of a direct recycling of the nutrients content of a high ash marine algae, contributes to the

overall sustainability of the FH process and its downstream processing to biofuel and bioproducts.

Another aspect of nutrient management were discussed in chapter 4 of this dissertation. In the previous chapter, we have confirmed the feasibility of recycling the nutrient-rich hydrolysate directly to be used for algal cultivation. However, this approach is not always possible and includes several challenges. Shipping, handling, and storage of hydrolysate, due the huge amount of water associated with the nutrients is very costly. Furthermore, organic content of the hydrolysate is high enough to be a favorable medium for bacterial growth. These limitation eliminates the potential for long-term storage of these nutrients. Chapter 4 addressed these concerns by providing two pathways for onsite recovery of nutrients in the microalgae in forms of two value-added bioproducts. Hydrothermal mineralization (HTM) and atmospheric precipitation (AP) were proposed to be integrated with the FH process to produce hydroxyapatite ($Ca_{10}(PO_4)6(OH)_2$, HAp) and dittmerite (magnesium ammonium phosphate salt, MAP, $MgNH_4PO_4 \cdot H_2O$), respectively. This is the first study that systematic methods were proposed that could recover phosphate in the form of HAp and MAP from a complex ionic/cationic algal hydrolysate with high organic content. The effect of seed inoculation on the nutrient removal and precipitates' composition and structure in both pathways were evaluated. In addition, the effect of temperature, Mg/PO_4 molar ratio, and the reaction time on the phosphate removal in the FH-AP process were determined. The structure, morphology and crystallinity of the precipitates were also fully assessed as part of this chapter.

In chapter 5, the effect of HTM reaction time on the phosphate mineralization process and the chemistry of the precipitates (calcium phosphate salts) were investigated.

In this regard, the calcium and phosphate removal from the aqueous phase after each reaction time (5, 15, 30, 45, 60, and 90 min) were evaluated. The reaction temperature was set at 280 ºC, which is similar to the FH process temperature. This is due to efficient heat integration alongside the process. Each liquid or solid fraction, which produced in every stage of the process were fully characterized in terms of structure, thermal stability, crystallinity and morphology.

Our prior studies indicated that lipid-rich BI had more than 90 wt% of the lipids while having the same fatty acid profile (Teymouri, Kumar, et al., 2017). However, the lipid extractability were never analysed. Chapter 6 presented the study on evaluating the efficiency of the lipid extraction of three algal species including *Scenedesmus* sp., *Nannochloropsis* sp., and *Chlorella vulgaris* after the FH process. A kinetic study were conducted on the lipid extractability of the above mentioned microalgae species for both raw and the corresponding BIs and the difference in the fatty acid profiles for each species were compared. Furthermore, hydrothermal liquefaction experiment were performed using raw and BI of the *Chlorella vulgaris* as a feedstock and the products' yields were compared and characterized for its fuel potential.

Recommendations and suggestions for future work of this study were stated in chapter 7 of this dissertation.

CHAPTER 2

KINETICS OF PEPTIDES AND ARGININE PRODUCTION FROM MICROALGAE (SCENEDESMUS SP.) VIA FLASH HYDROLYSIS

Note: The contents of this chapter have been published in the Industrial & Engineering Chemistry Research Journal. Only, experiments conducted at 240 ºC and 280 ºC were part of the Jose L. Garcia-Moscoso's (former graduate student) work and the rest including experiments performed at 320 ºC, all kinetics calculations, results, discussion, and conclusions section has performed by the author of this dissertation.

Garcia-Moscoso, J. L.; Teymouri, A.; Kumar, S., Kinetics of Peptides and Arginine Production from Microalgae (Scenedesmus sp.) by Flash Hydrolysis. Industrial & Engineering Chemistry Research 2015, 54 (7), 2048-2058.

Water under subcritical conditions in a continuous-flow reactor (flash hydrolysis) has proved to be an efficient and environmentally friendly method hydrolyzing proteins from microalgae biomass in a very short residence time (few seconds). In this study, flash hydrolysis experiments were conducted at three different temperatures (240, 280, and 320 °C) and three residence times (6, 9 and 12 s) to understand the kinetics of the hydrolysis of algae proteins to water-soluble peptides and arginine. Laboratory-grown protein-rich *Scenedesmus* sp. with an average composition of 54% proteins, 17% lipids, and 23% carbohydrates was used as the feedstock. After flash hydrolysis both liquid and solid products were collected and the contents of soluble peptides and arginine in the liquid fraction and of remaining proteinaceous material in the solids were analyzed. For all experiments above 240˚C at all residence times, the yield of soluble peptides was in the range of 57–67% of the algae protein whereas the maximum arginine yield (81.51%) was

achieved at 320 ˚C and residence time of 6 s. The protein solubilization to soluble peptides fitted second-order reaction kinetics, whereas for arginine the process was zeroth-order; the activation energies were calculated to be 43.0 and 34.1 kJ/mol, respectively. The results of this study suggest that the flash hydrolysis can be an environmentally benign method for hydrolyzing proteins from microalgae to produce valuable coproducts such as arginine as free amino acid and water-soluble peptides along with lipid-rich solids (biofuels intermediate) as a feedstock for biofuel production.

2.1. Introduction

Microalgae are highly versatile organisms that can be cultivated using natural or artificial light in diverse systems, including fresh water, brackish water, seawater, and even wastewater, providing an additional benefit by removing nutrients and organic pollutants from wastewater. Once the algae has grown and been harvested, good-quality biomass comprising mostly proteins, lipids, and carbohydrates is produced. The carbohydrate and lipid fractions of the biomass can be converted into liquid transportation fuels such as biodiesel, (Martinez-Guerra, Gude, Mondala, Holmes, & Hernandez, 2014; Patil et al., 2011) bioethanol, (K. H. Kim, Choi, Kim, Wi, & Bae, 2014) and renewable diesel. (Knothe, 2010) The proteins can be recovered and converted into high-value coproducts. The problem resides not in how to produce algal biomass, but in how to fractionate the biopolymeric components and process them cost-effectively using green technologies to minimize the chemical footprint. In this regard, it is important to note the need to achieve comprehensive recovery systems for biomass and all of its components in order to exploit the potential of microalgae. (C.-Y. Chen, Yeh, Aisyah, Lee, & Chang, 2011)

The processing of algae to biofuels consists of four major steps, including cultivation, harvesting, lipid extraction, and lipid upgrading. (Silva et al., 2013) Among all of the steps, the dewatering of algae is one of the most energy-intensive processes that can be avoided by working with wet biomass. In this regard, hydrothermal processes represent an efficient and environ- mentally benign option when compared to traditional means of lipid extraction using organic solvents. (Bligh & Dyer, 1959; Halim, Gladman, Danquah, & Webley, 2011; J.-Y. Lee, Yoo, Jun, Ahn, & Oh, 2010; Mendes et al., 1995)

The conventional hydrothermal liquefaction (HTL) of algae can potentially be used to produce biocrude, which can subsequently be upgraded to liquid hydrocarbons. The HTL of algae is conducted at high pressure (20 MPa) to maintain subcritical water at temperatures in the range of 300−350 °C. (D. C. Elliott, Hart, Neuenschwander, et al., 2013; D. C. Elliott, Hart, Schmidt, et al., 2013)

However, the liquefied products (biocrude) from HTL contain a mixture of oxygenated hydrocarbons including nitrogen- derived compounds from algae proteins. The protein fraction is usually degraded in the other thermochemical processes (e.g., pyrolysis, gasification) (Guo, Wang, Huelsman, & Savage, 2013; Harman-Ware et al., 2013; Hu, Zheng, Yan, Xiao, & Liu, 2013; Sanchez-Silva, López-González, Garcia-Minguillan, & Valverde, 2013) used for biofuel production. Some algae species have high protein contents (more than 50 wt %), and the biochemical composition of algal proteins can vary significantly as a result of environmental factors, including the availability of nutrients in the media in which they are cultivated. (Griffiths & Harrison, 2009; Li, Horsman, Wang, Wu, & Lan, 2008) The high protein content of microalgae requires an extraction step prior to biofuel production. It would be advantageous to

combine biofuel production from algae with protein coproducts such as peptides and free amino acids.

This idea was developed on the basis of our previous publication, (Jose Luis Garcia-Moscoso et al., 2013) when we noticed the presence of arginine as the only free amino acid in significant amounts in the algal hydrolyzate obtained after flash hydrolysis of *Scenedesmus sp.* without any additional processing. Separating arginine and peptides from the hydrolyzate mixture as valuable coproducts using available techniques will make the algae-to-biofuels/ bioproducts process more cost-effective.

The algae used in this study were *Scenedesmus sp*. with an average composition of 54% proteins, 17% lipids, 23% carbohydrates, and 6% ash. It was reported that the amino acid profile of *Scenedesmus* protein can also show high variability during the growth cycle mostly because of the nitrogen species in the growth medium and the changes in nitrogen metabolism produced. One of the most abundant amino acids in *Scenedesmus* protein is arginine (Arg), which can represent up to 30% of the protein weight (0.3 g of Arg/g of protein), and the highest contents are reported when nitrate (NO_3^-) or urea is the primary nitrogen source. (Thomas & Krauss, 1955) The specific functions of arginine in the algal cell might provide a clue to the content variability, as arginine intervenes in the regulation of the osmotic pressure in the cell membrane, prevents the aggregation of soluble protein, and also solubilizes proteins from loose inclusion bodies. (Arakawa, Tsumoto, Kita, Chang, & Ejima, 2007)

L-Arginine ($C_6H_{14}N_4O_2$) is commercially produced by aerobic fermentation (Utagawa, 2004) using specific strains of *Corynebacterium glutamicum* and is used as a food supplement for both human and animal consumption. Arginine present in

fermentation liquor can be separated by removing microbial cells and any other precipitates by ion-exchange resin treatment or precipitation. The partial purification and recovery of arginine can be standardized with strongly acidic cation-exchange resin such as Amberlite. (Glansdorff & Xu, 2006; Utagawa, 2004) Previous studies have reported the suitability of algae biomass as a valuable feed supplement or substitute for conventional protein sources (soybean meal, fish meal, rice bran, etc.); additionally, it has been reported that, despite the high content of nutritious protein in microalgae biomass, its use as a food or food additive has not gained importance because of the organoleptic characteristics of the product that limits its incorporation into conventional food. (Becker, 2007a) To make a better use of the biomass production potential of this species, protein fractionation and recovery as a preceding step to biofuel production seems to be one of the best approaches. Few studies have focused on protein hydrolysis of algae biomass for the production of free amino acids (Arg) and peptides using subcritical water. Protein extraction and amino acid production under subcritical water conditions from agricultural biomass has been reported using different types of feedstocks. For example, it was reported that, for rice bran protein production, a working temperature of 200 °C and a reaction time of 30 min provided close to 100% protein recovery. When hog hair was used as the protein source, longer residence times were employed (up to 60 min), and it was reported that the yields of total and individual amino acids gradually increased with reaction time up to 60 min and gradually decreased with longer reaction times. (Esteban, Garcia, Ramos, & Marquez, 2008; Sasithorn Sunphorka, Warinthorn Chavasiri, Yoshito Oshima, & Somkiat Ngamprasertsith, 2012)

Our previous study was focused on developing the flash hydrolysis process to extract proteins from algae while preserving the energy-rich macromolecules (lipids and carbohydrates) in the solids (biofuel intermediate). (Jose Luis Garcia-Moscoso et al., 2013) Flash hydrolysis uses subcritical water conditions in a continuous- flow system, which allows for the use of very short residence times and also reduces the size of the reactor required for processing the biomass. With minor adjustments to the experimental setup, a kinetics study on the hydrolysis of algae proteins to peptides and free amino acids (arginine) could be conducted. The objectives of this study were to (i) optimize the experimental conditions to maximize the yields of arginine and water-soluble peptide, (ii) characterize both the solid and liquid products obtained after flash hydrolysis, and (iii) estimate the kinetic parameters for protein and arginine solubilization using the flash hydrolysis process.

2.2. Experimental section

2.2.1. Material

Scenedesmus sp. was cultivated in our laboratory using photobioreactors and a modified BG-11 medium to provide a sufficient amount of balanced micro- and macronutrients to maintain optimal growing conditions. (C.-Y. Chen et al., 2011; Singh & Sharma, 2012) Once a high concentration of algae was reached in the container (800 mg/L), it was harvested using a high-cationic- charge, high-molecular-weight polymer (Hychem Hyperfloc CP913HH) at a dose of 2 mg/L capable of removing up to 95% of the algae biomass. Once harvested, the biomass was freeze-dried and stored until use. The elemental composition of the dry algae biomass was determined with a Thermo

Finnigan Flash 1112 elemental analyzer as described in our previous study. The biomass composition was determined to be 50.5% carbon, 9.4% nitrogen, 7.9% hydrogen, and 6.1% ash on a dry-weight (dw) basis.

Compositional analyses of the algae biomass were performed to quantify proteins, lipids, and carbohydrates; additionally, amino acid profiles were obtained after hydrochloric digestion of the biomass (Ion Chromatography Dionex ICS 5000 module with an AminoPac PA 10 column using a 17 amino acid standard from Sigma-Aldrich). A single arginine standard (Sigma-Aldrich), added to the sample in different dilutions, was used to verify the presence of the amino acid in the hydrolysate. It was verified that only the arginine peak increased proportionally to the new concentration. The fractions of carbohydrates (reducing sugars) and proteins in the biomass were measured by colorimetric methods [3,5-dinitrosalicylic acid (DNS) method for sugars and Lowry's protein estimation] with a spectrophotometer. (Lowry, Rosebrough, Farr, & Randall, 1951; Sereewatthanawut et al., 2008) Lipids (extractables) were measured after chloroform/methanol (2:1) extraction and quantified gravimetrically for experiments performed at 240 and 280 °C. (Bligh & Dyer, 1959) The ash content in the biomass was measured using the method of the U.S. National Renewable Energy Laboratory (NREL/TP-510-42622). Figure 1 shows the results of the biochemical composition analysis of the *Scenedesmus sp*. biomass used in this study. As can be seen in Figure 1, the major component of the algae biomass was protein (54% dw), with arginine being the most abundant amino acid (16% of total protein).

Figure 1. Biochemical composition of *Scenedesmus* sp. used in this study

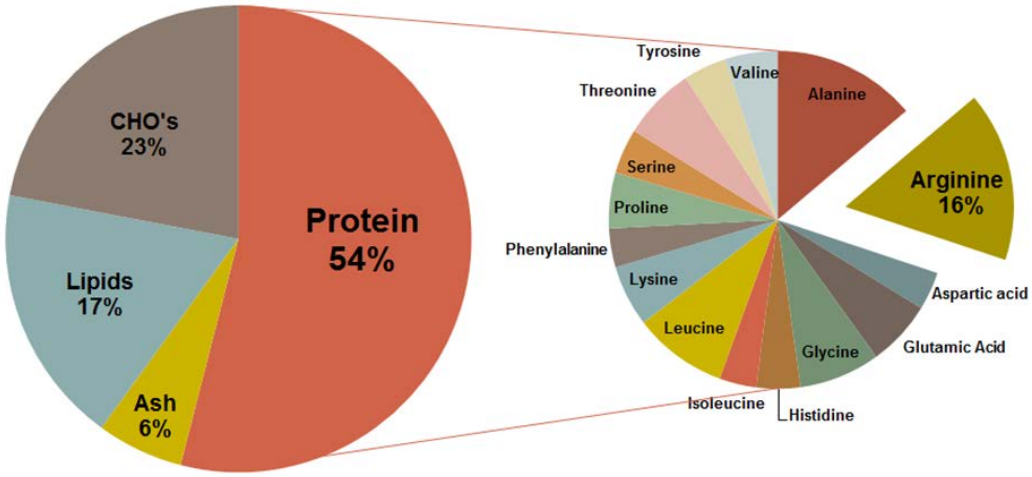

2.2.2. Procedure

To obtain a flowable algae slurry, the freeze-dried algae was well-mixed with water and homogenized. The freeze-dried (FD) algae used in this study was collected and preserved at −4 °C. By the time it had been collected and homogenized, a moisture content of only 3% was measured in the powder. The biomass was preserved in a freezer inside an airtight container. Before starting the experiments, algae slurry was prepared by mixing 50 g of FD algae and 500 mL of deionized water. To verify the amount of solids in the slurry, three different samples were collected and dried for 24 h at 45 ºC. The actual measured values were 7.76%, 7.81% and 7.74% (average = 7.8%; SD=0.03%) of solids.

The flash hydrolysis experimental setup and process was described in a previous study (J. L. Garcia-Moscoso, W. Obeid, S. Kumar, & P. G. Hatcher, 2013). In brief, the method involves a rapid hydrolysis process that capitalizes the difference in reaction kinetics of

algae components and solubilizes proteins into the liquid phase in a very short residence time (few seconds) by using a continuous-flow reactor under subcritical water conditions.

In our previous study we compared a constant residence time of 9 s at five different temperatures and concluded that the optimal conditions to maximize the soluble peptides recovery and lipids preservation in the solid product for *Scenedesmus* was around 280 °C (J. L. Garcia-Moscoso et al., 2013). In fact, that study provided the basis for extending our research to the production of free amino acid (arginine) and peptides, which was achieved by conducting experimental studies at three different residence times, three different reaction temperatures, and a constant pressure of 3000 psi (20.7 MPa) to keep subcritical water conditions (Table 2). Each experiment was performed in duplicate, and the reported values are the averages of the duplicate experiments. To understand the combined effect of temperature and residence time, we estimated the severity factor (R_0) at each set of experimental conditions. The severity factor has been used by several researchers to measure the combined effect of temperature and residence time in processes involving the hot-water treatment of biomass (S. Kumar, Gupta, Lee, & Gupta, 2010). The severity index is defined as:

$$R_0 = t \times \exp\left\{\frac{T-100}{14.75}\right\} \quad (1)$$

where t is the residence time in minutes and T is temperature in ˚C. The logarithmic values of R_0 are listed in Table 2.

Table 2. Experimental conditions

	Temperature (°C)	**Residence time (s)**	**ln R_0**
Run 1	240	6	7.2

Run 2	240	9	7.6
Run 3	240	12	7.9
Run 4	280	6	9.9
Run 5	280	9	10.3
Run 6	280	12	10.6
Run 7	320	6	12.6
Run 8	320	9	13.0
Run 9	320	12	13.3

The biomass residence time was calculated using the formula:

$$t = \frac{V}{F\left(\frac{\rho_{pump}}{\rho_{P1,T1}}\right)} \quad (2)$$

Where, *V* is reactor volume (mL); *F* is the combined volumetric flow rate of pumps 1 and 2 (mL/min); ρ_{pump} is the density of water at pump conditions (g/mL); $\rho_{P1,T1}$ is the density of water at reactor conditions (i.e., pressure 1 and temperature 1). Residence time was calculated based on the temperature indicated by the thermocouple inserted inside the reactor. The thermocouples used were OMEGACLAD® XL probes of standard dimensions (1/16 in.) that provided very low drift at high temperatures (±2 ºC).

2.2.3. Analyses of flash hydrolysis products

After each experiment, a mixture of liquid and solid products was recovered and separated by centrifugation followed by filtration. The aqueous-phase products were stored at 2 °C until being analyzed for total nitrogen, total organic carbon (Shimadzu

TOC/TN analyzer), total phenols (which were measured only for the first six runs based on U.S. Environmental Protection Agency method 420.4), soluble peptides (Lowry's colorimetric method), and arginine content (Ion Chromatography Dionex ICS-5000 AminoPac column and guard). The solid products were freeze-dried; weighed; stored at −4 °C; and analyzed to determine the biochemical composition by elemental analysis, Fourier transform infrared (FTIR) spectroscopy, nuclear magnetic resonance (NMR) spectroscopy, and lipid measurement (the last three analyses were performed only for runs 1−6). Also, the hydrolysate from run 5 was selected because achieving a slightly lower amount of protein (3.8% less soluble peptides) at lower temperature farther from the critical temperature of water (280 vs 320 °C) would be much more favorable for industry in terms of energy savings and cost efficiency.

FTIR spectroscopy (Shimadzu IR Prestige 21) and NMR spectroscopy were used to determine the biochemical composition before and after flash hydrolysis for all solid samples, except those of runs 7−9 because the six previous experiments provided a clear indication of the compositions.

2.3. Results and discussion

The analyses of liquid hydrolysate after flash hydrolysis under different conditions are provided in Table 3. The total nitrogen (TN) and total organic carbon (TOC) values increased gradually with increasing temperature and residence time. The contents of both soluble peptides and arginine in the liquid hydrolysate increased consistently at higher temperatures. It can easily be seen that the soluble peptides followed a similar trend at all temperatures: First, their concentration increased up to a residence time of 9 s, and then, as the residence time continued to increase, the amount of peptides started to decrease.

This might be due to the partial decomposition of peptides to ammonia and other degradation products at longer residence times. (Becker, 2007b)

Table 3. Results of liquid hydrolysate analysis from different Runs.

	TOC		TN		Soluble peptides		Arginine	
	mg/L	Input %	mg/L	Input %	mg/L	Input %	mg/L	Input %
Run 1	1145 ±31	44.1	218.1 ±9	45.1	1294 ±93	42.9	64 ±3	13.5
Run 2	1264 ±10	48.2	265.0 ±7	54.3	1429 ±66	46.9	112 ±12	23.5
Run 3	1324 ±20	50.2	262.9 ±6	53.6	1382 ±30	45.1	90 ±5	18.8
Run 4	1369 ±61	52.5	313.3 ±1	64.6	1825 ±34	60.2	183 ±6	38.5
Run 5	1483 ±35	56.9	350.3 ±2	72.2	1930 ±51	63.7	198 ±16	41.6
Run 6	1582 ±35	59.9	334.5 ±21	68.1	1743 ±47	56.8	262 ±19	54.4
Run 7	1610 ±83	49.6	480.6 ±32	79.6	2377 ±216	63.0	471 ±18	81.5
Run 8	1713 ±38	54.5	522.8 ±13	89.3	2483 ±125	67.5	407 ±36	70.6
Run 9	1737 ±23	55.3	541.4 ±2	92.6	2430 ±8	66.5	306 ±40	56.1

On the other hand, it can be noted that the arginine content reached the highest value at a temperature of 320 °C (run 7) and that it decreased for longer residence times regardless of the temperature of the experiments (Table 3, Figure 4-b). This might be due to the partial decomposition of arginine to ammonia, organic acids, amines, amino acids

with lower molecular weights such as glycine, and other degradation products. (Becker, 2007a; Esteban, García, Ramos, & Márquez, 2008)

Analysis of the hydrolysate at temperatures of 240 and 280 °C demonstrated that arginine was the only free amino acid (Figure 2) that was identified and quantified in significant amounts after flash hydrolysis without any other additional processing. The ion chromatogram clearly showed the presence of glycine in significant amounts (12.5−21.3% of the amino acid profile) along with arginine as free amino acids for the runs conducted at 320 °C, with the lowest amount occurring for run 7 (320 °C and 6-s residence time) and the highest amount for run 9 (320 °C and 12-s residence time). The amounts of other free amino acids at this temperature were still negligible. These results are in agreement with previous findings that amino acids of high molecular weight such as arginine at high temperature and residence time are more susceptible to degradation not only to ammonia, organic acids, and amines but also to other amino acids with lower molecular weight (Figure 2) (Esteban, Garcia, et al., 2008).

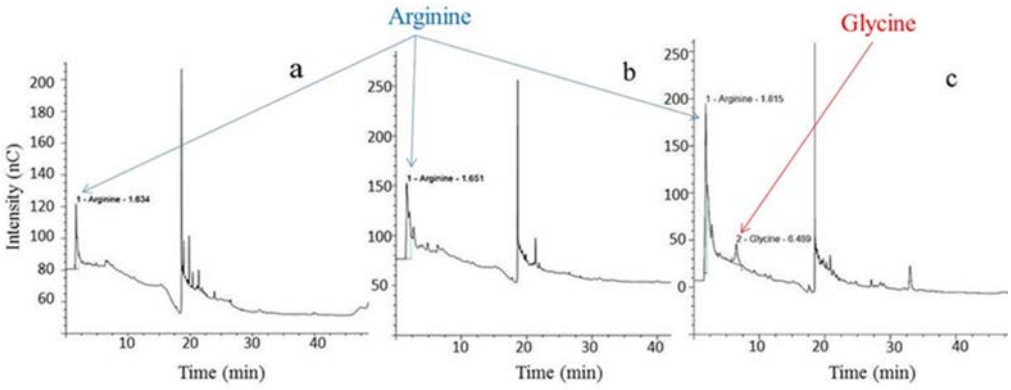

Figure 2. IC chromatogram of liquid hydrolysate from Runs 1, 6 and 7.

The yields of soluble peptides and arginine are shown in Figure 3 in milligrams per gram of protein input. The yields of soluble peptides and arginine reached their

maximum values at run 8 (674.7 mg/g of protein) and run 7 (127.8 ± 6.9 mg/g of protein), which represent 67.5% and 81.5%, respectively, of the total amount of proteins in the algae biomass.

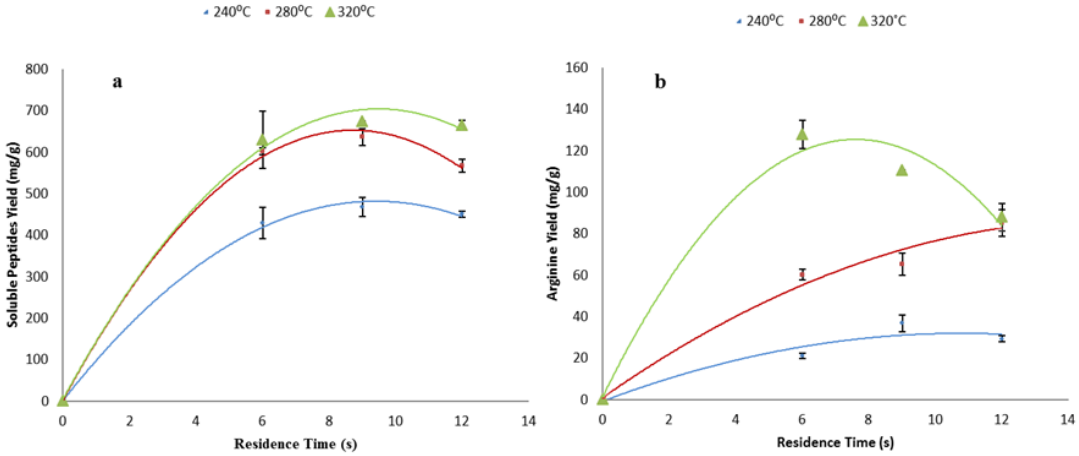

Figure 3. a) Soluble peptides yield (mg/g of protein); b) Arginine yield (mg/g of protein).

Figure 4a,b compares the soluble peptides as a percentage of algae protein and arginine in the hydrolysate as a percentage of arginine in *Scenedesmus* protein for all experimental conditions. In aqueous media, proteins undergo hydrolysis to form oligopeptides and amino acids. Amino acids further degrade to form low-molecular-weight amino acids and carboxylic acids. Taking alanine and glycine as model compounds, the amino acid decomposition was studied in detail by researchers such as Sato et al., Klinger et al., and Faisal et al. (Quitain, Sasaki, & Goto, 2014) The reaction networks of amino acids under hydrothermal conditions take two main paths, namely, decarboxylation to produce carbonic acid and amines and deamination to produce ammonia and organic acids. The ratio of deamination to decarboxylation differs depending on the type of amino acid. Both deamination and decarboxylation occur for most of amino acids. (Quitain et al., 2014) The arginine yields observed under different

conditions were in agreement with the above-mentioned scenario. Arginine increased up to run 7 (320 °C and 6 s), suggesting that there was a higher concentration of this amino acid in the hydrolysate, and as soon as the temperature reached 320 °C, which is high enough for degradation, longer residence times led to more degradation.

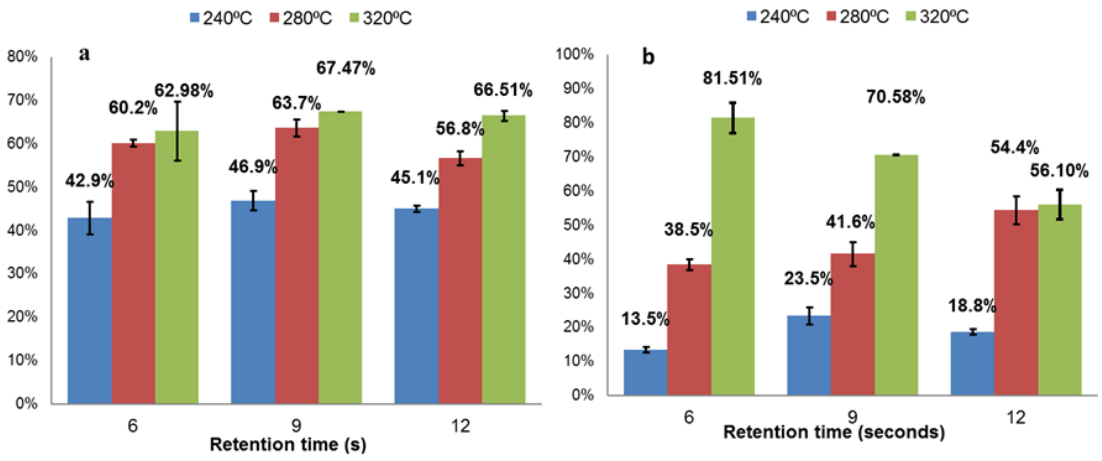

Figure 4. a) Solubilized peptides as % of algae protein; b) Arginine in hydrolysate as % of arginine in Scenedesmus protein

Figure 5 displays the amount of arginine in the hydrolysate (mg) per protein in algae (mg) as a function of temperature (°C) and residence time (s) in a three-dimensional graph prepared using the Matlab R2014b computational program.

Guo et al. (Guo et al., 2013) and Chakinala et al. (Chakinala, Brilman, van Swaaij, & Kersten, 2009) reported that, at high temperature in aqueous medium, proteins hydrolyze to peptides and amino acids, which subsequently degrade and also form free stable radical anions through the Malliard reaction between proteins and carbohydrates. Rodriguez- Meizoso et al. also reported the presence of simple phenolics (gallic acid), caramelization products, and other possible Malliard reaction products in a sample

produced at 200 °C from *Haematococcus pluvialis* microalgae. (Rodríguez-Meizoso et al., 2010)

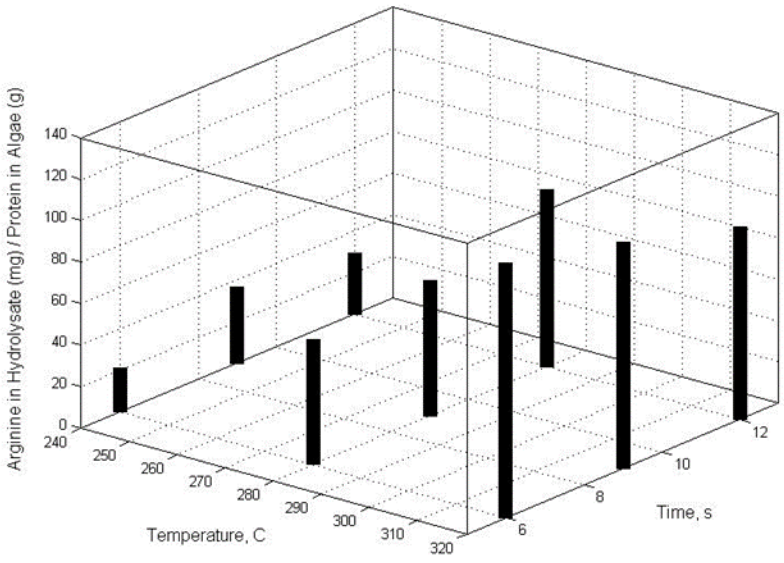

Figure 5. Arginine in hydrolysate (mg)/ Protein in algae (g) vs. Temperature (˚C) vs. Time (s)

During the reaction, the condensation of a reducing group from a carbohydrate and an amino group from a protein or amino acid ultimately results in a polymeric carbonyl amine compound of low solubility. The reacting amino acids and sugars rearrange themselves to form ring-type structures. The formation of these undesirable ring-type Malliard products is minimized by the flash hydrolysis process. This study showed that the algae proteins can be fractionated by hydrolyzing them as peptides and amino acids (building blocks).

The majority of hydrolyzed nitrogen was present as protein building blocks (not degraded to ammonia, nitrate, nitrite, or others). In the subcritical water medium under similar reaction conditions, total nitrogen distributions are expected to be sums of the following three major compounds

Total nitrogen = nitrogen as peptides and amino acids + nitrogen as ammonia + nitrogen as nitrate and nitrite (3)

The ammonia content measured for run 5 was 88.61 mg/L (about 15% of total nitrogen), the nitrate plus nitrite content was only 0.09 mg/L in the liquid phase for this particular experiment, and the rest of the nitrogen was available as peptides and amino acids. The novelty of the process is the preservation of protein building blocks (peptides and amino acids) during hydrolysis reactions. It is important to note that, during the conventional HTL of algae, the nitrogen-derived water-soluble compounds mostly comprise ammonia.

Phenolic compounds are also reported as a byproduct during HTL. (Nenkova, Vasileva, & Stanulov, 2008) These phenolic compounds are reported to have inhibitory effects on algae growth (Nakai, Inoue, & Hosomi, 2001) when the hydrolysate is recycled to the growth medium. In this study, the hydrolysate from run 5 was analyzed for total phenols and quantified as 0.18 mg/L. Much higher values have been reported in conventional HTL experiments on algae biomass, (Biller et al., 2012b) as well as high amounts of unknown TOC that go to the liquid phase after hydrolysis. This limits the use of the aqueous phase for potential nutrient recycling or other coproduct development. Table 4 compares the amounts of phenolic compounds produced after conventional HTL with the amounts produced after flash hydrolysis of algae in this study.

Table 4. Comparison of amount of phenolic compounds produced by Flash Hydrolysis and conventional HTL (Biller et al., 2012a)

	Total carbon in algae (mg/L)	TOC in hydrolysate (mg/L)	Phenols measured (mg/L)	Carbon in phenol (mg/L)	% C (from algae to phenol)	% C (phenol in hydrolysate)

ODU Flash hydrolysis 280C 9 seconds (Run 5)	2619.9	1484	0.18	0.14	0.01	0.01
Chlorogloeopsis 300 °C 1h	59345.5	9060	178	136.18	0.23	1.50
Spirulina 300 °C 1h	60763.6	15123	98	74.98	0.12	0.50
Chlorella 300 °C 1h	57381.8	11373	108	82.63	0.14	0.73
Chlorella 350 °C 1h	21040.0	13764	158	120.88	0.57	0.88
Scenedesmus dimorphus 350 °C 1h	21360.0	11119	80	61.21	0.29	0.55

Usually, batch reactor experiments work with higher residence times and solids loadings, resulting in TOC values that are orders of magnitude higher to those obtained by flash hydrolysis. Also, higher residence times (1 h vs 9 s) allow for the degradation of carbohydrate and protein components. As can be seen in Table 4 the amount of carbon converted to phenol in this study was 200−1000 times lower than that obtained in conventional HTL.

The quantified amounts of soluble peptides and amino acids (arginine) extracted from the liquid phase after flash hydrolysis provided data for calculating the activation energy and modeling the kinetics of protein hydrolysis reactions. Similar kinetics models have been described for the hydrothermal liquefaction of algae and other types of biomass under HTL conditions. (Abdelmoez, Nakahasi, & Yoshida, 2007; Sereewatthanawut et al., 2008; Sasithorn Sunphorka et al., 2012) The following simplified reactions were used assuming that the protein in the algae biomass was hydrolyzed to both soluble peptides and arginine

Algae proteins + water (excess) → soluble peptides (4)

Arginine in algae protein + water (excess) → arginine in aqueous phase (5)

Water was assumed to be present in large excess (1 wt % solids) in the reaction medium, and its concentration change due to reaction was assumed to be negligible. As stated earlier, arginine was the only free amino acid identified and quantified in algae hydrolysate after flash hydrolysis in runs 1−6. In experiments conducted at 320 °C, some amount of glycine was observed. However, based on the ion chromatography results and for the sake of simplicity, it was assumed that arginine was the only free amino acid in the reaction medium for our calculations.

The reaction rate constant (k), reaction order, and activation energy (E_a) were calculated by fitting the experimental values in the mathematical model of integrated rate law and Arrhenius equation

$$k = A\, e^{-Ea/RT} \quad (6)$$

$$\ln k = -(E_a/R)\, 1/T + \ln A \quad (7)$$

Equation 7 is a linear form of eq 6, where A is a constant that includes the orientation factor and T is the temperature in Kelvin.

The rate constant k for protein hydrolysis to soluble peptides and arginine was obtained by fitting the experimental values (C_t vs time for zeroth-order, ln C_t vs time for first-order, and $1/C_t$ vs time for second-order, where C_t is the concentration at time t). The most accurate k value was obtained from the slope of the plotted graph with the best correlation value (r^2) (Figures 6 and 7). Calculating k at the three temperatures and plotting ln k versus $1/T$ provided a line with a slope equal to $-E_a/R$, where R is the gas constant (8.314 J mol^{-1} K^{-1}) (Figure 8).

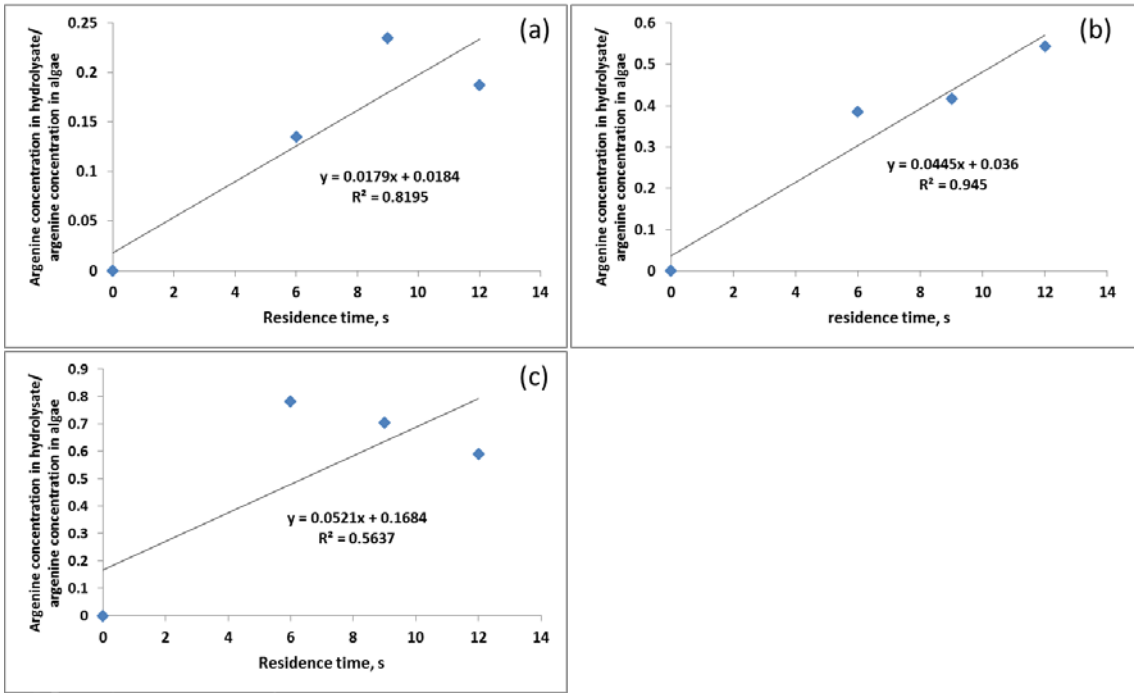

Figure 6. Zeroth-order reaction determination for arginine based on the experimental data and the highest correlation value at a) 240˚C, b) 280˚C, c) 320˚C.

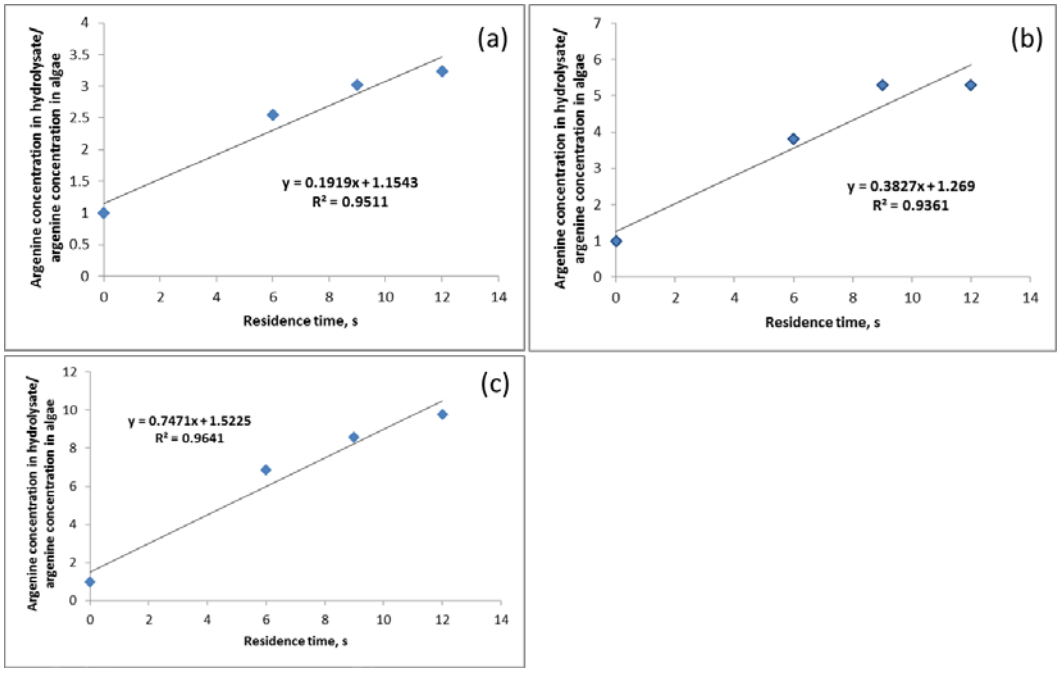

Figure 7. Second-order reaction determination for soluble peptides based on the experimental data and the highest correlation value at a) 240˚C, b) 280˚C, c) 320˚C

Table 5 lists the values obtained by the kinetics study for protein hydrolysis to soluble peptides and soluble arginine. The correlation factors (r^2) range from 0.82 to 0.99, except for that for arginine solubilization at 320 °C, which was 0.56. This might be due to the fact that, at this temperature, at a residence time of 6 s, the arginine yield increased to its maximum and then dropped significantly as the residence time increased, due to the degradation of arginine to lower-molecular-weight amino acids or parallel reactions that could have occurred, which consequently affected the trend of the graph and its linearity as well.

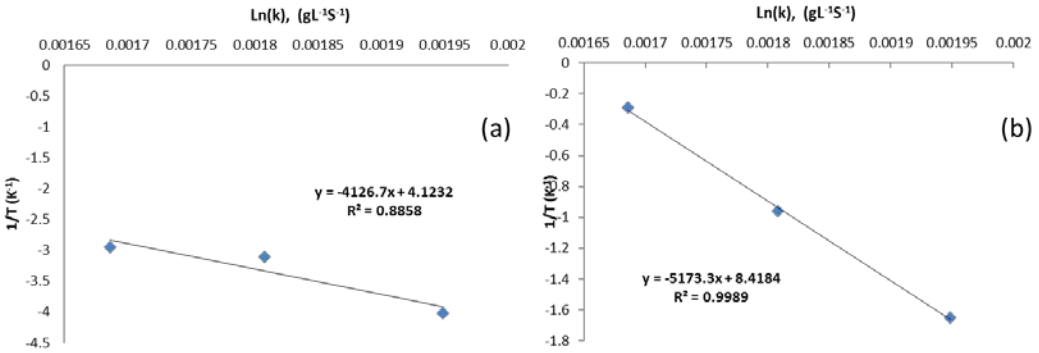

Figure 8. Activation energy slopes and data for a) arginine b) soluble peptides

Table 5. Calculated kinetics parameters (protein and arginine solubilization)

Parameter	Protein Solubilization	Arginine Solubilization
k_{240}	0.19 L g^{-1} s^{-1}	0.02 g L^{-1} s^{-1}
k_{280}	0.38 L g^{-1} s^{-1}	0.04 g L^{-1} s^{-1}
k_{320}	0.75 L g^{-1} s^{-1}	0.05 g L^{-1} s^{-1}
Reaction order	2	0
Activation energy (E_a)	43.01 kJ/mol	34.31 kJ/mol

Obviously, it can be seen that, for both soluble peptides and arginine, the reaction rate constant *k* increased with temperature. However, partial degradation of the product was observed when hydrolysis was carried out at higher temperature (320 °C) for extended residence times. (Quitain et al., 2014) These observations are considered to be in agreement with a low correlation value (r^2 = 0.56) for runs conducted at 320 °C. As explained earlier, at this temperature and longer residence time, amino acids such as arginine can further convert by following two pathways, namely, decarboxylation to produce carbonic acid and amines and deamination to produce ammonia and organic acids. (Quitain et al., 2014) In other words at 320 ˚C couple other parallel reactions are occurring that have higher reaction rates than arginine production which make the *k* value calculations very complicated.

Sunphorka et al. (S. Sunphorka, W. Chavasiri, Y. Oshima, & S. Ngamprasertsith, 2012) reported that that the aggregated protein was decomposed into smaller polypeptides by a second-order process, whereas amino acid production followed a zeroth-order reaction kinetics; these values coincide with those observed in our study (protein and arginine solubilization).

For the biofuels intermediate (solid fractions), the solids recovered after each run (after centrifugation followed by filtration) were freeze dried and stored at -4 °C until analysis. These solids appeared greenish, indicating that chlorophyll was still present. It was also observed that the solid products from the experiments conducted at higher temperatures (runs 4−9) settled to the bottom of the collection containers and were more easily separated than those from lower-temperature experiments (runs 1−3). Table 6

reports the results of the analysis of the biofuel intermediates (solid products) from different runs. Each run was performed in duplicate, and for elemental analysis, each sample was evaluated in triplicate; the reported values in Table 6 are the averages of nine individual measurements.

Table 6. Elemental analysis of solid residues and lipid contents

Sample	Carbon (%)	Nitrogen (%)	Hydrogen (%)	Lipid contents (%)
Algae biomass	50.5 ±0.3	9.4 ±0.1	7.9 ±0.3	17.0
Run 1	56.7 ±0.2	9.0 ±0.3	8.4 ±0.5	35.0
Run 2	57.0 ±0.6	8.3 ±0.2	8.9 ±0.2	37.6
Run 3	57.8 ±0.3	8.6 ±0.2	8.7 ±0.4	42.7
Run 4	61.2 ±1.4	8.1 ±0.1	9.0 ±0.3	47.8
Run 5	61.4 ±0.8	6.5 ±0.2	8.9 ±0.3	61.0
Run 6	65.1 ±1.3	7.2 ±0.1	9.8 ±0.4	74.1
Run 7	61.5 ±0.3	5.9 ±0.4	9.9 ±0.1	-
Run 8	62.6 ±3.2	5.2 ±1.8	9.8 ±0.8	-
Run 9	64.0 ±1.9	5.3 ±1.2	10.0 ±0.2	-
Hydrolysate Run 5	48.0 ±0.1	11.4 ±0.2	7.1 ±0.1	-

The carbon content in the biofuel intermediate increased gradually with temperature and residence time. In the case of nitrogen, it was observed that the value decreased for the experiments conducted at 6 and 9 s, but it increased slightly for the experiments with a residence time of 12 s. It is possible that the observed increase in

nitrogen value (run 3 vs run 2, run 6 vs run 5, and run 9 vs run 8) might be due to the recondensation of proteinaceous material, which was then recovered with the solid products. The higher carbon content in the residue can be explained by the lipid material concentration and also the nitrogen depletion from the original material. (J. L. Garcia-Moscoso et al., 2013).

The amount of solids recovered after each experiment and the respective protein contents are reported in Table 7. It can be seen that the amount of solids recovered diminished gradually at higher temperatures and longer residence times, which indicates a higher biomass solubilization rate. The protein content decreased significantly, matching the observed higher total nitrogen and soluble peptides values in the hydrolyzate. Also, the lipids were preserved (Table 6) and concentrated in the solids recovered, making the solids a better feedstock for biofuels than the original algae biomass. The amounts of carbon and nitrogen recovered in both liquid and solid products after each run are reported in Table 7. However, the carbon recovery (%) differs from the mass balance. Because it is difficult to determine mass balances in hydrothermal media such as flash hydrolysis process because of the occurrence of complex reactions, carbon recovery has been used in many studies instead. (Biller & Ross, 2011a; J. L. Garcia-Moscoso et al., 2013).

Table 7. Percentage of solids (biofuels intermediate) recovered, their protein content, carbon, and nitrogen recovered in both liquid and solid products.

	Solids recovered, %	**Protein in Solids, %**	**C recovered (%)**	**N recovered (%)**
FD algae	-	54	-	-

Run 1	41.1	±1.4	39.3	±0.3	90.2	84.4
Run 2	37.8	±1.0	33.2	±0.1	90.8	87.5
Run 3	33.6	±0.8	30.9	±0.6	88.6	84.5
Run 4	30.5	±0.7	26.2	±1.0	89.4	90.8
Run 5	27.5	±1.6	18.9	±0.9	90.2	91.1
Run 6	24.7	±0.4	18.9	±0.5	91.8	87.0
Run 7	23.0	±5.6	14.5	±4.6	94.1	87.0
Run 8	22.2	±6.6	11.6	±0.7	99 ±2	87.0
Run 9	19.0	±6.9	10.2	±1.4	99 ±2	87.0

To characterize these solids, FTIR spectra (Figures 9 and 10) were obtained. The advantage of an infrared spectroscopic technique is the direct, fast, and nondestructive nature of the screening method. The application of IR spectroscopy to identify and quantify chemical constituents in biomass is based on the chemical bonds of molecules that absorb energy in the IR region of the electromagnetic spectrum. (Dean, Sigee, Estrada, & Pittman, 2010; L. M. L. Laurens & Wolfrum, 2011). The FTIR spectra provided biochemical profiles containing overlapping signals from a majority of the compounds present in the samples of algae biomass. Figure 9 shows the overlapping spectra of a sample of freeze-dried algae and biofuel intermediates from runs 1−3.

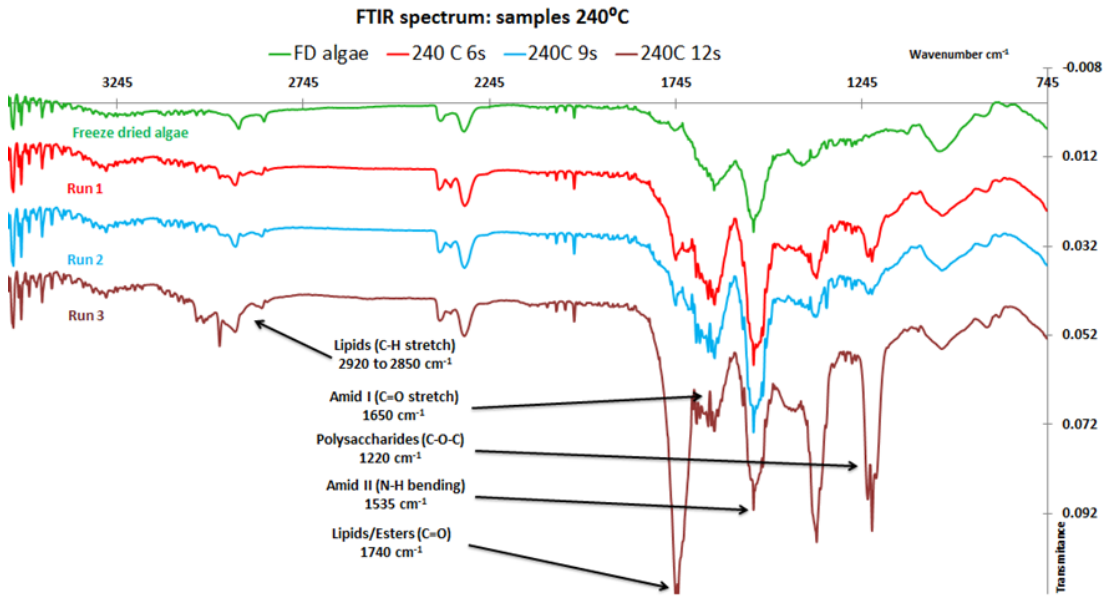

Figure 9. FTIR spectra of freeze-dried algae and biofuels intermediates of runs 1–3.

In the same way, Figure 10 shows overlapping spectra for biofuel intermediates from runs 4−6. The use of FTIR spectroscopy to identify and quantify the biomolecular composition of algae cells has beeb reported in several studies (Dean et al., 2010; Giordano et al., 2001; Meng, Yao, Xue, & Yang, 2014). Peaks and bands can be assigned to different types of macromolecules as follows: 2920–2850 cm^{-1} for lipids (C–H stretch); 1740 cm^{-1}, lipids/ester (C=O stretch); 1650 cm^{-1}, amide I (C=O stretch); 1535 cm^{-1}, amide II (N–H bend); and 1220 cm^{-1}, polysaccharides (C–O–C stretch).

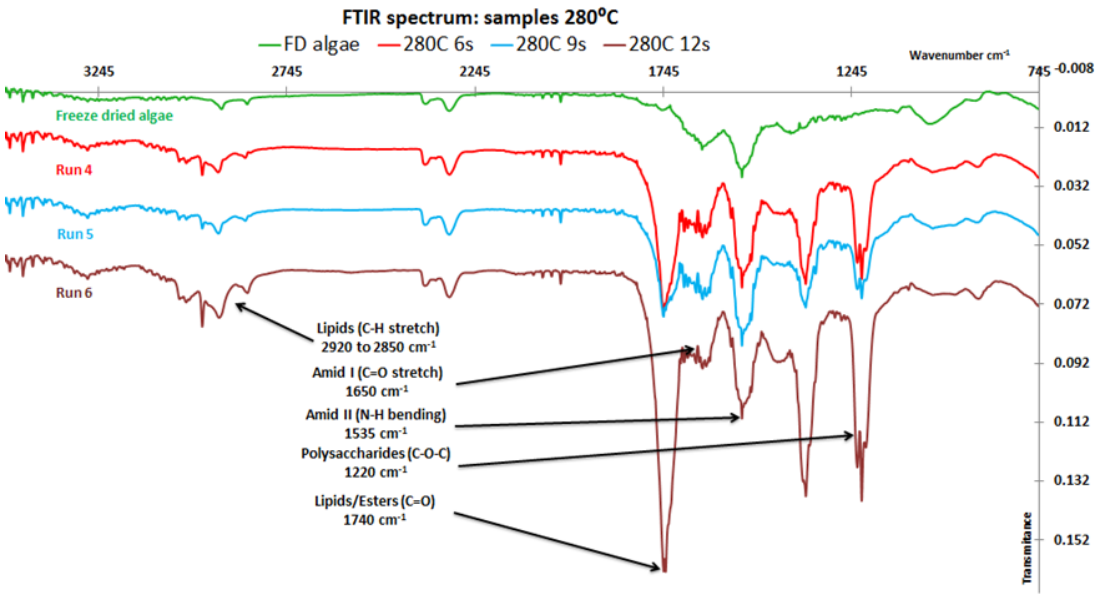

Figure 10. FT-IR spectra of freeze-dried algae and biofuels intermediates of runs 4–6.

These solid products were further analyzed to obtain solid-state ^{13}C NMR spectra. The NMR data were collected on a 400 MHz Bruker AVANCE II spectrometer with ^{13}C resonating at 100 MHz and ^{1}H resonating at 400 MHz. The samples were placed in a 4 mm NMR rotor and covered with a Kel-F cap, and they were rotated with a frequency of 12 kHz and spun at the magic angle (54.7˚). Direct polarization-magic angle spinning (DP-MAS) with broad band proton decoupling was used to obtain quantitative analysis of the different regions in the ^{13}C spectra (X. Zang, Nguyen, Harvey, Knicker, & Hatcher, 2001). The parameters were optimized for 90˚ pulse with maximum signal, and the sample was run with a 30-s recycle delay to allow for full T_1 relaxation.

Several researchers have used this technique to characterize major components in algae biomass (Meng et al., 2014; Nguyen et al., 2003; Ruhl, Salmon, & Hatcher, 2011). Strong signals in the 0-60 ppm region indicates the presence of lipid-like aliphatic carbons and proteins. The contents of carbohydrates, proteins, and lipids can be

quantified by identifying peaks at 72 and 105 ppm; 22, 50, 130, and 175 ppm; and 30 and 40 ppm, respectively (Figure 44, Appendix A). Peaks in the region of 105−160 ppm are subordinate and indicate the presence of aromatic/carbons, reflecting aromatic amino acids comprising proteinaceous components and olefinic structures. The large peak at 175 ppm is assigned to amide and carboxyl groups, structural components of both lipids and proteins (Johnson, Liu, Salmon, & Hatcher, 2013). Table 8 summarizes the observed differences in composition after integration of the NMR spectra obtained for all samples.

Table 8. Integrated values from ^{13}C cross-polarization MAS NMR (%)

	Algae	**Run 1**	**Run 2**	**Run 3**	**Run 4**	**Run 5**	**Run 6**	**Hydrolysate (Run 5)**
Aliphatic	45.3	54.4	56.6	56.3	56.3	61.1	59.0	33.0
Proteinaceous	20.1	17.5	16.4	15.6	14.3	12.4	13.0	17.0
Carbohydrates	11.7	5.7	5.2	5.9	5.5	4.5	4.0	18.2
Olefins/Aromatics	7.2	8.0	8.4	8.3	10.9	11.1	12.6	17.1
-C=C-COOR/-C=C-CHO	0.7	0.6	0.5	0.6	0.6	0.5	0.5	1.3
Carboxyl/Amide-C	15.0	13.9	12.9	13.4	12.3	10.4	10.9	13.4

The NMR and FTIR spectra of the recovered solid products indicated that the protein was extracted and solubilized whereas the lipids and carbohydrates were still present in the solids. The NMR spectrum of the freeze-dried product showed peaks that are characteristic of protein/peptide side-chain carbons.

Thermogravimetric (TG) and differential thermogravimetric (DT) analyses were conducted to understand the thermal stability of the biofuel intermediates up to 700 °C,

based on the continuous measurement of the weight loss as a function of temperature increase. In TGA with nitrogen as the carrier gas, the first-stage mass loss (up to 110 °C) generally refers to the moisture content, and the mass loss after that (between 110 and 700 °C) corresponds to the volatile matter. (Bi & He, 2013).

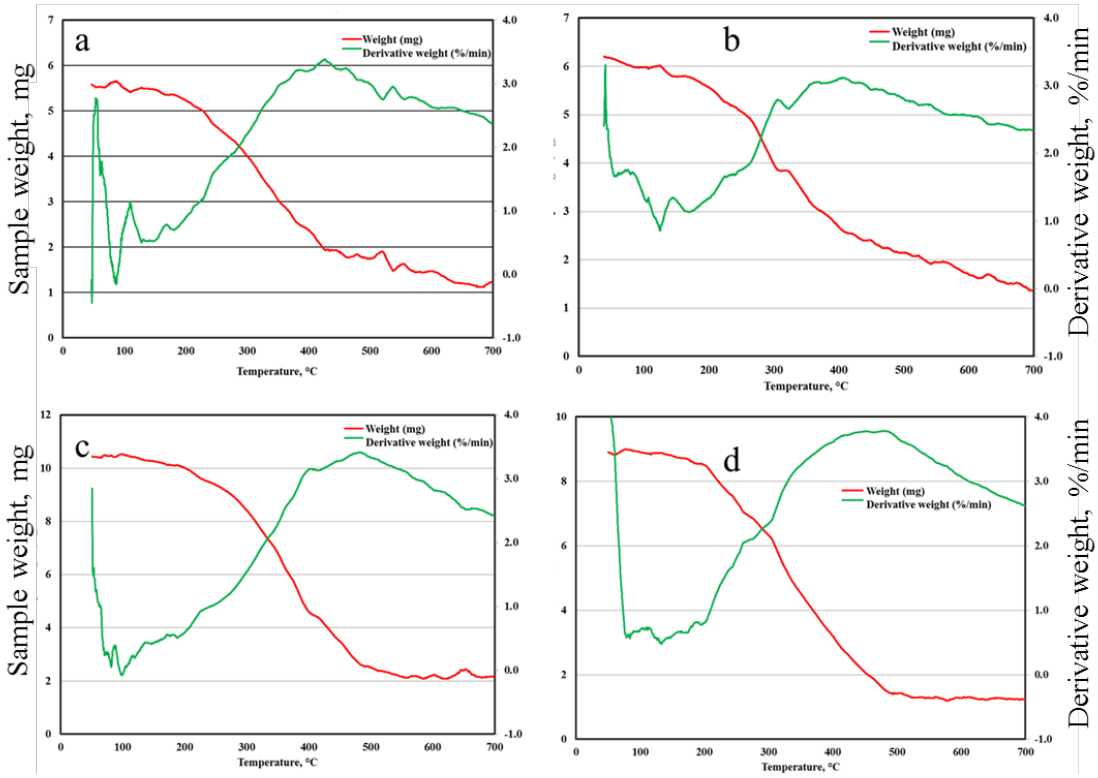

Figure 11. TGA profiles of (a) algae biomass, (b) freeze-dried hydrolysate from run 5, (c) biofuel intermediate from run 2, and (d) biofuel intermediate from run 5.

As shown in Figure 11, after moisture loss at around 110 °C, another stage of weight loss was observed at approximately 240 and 580 °C due to the loss of volatile matter and the decomposition of algae biomass. The DTA profiles for *Scenedesmus* sp. and the freeze-dried hydrolysate from run 5 have the highest values around 400 °C, whereas the highest values for the biofuel intermediates from runs 2 and 5 are over 500 °C, probably because of the higher lipid and lower protein content.

2.4. Conclusions

Flash hydrolysis can be an environmentally benign process for recovering protein-derived coproducts from microalgae. During the flash hydrolysis of *Scenedesmus* sp., water-soluble peptides were found to be the most abundant compounds recovered from the hydrolysis of the protein component. Arginine as a free amino acid was also present in significant amounts, providing another potential coproduct from this process. Peptides and arginine can be separated and purified from the hydrolysate to be developed as high-value coproducts from microalgae. The soluble peptides yield reached its maximum value in run 8 at 675 mg/g of protein, and in run 7, the maximum arginine yield was 123 mg/g of protein. The solubilization of protein to soluble peptides followed a second-order reaction with an activation energy of 43.0 kJ/ mol, whereas the solubilization of arginine fitted zeroth-order reaction kinetics with an activation energy of 34.1 kJ/mol. Arginine is a semiessential amino acid already being sold as a nutrient supplement. Soluble peptides could also be used as food/feed supplements, but there are other potential uses including as additives for composite materials or the production of polyols.

The present study showed that, by tuning the temperature and residence time of the flash hydrolysis process, not only can the protein content be reduced significantly, but also the lipid content can be increased from 17% in raw algae biomass to around 75% in biofuel intermediates (solids) after the flash hydrolysis process. TGA showed that, among the first six runs, the highest weight loss for the *Scenedesmus* biomass and the freeze-dried algae hydrolysate from run 5 was around 400 °C. However, TGA and DTA profiles of the biofuel intermediate from run 5 showed that the highest weight loss occurring at

temperatures over 500 °C, indicating a lower protein content and a higher lipid content after the flash hydrolysis process.

2.5. Acknowledgements

The authors are thankful for the financial support from the National Science Foundation (NSF CAREER Award CBET- 1351413). Our special appreciation goes to the Virginia Coastal Research Consortium for providing all of the analytical instrument support and Mr. Isaiah Ruhl for helping with NMR analysis. We also extend our thanks to Applied Research Center, Newport News, VA, for support with FTIR and TG analyses.

CHAPTER 3

INTEGRATION OF BIOFUELS INTERMEDIATES PRODUCTION AND NUTRIENTS RECYCLING IN THE PROCESSING OF A MARINE ALGAE

Note: the contents of this chapter have been published in the AIChE Journal. The nutrient recycling part of this study (sections 3.2.7 and 3.3.4) was performed by a visiting scholar Dr. Elena Barbera from the University of Padova.

Teymouri, A.; Kumar, S.; Barbera, E.; Sforza, E.; Bertucco, A.; Morosinotto, T., Integration of Biofuels Intermediates Production and Nutrients Recycling in the Processing of a Marine Algae. AIChE Journal 2017, 63 (5), 1494-1502.

The cost-effective production of liquid biofuels from microalgae is limited by several factors such as recovery of the lipid fractions as well as nutrients management. Flash hydrolysis (FH), a rapid hydrothermal process, has been successfully applied to fractionate the microalgal biomass into solid biofuels intermediates while recovering a large amount of the nutrients in the aqueous phase (hydrolysate) in a continuous flow reactor. The aim of the work is to enhance the quality of a high-ash containing marine algae *Nannochloropsis gaditana* as biofuel feedstock while recycling nutrients directly for algae cultivation. Characterization of products demonstrated an increase in extractable lipids from 33.5 to 65.5 wt% (dry basis) while retaining the same FAME profile, in addition to diminution of more than 70 wt% of ash compared to raw microalgae. Moreover, the hydrolysate was directly used to grow a microalga of the same genus.

3.1. Introduction

The world energy sector is mainly dependent on fossil fuels. The U.S. Energy Information Administration (EIA) recently reported that around 87% of energy consumption in the year 2014 was produced from fossil resources (Gençer & Agrawal, 2016). It is expected that these resources will be considerably diminished in the next 100 years (Gençer & Agrawal, 2016). Renewable resources such as solar , wind, hydropower, ocean waves, geothermal, and biomass are alternatives that will address the issue (Twidell & Weir, 2015). Among all renewable sources, biomass has been widely used due to its fuel supply diversity (efficient conversion to electricity, liquid, and gaseous fuels)(Johansson, 1993) and particularly, microalgal biomass has brought a large degree of attention (Demirbas & Fatih Demirbas, 2011; Makareviciene, Skorupskaite, & Andruleviciute, 2013).

The idea of utilizing these green unicellular microalgae as an energy source was proposed many years ago (Benemann, Weissmann, Koopman, & Oswald, 1977). There are a variety of advantages utilizing microalgae as a promising renewable energy source, including but not limited to their high capabilities for carbon dioxide fixation (Mata et al., 2010), growth in variety of conditions such as lacustrine, freshwater, brackish or even hyper saline, and wastewater (Ahmad et al., 2011; Mutanda et al., 2011), occupying less land compared to terrestrial crops (Chisti, 2007), efficient photosynthesis process (Vonshak, 1990), and high growth rate and productivity compared to conventional crops.

Despite the above advantages, there are challenges in scaling-up the process economically. These challenges are related to algal species resistance to contamination, tolerance of various stresses in the growth conditions (pH, temperature, light intensity,

ionic strength, etc.), downstream processing, nutrients cost and availability (Griffiths & Harrison, 2009; Mata et al., 2010). Among these, nutrients cost and requirements, in particular concerning phosphorus and nitrogen, were found to be highly critical for large-scale algal oil production (Canter, Blowers, Handler, & Shonnard, 2015; Pate, Klise, & Wu, 2011; Quinn & Davis, 2015; Yun, Smith, & Pate, 2015). A typical algal biomass contains around 7 wt% nitrogen and 1 wt% phosphorus (dry-basis) suggesting that application of fertilizers for large scale algal cultivation is likely inevitable (Slade & Bauen, 2013). Venteris *et al.* showed that assuming complete nitrogen and phosphorus consumption, in order to reach the Energy Independence and Security Act (2007) advanced biofuel goals (21 BGY: billion gallon per year), the nitrogen and phosphorus demand would vary between 1.4–4 and 1.3–2.9 times of the total U.S. consumption for agricultural fertilizers respectively, depending the technology pathways (Venteris, Skaggs, Wigmosta, & Coleman, 2014). These estimations strongly support, as the comprehensive study carried out by Canter *et al.*, that nutrients supply for algal growth are too large to just rely on the agricultural fertilizers (Canter et al., 2015).

Cultivating marine microalgae would be a long-term promising solution to this issue. Most of the above mentioned nutrients are available in the marine environments (estuarine, coastal, and oceanic ecosystems) to meet or exceed the stoichiometric amounts required for algal growth of most species; although, the N:P ratio might be different depending on the marine systems (Hecky & Kilham, 1988). Nonetheless, in order to make it sustainable, it is crucial to manage, recover and recycle the nutrients, especially phosphorus and nitrogen, directly from the source (*i.e.*, the non-lipid fractions of microalgal biomass) to eliminate the potential of non-point environmental pollution. In

fact, increasing level of nutrients is the main cause of eutrophication in lakes (Correll, 1998; Schindler, 2006). Nitrogen will also lead to the undesired production of NO_x compounds during the combustion process (Biller & Ross, 2011b). Venteris *et al.* also emphasized the importance of nutrients recycling and recovery as a key factor for industrialization of microalgae to biofuel production and its impact on the agricultural fertilizers market and food security (Venteris et al., 2014).

In order to select the appropriate marine species as a feedstock for biofuel production, measuring oil productivity which is related to both algal growth and the oil content of microalgae (Chisti, 2007; Griffiths & Harrison, 2009) seems to be an attractive characterization of the algal biomass. Most common microalgae have a lipid content of 20–50 wt% of dry biomass, however, higher amounts in the range of 70–85 wt% are also reported (Mata et al., 2010; Rawat, Ranjith Kumar, Mutanda, & Bux, 2013). Rodolfi *et al*. concluded that *Nannochloropsis* sp. can produce 3.5 and 20 times higher amount of oil annually per hectare than palm and sunflower, respectively (Rodolfi et al., 2009). Accordingly, the microalgal feedstock applied in this study was *Nannochloropsis gaditana*, which is a well-known high-lipid marine microalgae with high growth rates that make it an outstanding candidate for biofuel productions (Gouveia & Oliveira, 2009; Mendoza, Vicente, Bautista, & Morales, 2015; Rodolfi et al., 2009).

There are different conversions of algal biomass into fuels, classified under physical and chemical processes. Since techno economic and life cycle analysis have confirmed dewatering as one of the most energy intensive processes in the algal-biofuel refineries (R. E. Davis et al., 2014; Handler et al., 2014; Lardon, Hélias, Sialve, Steyer, & Bernard, 2009), abounding numbers of recent studies have been focusing on the

hydrothermal (HT) processing of wet algal biomass as an inexpensive, scalable, and sustainable method which is based on conversion followed by fractionation (Patel et al., 2016; Peterson et al., 2008).

A variety of techniques are available to treat algal biomass in HT conditions. Hydrothermal liquefaction (HTL) has gained more attention in current studies due to its ability to convert solid biomass to liquid fuel precursor in the form of biocrude. However, the biocrude yield and its components substantially depend on the temperature and residence time (Patel et al., 2016). At low temperature, due to incomplete cell rupture, biocrude yield is low (Patel et al., 2016). Elevated temperatures and longer residence times, increase deoxygenation resulting in higher HHV of the biocrude (Saqib S. Toor et al., 2013). However, it will reduce the mass of the aqueous phase due to gasification and raise nitrogen content in the biocrude (Patel et al., 2016).

On the other hand, flash hydrolysis (FH) has been proven to be an environmentally-friendly continuous process that can utilize the wet algal biomass (slurry) at 280˚C temperature and very short residence time (9 s) to fractionate macronutrients such as nitrogen and phosphorus while preserving lipids in the solid residue (biofuels intermediates) (Barbera, Sforza, Kumar, Morosinotto, & Bertucco, 2016; Jose Luis Garcia-Moscoso et al., 2013; Garcia-Moscoso, Teymouri, & Kumar, 2015). The successful realization of short residence times for fractionating algae components (proteins and lipids) would greatly reduce the reactor volume, significantly reduce CAPEX and OPEX, and provides product stream of small peptides and amino acids as a co-product along with the lipid-rich solids as biofuels precursors. This is much more favorable and economical compared to conventional HTL that uses long residence

times (several minutes) and temperatures ($\geq$ 300 ºC) (Patel et al., 2016). Moreover, the studies performed by Biller *et al.* have shown that based on the algal strains, dilutions of 200-400 times are required in order to obtain optimum growth in the aqueous phase yield from HTL to eliminate the effect of inhibitors such as nickel, fatty acids, and phenols (Biller et al., 2012b), while these toxic compounds are present in much lower concentrations in the aqueous phase produced from FH (Jose Luis Garcia-Moscoso et al., 2013; Garcia-Moscoso et al., 2015).

In a recent study carried out by Barbera *et al.*, it was shown that the same hydrolysate obtained from FH could be used for cultivation of *Scenedesmus obliquus*, without requiring the addition of any other nutrients (Barbera et al., 2016). In particular, the growth rate obtained in batch experiments resulted to be higher compared to that in standard medium, due to mixotrophic growth exploiting residual organic carbon molecules in the hydrolysate. In addition, continuous steady-state production was also obtained under various conditions (Barbera et al., 2016).

The objectives of the present study are to (i) perform the FH process on *Nannochloropsis gaditana* to investigate the extent of nutrients removal and biofuels intermediate production from a high-ash marine algal biomass, (ii) characterize the biofuels intermediates obtained from the FH process for its use for producing biofuels, (iii) evaluate the feasibility of direct recycling of the nutrients-rich hydrolysate for algae cultivation. The extraction of both macro- and micro- nutrients from a high-ash marine algae through the FH plus the direct uptake potential of these nutrients (without any additives or dilutions) by an alga has not been previously studied. In addition, the FH process with direct nutrients recycling possibility for marine algae makes the process

environmentally sustainable with respect to nutrients management and downstream processes for producing biofuels.

3.2. Materials and methods

The *Nannochloropsis gaditana* biomass used for FH was cultivated in ponds in greenhouses provided by Algaespring B.V (http://www.algaspring.nl). Algal biomass after harvesting was freeze-dried (FD) and stored in an airtight container at a temperature below -20˚C.

3.2.1. FH experiments

Prior to the experiments, the algal biomass was mixed and homogenized with an appropriate amount of deionized water to obtain a flowable slurry. In this regard, 60 mL of deionized water (DI) was added to 16 g of FD *N. gaditana* microalgae. To measure the amount of solids in the slurry, three different samples were collected and dried for 24 h at 60˚C. The average solid content was 20.56 wt% with relative standard deviation (RSD) of 0.24%. The FH experimental set-up and process have been described in detail previously (Jose Luis Garcia-Moscoso et al., 2013; Garcia-Moscoso et al., 2015). All three experiments were conducted at the temperature of 280˚C and 9 s of residence time. These conditions were selected based on previous studies, which was found to be optimum for nutrients extraction and lipid preservation in the form of biofuels intermediates (Jose Luis Garcia-Moscoso et al., 2013).

After each experiment, the greenish product slurry was centrifuged and filtered to separate the biofuels intermediates from the hydrolysate. The liquid and solid products were stored at 2˚C and -20˚C respectively, until further experiments or analyses were done.

3.2.2. Moisture, ash, and elemental analysis

Ash analyses of the FD microalgae were done in triplicate using the standard procedure suggested by National Renewable Energy Laboratory (NREL) Technical Report (Van Wychen & Laurens, 2013). Moisture content was measured at 105 ˚C with an infrared moisture analyzer (IR 35, Denver Instrument, Bohemia, NY). The elemental composition of the dry algae biomass was determined in triplicate using an elemental analyzer (Thermo Finnigan Flash EA 1112 Automatic Elemental Analyzer, Thermo Fisher Scientific, Waltham, MA) as described in a previous study (Jose Luis Garcia-Moscoso et al., 2013).

3.2.3. Carbohydrates, proteins, and amino acids profile

Carbohydrates (reducing sugars) and protein content of microalgae were estimated using colorimetric 3,5-dinitrosalicylic acid (DNS) and Kjeldahl method, respectively (Lowry et al., 1951). The nitrogen to protein factor of 6.25 were used for protein content determination in microalgae (Jones, 1941). To identify the relative amounts of different amino acids in the peptides present in the hydrolysate, amino acid profiles were obtained before and after a complete acid digestion process. Both microalgae and the hydrolysate were hydrolyzed with hydrochloric acid 6N for 18–24 h in a 110 ˚C heating block (Karty, 2014). Chromatography analysis was performed using the Dionex ICS-5000 AAA-Direct Ion Chromatography instrument (Thermo Fisher Scientific, Waltham, MA) equipped with an AminoPac PA10 column and a guard column. Sigma-Aldrich 17 amino acid standard was used and all samples were analyzed in duplicate.

3.2.4. Total organic carbon, total nitrogen, and total phosphorus

After each FH experiment, the obtained aqueous-phase was analyzed for total nitrogen (TN), total organic carbon (TOC) using Shimadzu TOC/TN analyzer (TOC-VCSN, Shimadzu, Kyoto, Japan), and total phosphorus (TP) using HACH DR 2800 spectrophotometer (Hach Company, Loveland, CO) to confirm the consistency of the runs and to prepare material balance.

3.2.5. X-Ray fluorescence (XRF)

In order to determine the elemental composition of the hydrolysate being used for algal cultivation, X-Ray Fluorescence (XRF) spectroscopy analysis (Bruker S4 Pioneer, Bruker Corp., Billerica, MA) was conducted on the FD aliquot.

3.2.6. Gas Chromatography-Mass Spectrometry (GC-MS) and Pyrolysis GC-MS

A modified tetramethylammonium hydroxide (TMAH) solution was used to analyze the lipids present in biofuels intermediate by converting them to fatty acid methyl esters (FAMEs) (Woo & Kim, 1999). Lipids of both the FD raw microalgae and biofuels intermediates were Soxhlet extracted with 2:1 (v/v) chloroform/methanol for 24 h, dried and weighed (Bligh & Dyer, 1959). Approximately 1 mg aliquot plus 250 µl TMAH solution (25 wt% in methanol from Sigma–Aldrich, PN: 334901) were transferred to a sealing glass ampule. A vacuum line was attached to the ampule in order to dry out the methanol. After most of the methanol was removed, ampules were flamed-sealed and moved to a muffle furnace at 250˚C for 2 h. The tubes were then cooled to ambient temperature. Samples were reconstituted using ethyl acetate followed by filtering to remove any solid particles. The FAMEs were compared with internal standard (F.A.M.E. Mix, C4-C24 from Sigma–Aldrich, PN: 18919-1AMP) for identification and

quantification using a coupled gas chromatography (HP 6890 series GC system, Hewlett–Packard Agilent, Ramsey, MN) – mass analyzer (Pegasus III time-of-flight (TOF) mass spectrometer, Leco Corp., St. Joseph, MI) system(Obeid, Salmon, Lewan, & Hatcher, 2015). Pyrolysis–gas chromatography-mass spectrometry was carried out on the samples using a Chemical Data Systems (CDS) pyrolysis system CDS 2000 Plus coupled to a Leco Pegasus II GC–MS system with the GC operating in the split mode (50:1) (Obeid, Salmon, & Hatcher, 2014).

3.2.7. Algal cultivation using hydrolysate

3.2.7.1. Algal strain and culture media

Nannochloropsis gaditana (strain 849/5, obtained from CCAP) was used to carry out growth experiments exploiting the hydrolysate as culture medium. The algal strain was maintained in sterile f/2 medium, with 33 g L^{-1} sea salts (Sigma -Aldrich), having a concentration of 1.5 g L^{-1} $NaNO_3$ (247 mg L^{-1} N) and 5 mg L^{-1} of $NaH_2PO_4 \cdot H_2O$ (1.12 mg L^{-1} of P), buffered with 40 mM TRIS HCl pH 8. The same medium was used for all control experiments, as a reference. For all growth experiments in the hydrolysate, an appropriate amount of FD powder was re-dissolved in sterile distilled water (although experiments were not carried out in sterile conditions) in order to match the same total N concentration of f/2 used as a control (247 mg L^{-1}), which corresponds to a P concentration of 40 mg L^{-1} (mainly present as orthophosphates, PO_4-P). In addition, 33 g L^{-1} of sea salts were added to the medium.

3.2.7.2. Experimental set-up for algal cultivation

Batch growth experiments were conducted in Drechsel bottles of 5 cm diameter, with a total culture volume of 100 mL. A continuous light intensity of 150 μmol m^{-2} s^{-1}, measured with a photoradiometer (HD 2101.1 from Delta OHM) which quantifies the PAR (Photosynthetically Active Radiation, 400-700 nm), was artificially provided by fluorescent lamps. Cultures were placed in an incubator with a constant temperature (24 ± 1°C). A mixture of air enriched with CO_2 (5% v/v, regulated by two flowmeters) was supplied to the cultures at a total flow rate of 1 L h^{-1}. All experiments started with an initial microalgae inoculation of OD_{750} = 0.45, which corresponds to a cell concentration of about $5 \cdot 10^6$ cells mL^{-1}, and were carried out at least in duplicate.

3.2.7.3. Analytical procedures used in algae cultivation

Algal growth was monitored daily by measuring the optical density (OD) at 750 nm with a UV-visible UV 500 double beam spectrophotometer (Spectronic Unicam, UK), as an indirect indication of biomass concentration. In addition, cell count was performed using a Bürker Counting Chamber (HBG, Germany). Specific growth rates were calculated by linear regression of the logarithm of the experimental points during the exponential phase of growth, taken as the average of the two independent biological replicates. At the end of the growth curve, the final biomass concentration was measured in terms of dry weight (DW, g L^{-1}). DW was measured gravimetrically by filtering 5 mL of culture sample (previously diluted 1:5 in order to dissolve salts) with 0.45 μm cellulose acetate filters, which were then dried for 4 h at 90 °C in a laboratory oven. In the case of growth experiments using the hydrolysate, the DW of the medium itself was previously measured and subtracted from that of the total sample. Nitrogen, Phosphorus and Chemical Oxygen Demand (COD) concentrations were measured

spectrophotometrically, using standard test kits, at initial and final conditions. A sample of culture was previously filtered using a 0.22 μm filter, to measure only the dissolved nutrients. Total nitrogen (TN) was measured using the persulfate digestion method, based on oxidation of most nitrogen forms to nitrate, at high pH. Samples were digested at 121°C for 60 min in an autoclave. Nitrates (NO_3-N) were then measured using test kits provided by Carlo Erba Reagenti, Italy. Ammonium (NH_4-N) was measured using HYDROCHECK SPECTRATEST (Reasol®), based on the reaction with Nessler reagent in alkaline conditions, and followed by absorbance measurement at 445 nm. Phosphorus (PO_4-P) was measured by the absorbance (at 705 nm) of a dying complex formed between orthophosphate ions and molybdenum in reducing environment. Finally, COD was measured with an analytical kit provided by Sigma-Aldrich, USA (AQUANAL®), which is based on oxidation of organic compounds by potassium dichromate in sulfuric acid solution.

3.3. Results and discussion

3.3.1. Microalgae characterization

The elemental composition of the FD *Nannochloropsis gaditana* was 47.7% carbon, 7.0% nitrogen, 6.9% hydrogen, and 12.4% ash on a dry weight (DW) basis. Using the 6.25 conversion factor, proteins content was estimated as 43.8 wt% in the microalgae(Jones, 1941) and this value was used for material balance and yield calculations. However, different nitrogen to protein factors from 2.53 to 5.77 has been also reported recently which is highly dependent on growth condition and physiology of the cultures (Lourenço, Barbarino, Lavín, Lanfer Marquez, & Aidar, 2004). Figure 12 illustrates the results for the composition analysis of *N. gaditana* including the amino acid

profiles. As can be seen, arginine, aspartate, and alanine each with 19.9 wt%, 10.4 wt%, and 9.8 wt% are the predominant amino acids, respectively. A similar amino acid profile was seen for the hydrolysate. Arginine (21.2 wt%), alanine (11.4 wt%), and aspartate (10.5 wt%) were still the most abundant amino acids. Different amino acids profiles have been reported in the literature based on the microalgae's strain (Lourenço et al., 2004; Lourenço, Barbarino, Marquez, & Aidar, 1998; Templeton & Laurens, 2015; Tibbetts, Milley, & Lall, 2014).

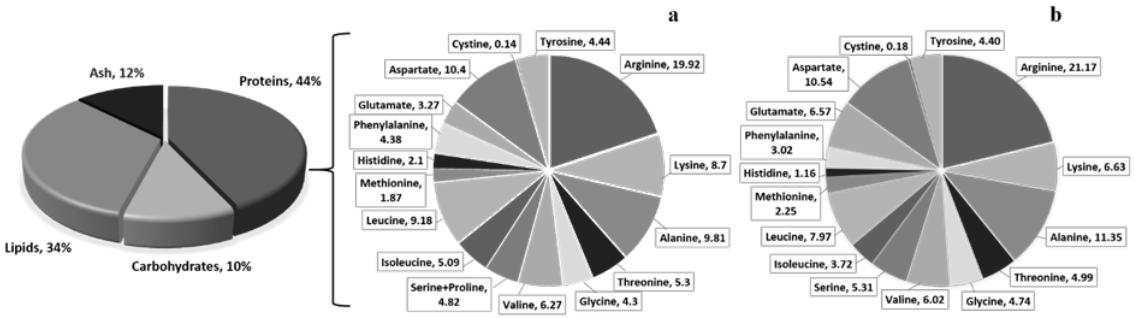

Figure 12. Biochemical composition and amino acids profile of *Nannochloropsis gaditana* (a) and hydrolysate recovered after FH (b) (all numbers and percentages are in dry weight basis)

The analysis showed 34 wt% of lipids in the algal strain. Similarly, Huerlimann *et al.* reported 22-32 wt% oil content for *Nannochloropsis* sp. grown in f/2 medium thus without any particular deprivation treatment (depending on their growth phase) (Huerlimann, de Nys, & Heimann, 2010). Even higher lipid content for *Nannochloropsis* sp. has been reported, depending on the growth condition of algal biomass including nutrient (nitrogen and phosphorus) deprivation, irradiances, etc. (Griffiths & Harrison, 2009; Simionato et al., 2013).

3.3.2. Biofuels intermediates

Data obtained from elemental analysis showed that the percentage of carbon, nitrogen, and hydrogen are 60.6, 6.5, and 9.6 wt% (dry-basis) respectively. Ash analysis conducted on both raw microalgae and biofuels intermediates demonstrate diminution of more than 70% in the ash content (reducing from 12.4 wt% to 3.6 wt%). Ash is an undesired by-product of most biomass thermal conversion processes that would very likely affect the process design and operation, as well as the product purification processes and product quality. Reducing the ash content of algal biomass is thus very crucial to reduce their impact on slagging, fouling and other ash-related problems in biorefineries for biofuel production (Ross, Jones, Kubacki, & Bridgeman, 2008). Reduction of the ash content of biomass also has a great impact on the transportation cost as well and will decrease the final product price. Yun *et al.* studies proved that reducing the ash content of algal turf from 52 to 13% dry weight basis will highly affect the capital and operational cost of the facility lead to reduction in the final fuel price by approximately 23.5% (Yun et al., 2015).

Figure 13 shows the average material balance of the three FH experiments. Based on the material balance and elemental analysis results, there is approximately 56 wt% decrease in the nitrogen content in the biofuels intermediates compared to the raw *N. gaditana* biomass, while hydrogen to carbon ratio (H/C) increased from 1.7 to 1.9. Having less nitrogen is favorable since nitrogen in the fuel directly produces NO_x compounds during combustion, which are undesirable in terms of environmental issues and legislative reasons (Biller & Ross, 2011b; Ross et al., 2010). The higher H/C content could be as a result of lipid accumulation in the biofuels intermediates. Performing the

aforementioned extraction method on both the *N. gaditana* biomass and the biofuels intermediates demonstrated an increase in extractable lipids from 33.5 to 65.5 wt% (dry basis). This is equal to more than 92 wt% of lipids presented originally in the feedstock. Dealing with lipid-rich feedstock will reduce the operational cost of biofuel production (including the transportation and storage costs). Lardon *et al.* reported that 90% of energy consumption in the process of biofuel production is related to drying (20%) and lipid extraction (70%) processes and any development will directly impact sustainability and the final fuel cost (Lardon et al., 2009). The results are comparable to former studies by Garcia *et al.* (Jose Luis Garcia-Moscoso et al., 2013; Garcia-Moscoso et al., 2015) and also Levine *et al.*, who stated a 77-90 wt% retention of total lipids from dry algal biomass in the solid residue after hydrolysis performed at 250˚C and 15-60 min of reaction time (Levine, Pinnarat, & Savage, 2010).

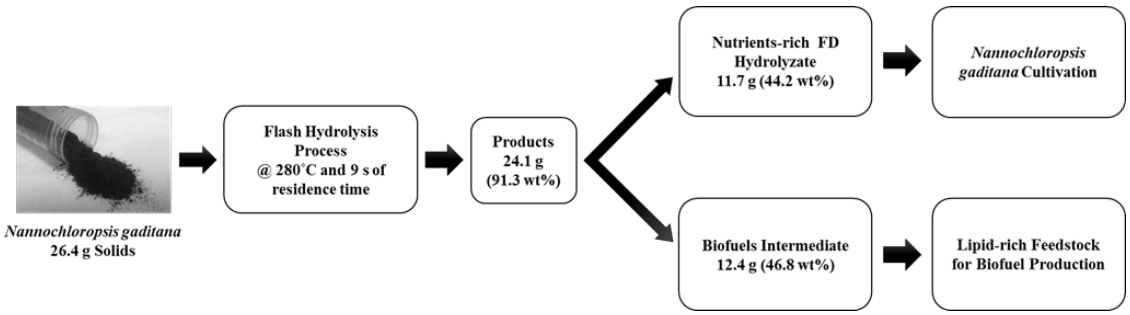

Figure 13. The average material balance of three experiments conducted at 280 ˚C and 9 s of residence time

In order to have a better understanding of the lipid profile and its consistency after the FH, a modified TMAH method was performed to convert fatty acids to FAMEs followed by GC–MS analysis. Figure 14 shows the GC-MS spectra for FAME standard which is used for quantification purposes (Figure 14a), *Nannochloropsis gaditana*

microalgae (Figure 14b), and biofuels intermediates (Figure 14c) yield from FH experiments. The peaks are identified by their retention time and fingerprint fragmentation pattern. As can be observed, the FAME distribution is very similar and consistent. In other words, the lipid profile has not changed, while the amount of lipids in the algae increased from 33.5 to 65.5 wt%. Table 9 illustrates the FAME profile of *N. gaditana* microalgae and the biofuels intermediates. As can be seen, in both samples, the two major fatty acids (palmitic acid and palmitoleic acid) constituted approximately 83.3 wt% in *N. gaditana* and 90.9 wt% in biofuels intermediates of the total fatty acids pattern. A variety of fatty acids profiles have been reported in different studies (Lang, Hodac, Friedl, & Feussner, 2011), also in dependence from environmental condition changes such as nitrogen availability, light intensity, and temperature that affects the fatty acids distribution (Simionato et al., 2013; Sukenik, Zmora, & Carmeli, 1993).

Table 9. FAME profile for *Nannochloropsis gaditana* and biofuels intermediates

	N. gaditana , wt%	Biofuels Intermediates, wt%
Myristic acid (C14:0)	4.7	4.8
Palmitic acid (C16:0)	46.9	50.0
Palmitoleic acid (C16:1)	36.4	40.9
Stearic acid (C18:0)	5.2	2.0
Oleic acid (C18:1)	6.8	2.3

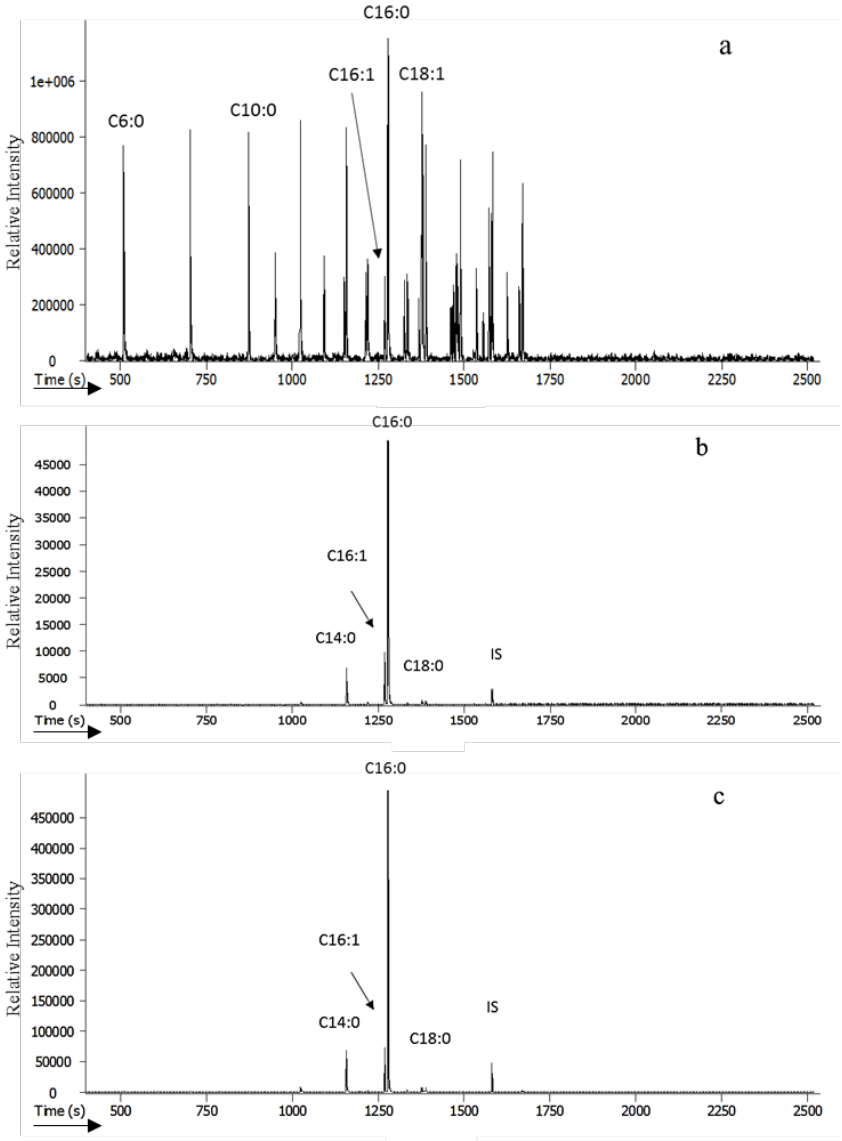

Figure 14. Gas chromatography-mass spectrometry spectra for: a) FAME standard, b) *Nannochloropsis gaditana* microalgae, c) biofuels intermediates yield from experiments carried at 280 ˚C and 9 s of residence time. (IS: Internal Standard)

Pyrolysis GC-MS has been proved to be a promising analyzing technique to quickly and simply verify the composition of the microalgal biomass with minimal pre-treatment (Biller & Ross, 2014). As can be observed in the pyrograms (Figure 15) the peaks identified as break down of Tryptophan and Tyrosine (a representative of proteins)

decreased from raw *N. gaditana* (Figure 15a) to biofuels intermediates (Figure 15b) (Marcos et al., 2016).

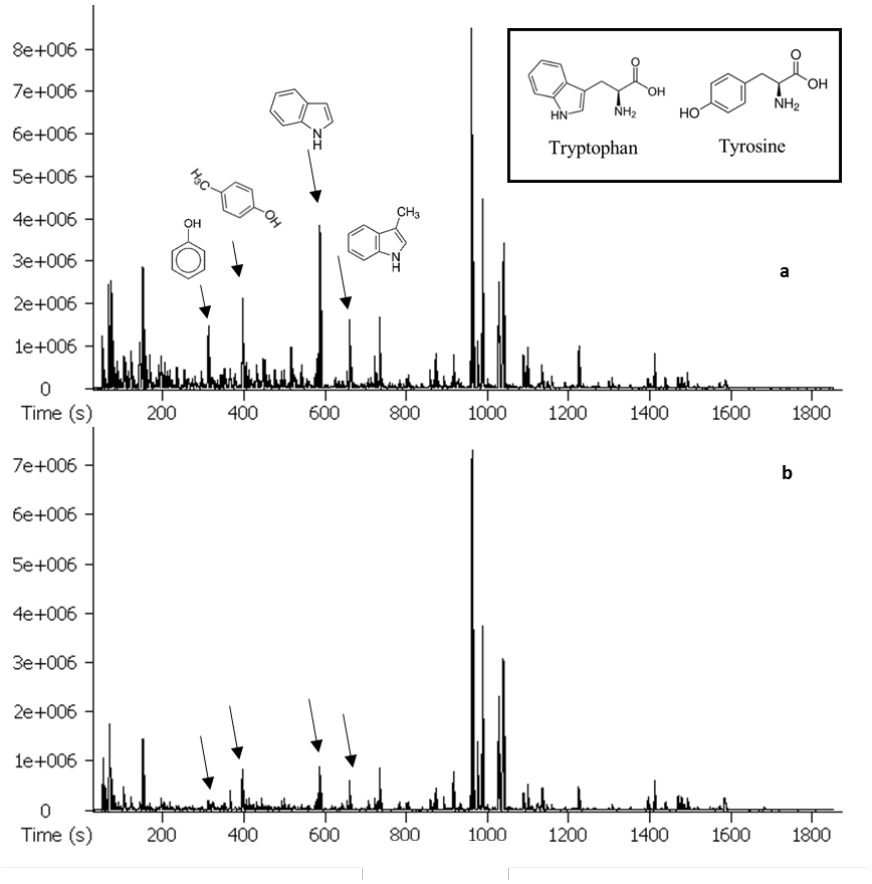

Figure 15. Pyro-GC-MS spectrum for *Nannochloropsis gaditana* microalgae (a) and biofuels intermediates (b). Notice the reduction in the peaks height representing proteins.

Furans and levoglucosan were used as representative of carbohydrates in the microalgae and the biofuels intermediate (Figure 16). Wand *et al.* reported levoglucosan as the major carbohydrate-derived compound identified by GC-MS after the pyrolysis of algal biomass (K. Wang, Brown, Homsy, Martinez, & Sidhu, 2013). As can be seen, peaks identified as furans and levoglucosan in the algal biomass reduced after the FH process expressing that more carbohydrates are available in the hydrolysate making it a rich source for algal cultivation.

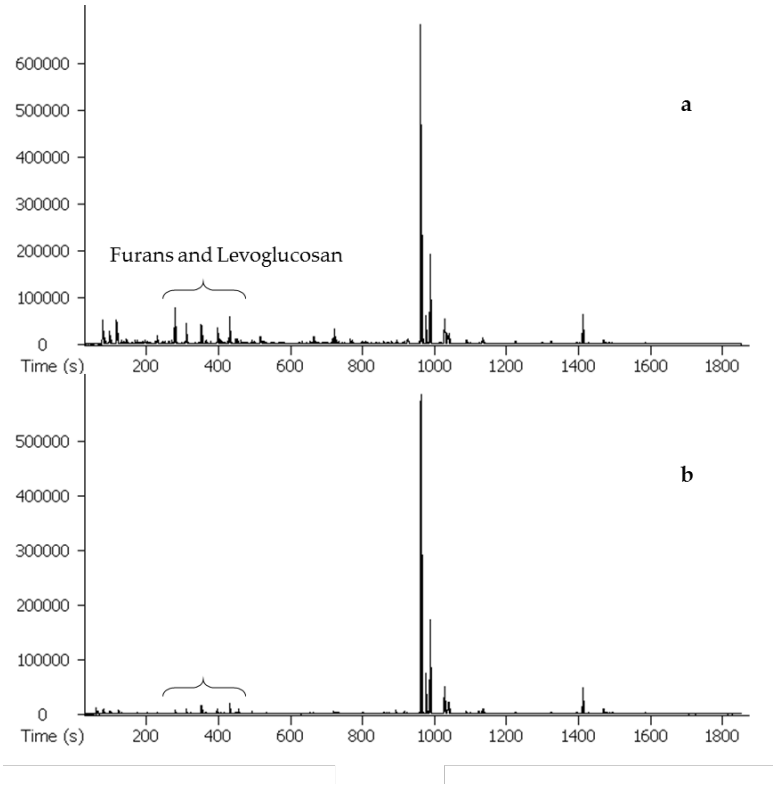

Figure 16. Carbohydrates representatives (furans and levoglucosan) comparison in the (a) *Nannochloropsis gaditana* microalgae and the (b) biofuels intermediates. Notice the reduction in the peaks height.

3.3.3. Algal hydrolysate: A nutrients-rich medium

Table 10 shows the average results of three FH experiments for TOC, TN, TP, and pH of the hydrolysate.

Table 10. Characteristics of *N. gaditana* hydrolysate (1.9 wt% of algae slurry input)

Characteristics	pH	TOC (mg/L)	TN (mg/L)	TP (mg/L)
N. gaditana Hydrolysate	6.2	3072	767	117

After all experiments were done, the nutrients–rich hydrolysate was freeze-dried in order to store, further analysis and be used as nutrients source for algal cultivation. In accordance with previous studies (Jose Luis Garcia-Moscoso et al., 2013; Garcia-Moscoso et al., 2015), the results from elemental composition and XRF spectroscopy analysis also confirmed that FH on *Nannochloropsis gaditana* efficiently extracted most of macronutrients such as nitrogen and phosphorus (between 50 to 60 wt%), and other micronutrients such as Cl, K, Ca, Na, S, Br, Mg, etc. in the aqueous phase (Table 11). This makes the hydrolysate a potential media for the direct use in algal cultivation.

Table 11. Elemental composition of *Nannochloropsis gaditana* nutrients-rich hydrolysate obtained from elemental analyzer and X-ray fluorescence. Values are wt% dried basis.

Elements	C	N	H	O	Cl	K	Ca	P	S	Na	Mg	Br
N. gaditana Hydrolysate	35.8	8.0	5.8	27.8	15.8	4.5	1.6	1.3	1.0	1.1	0.3	0.3

3.3.4. Algal cultivation via direct recycling

To ascertain the use of nutrients, *N. gaditana* was cultivated in the hydrolysate. Productivity results are shown in Figure 17 comparing the f/2 and hydrolysate based culture media.

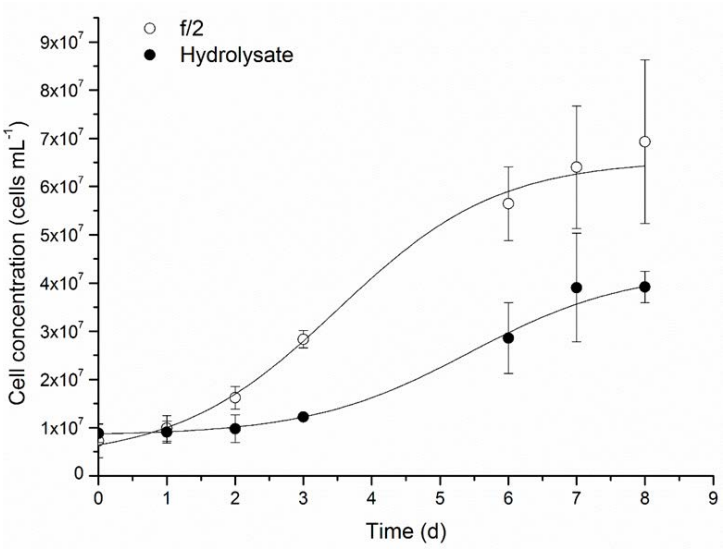

Figure 17. Growth curve of Nannochloropsis gaditana in f/2 (open circles) and in the hydrolysate (full circles)

It can be clearly seen that *N. gaditana* was able to grow in the hydrolysate, reaching a satisfactory final cell concentration of about 40×10^6 cells mL^{-1}. The growth rate appeared to be lower compared to that obtained in sterile f/2 medium, used as control, showing in addition an initial lag-phase, which indicates cells adaptation to the new cultivation conditions. In particular, the growth rate resulted to be equal to 0.46 d^{-1} in f/2, and 0.29 d^{-1} in the hydrolysate. Nonetheless, the final biomass concentration measured as dry weight resulted to be similar in the two cases (1.01 ± 0.27 g L^{-1} and 0.93 ± 0.18 g L^{-1} for control and hydrolysate cultures respectively).

To determine the bio-availability of the nutrients contained in the hydrolysate, initial and final concentrations were measured. As previously reported, nitrogen is mainly present in the hydrolysate in the form of soluble peptides and amino acids, while only about 10% is available as ammonium (NH_4–N). In a previous work, it was shown that *Scenedesmus* sp. was able to uptake the organic nitrogen forms contained in the medium

and use that for growth (Barbera et al., 2016; Caleb Talbot, 2016). However, the capability of up-taking simple organic nitrogen is species-dependent, and has therefore to be assessed for the species considered (Markou, Vandamme, & Muylaert, 2014).

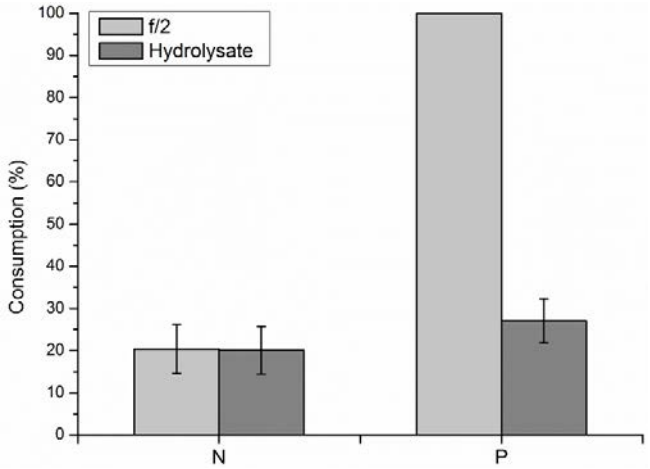

Figure 18. Nitrogen and phosphorus consumption in f/2 (light grey) and hydrolysate (dark grey).

As demonstrated in Figure 18, about 20% of the initial nitrogen (measured as TN) contained in the hydrolysate was consumed by the culture. On the other side, COD measurements show that no consumption of organic carbon is verified (Table 12), suggesting that *N. gaditana* did not in fact consume the organic nitrogen available in the medium. This result is consistent with what was reported in the work of López Barreiro *et al.* (López Barreiro et al., 2015), in which no significant organic carbon consumption was measured for *N. gaditana* grown in the aqueous phase obtained from HTL. This is consistent with the limited ability of this species to use organic carbon in mixotrophic conditions (Sforza, Cipriani, Morosinotto, Bertucco, & Giacometti, 2012).

Interestingly, as also shown in Table 12, the concentration of NH_4-N, initially very low, was found to be much higher at the end of the growth curve. This seems to

suggest that ammonium was slowly released in the medium, and that the slower growth rate obtained in the hydrolysate compared to that in f/2 could be due to an initially limiting inorganic nitrogen concentration. The slow release of ammonium in the medium, is therefore necessary in order to allow algal growth since algae are not able to use organic nitrogen molecules.

Table 12. Initial and final nutrients concentrations in f/2 and hydrolysate cultures

	Nutrient	**Initial concentration (mg/L)**	**Final concentration (mg/L)**
f/2	N (NO_3-N)	249.07 ± 14.07	198.20 ± 2.56
	P (PO_4-P)	0.68 ± 0.25	0
Hydrolysate	N (TN)	203.71 ± 11.23	162.88 ± 1.60
	N (NH_4-N)	18.16 ± 0.17	102.13 ± 1.03
	P (PO_4-P)	22.77 ± 1.05	16.60 ± 0.49
	COD	840.19 ± 158.37	1040.58 ± 80.58

Phosphorus, conversely, was mainly available in the hydrolysate in the form of orthophosphates, and could be efficiently assimilated by microalgal cells. The P in f/2 was entirely consumed (being the limiting nutrient under these experimental conditions), whereas only 27% of that initially present in the hydrolysate was uptaken by the culture (Figure 18), likely due to the limiting nitrogen bio-available in this case.

Overall, the liquid hydrolysate obtained from FH of *Nannochloropsis gaditana* was proved to be able to growth of a microalga of the same genus, even without the addition of other macro and micro-nutrients, highlighting the good potential of this technique for direct nutrient recycling. However, the species considered was found to have a low capability of assimilating the organic nitrogen forms present in the medium, requiring first inorganic ammonium to be released, which leads to slower growth rates. Nonetheless, the partial addition of other inorganic nitrogen forms (*e.g.*, nitrates) can help to improve the growth during the first days of cultivation. At the same time, the hydrolysate could be used as the sole source of phosphorus, providing therefore a quantitative recycle of this strategic resource.

3.4. Conclusion

The present work investigates the viability of the FH process on the high-ash marine microalga *Nannochloropsis gaditana*. A thorough characterization of both the biofuels intermediate and the nutrient-rich hydrolysate phases produced by the process was performed. Results show that the lipids contained in the original biomass are preserved in the solid phase, having the same FAME profile, while the ash and proteins contents are greatly reduced. The liquid hydrolysate is, on the other hand, rich in nutrients was tested for direct nutrients recycling for algae cultivation. Results show that *N. gaditana* was able to grow in this medium, even though the release of inorganic ammonium from amino-acids and peptides is necessary. Nonetheless, phosphorus resulted to be readily available. Overall, the results obtained show that FH could be a very promising and viable process to improve the performances of biofuels production and nutrients management.

3.5. Acknowledgements

The author would like to acknowledge the financial supports of this work by National Science Foundation (NSF CAREER award #CBET-1351413) and ERC starting grant BIOLEAP nr 309485 and PRIN 2012XSAWYM to TM. This study is a part of Research Opportunities in Europe for NSF CAREER Awardees program.

CHAPTER 4

HYDROXYAPATITE AND DITTMARITE PRECIPITATION FROM ALGAL HYDROLYSATE

Note: the contents of this chapter have been published in the Algal Research journal.

Teymouri, A., Stuart, B. J., & Kumar, S. (2018). Hydroxyapatite and dittmarite precipitation from algae hydrolysate. *Algal Research*, *29*, 202-211.

DOI: https://doi.org/10.1016/j.algal.2017.11.030

Several research efforts across the globe have been concerned with addressing the technical barriers in the commercialization of algae-based sustainable biorefineries. Nutrients cost and management and in particular, phosphorus, have been highlighted as one of the most significant challenges in algae cultivation and downstream processing. In this study, 83 wt% of phosphorus present in *Scenedesmus* sp. microalgae was extracted as water-soluble phosphate in aqueous phase via flash hydrolysis process while preserving the algae lipids. Subsequently, the phosphate containing aqueous phase (algae hydrolysate) was used for producing dittmarite and hydroxyapatite by two different mineralization processes. In the first pathway, more than 97 wt% of the phosphate in the hydrolysate was recovered in the form of carbonate-hydroxyapatite, a valuable biomaterial, at 280 ˚C within one hour of residence time via hydrothermal mineralization process. Whitlockite as the secondary phase was also observed along with the hydroxyapatite. In the second pathway, 67 wt% of the phosphate and 6 wt% of nitrogen were recovered as dittmarite (magnesium ammonium phosphate), an effective slow-

release fertilizer, at 20 ˚C via an atmospheric precipitation process. The effects of seeding, temperature, reaction time, and mineralizers to PO_4 molar ratio on phosphate removal as well as product yield were studied. This is the first kind of study in which flash hydrolysis and mineralization processes were integrated to provide an energy efficient platform for phosphorus recovery from microalgae in forms of value added compounds that could be suitable for long-term storage and handling. Through this experimental study, we report the shortest residence time for hydroxyapatite precipitation from an algal hydrolysate. The short residence time could substantially save in reactor size and processing time as well as provide an option for high throughput which could result in a significant cost reduction in algae to bioproducts and biofuels.

4.1. Introduction

Microalgae are as an attractive feedstock for biofuels and bioproducts due to its lipids, proteins, and carbohydrates content as well as its adaptable growth conditions (Langholtz, Stokes, & Eaton, 2016). A variety of pathway and process developments have been investigated in order to accelerate the commercialization of algal-based biorefineries (Mayfield, 2015; Pienkos, 2016). In spite of improvements in algal productivity and development on different downstream processing routes, the barriers for large-scale commercialization have not yet been removed (Pienkos, 2016). Algae biomass and biofuels production costs are dependent on the nutrients use; particularly nitrogen and phosphorus (Langholtz et al., 2016). Phosphorus is of greater concern in large-scale algae cultivation due to its irreplaceability and the fact that it is obtained from a non-renewable phosphate rocks through mining (Canter et al., 2015; Pate et al., 2011). Recent collaborative studies supported by the U.S. Department of Energy and the

National Academies Press outlined nutrients supply and recycling as a critical hurdle for a sustainable algae-to-fuel process (Council, 2012; Mayfield, 2015). Multiple studies have been dedicated to nutrients recycling and management either separately or in conjunction with the biofuel production processes, such as direct recycling of the aqueous phase produced by the hydrothermal liquefaction (HTL) of microalgae (Biller et al., 2012b; Garcia Alba, Torri, Fabbri, Kersten, & Brilman, 2013; López Barreiro et al., 2015) or the aqueous phase (hydrolysate) obtained from the flash hydrolysis (FH) (Barbera et al., 2016; Talbot, Garcia-Moscoso, Drake, Stuart, & Kumar, 2016; Teymouri, Kumar, et al., 2017) process. Although, the results from these studies have shown the feasibility of direct nutrients recycling approach, it possesses several practical challenges. One of the main challenges is the fact that all of these nutrients are dissolved in the aqueous phase; therefore, any type of handling, shipping or storage needs to account for the huge amount of water associated with these nutrients (Barbera et al., 2016; Biller et al., 2012b; Talbot et al., 2016). The need for dilution of the aqueous phase to reduce the concentration of growth inhibitors (e.g. phenolic compounds) (Talbot et al., 2016) in addition to N:P ratio adjustment are other challenges involved in this approach. Further, organic content and nutrients present in the aqueous phase is a rich medium for bacterial growth resulting in decomposition of the nutrients such as organic nitrogen (Talbot et al., 2016). All of these obstacles and limitations eliminate the potential for long-term storage. To address these challenges, the current study provides a novel method of on-site nutrients recovery from microalgae in the forms of two value-added products (hydroxyapatite and dittmarite) which can be stored and used for various applications.

In the proposed approach, nutrients are extracted in algae hydrolysate using FH process (Barbera et al., 2016; Barbera et al., 2017; Jose Luis Garcia-Moscoso et al., 2013; Garcia-Moscoso et al., 2015; Sandeep Kumar et al., 2014; Talbot et al., 2016; Teymouri, Kumar, et al., 2017). FH is a continuous subcritical water extraction process which has been shown to extract phosphorus (>80 wt%), nitrogen (>60 wt%) and inorganic elements (S, K, Na, Ca, Mg, Cl, etc.) in aqueous phase (algae hydrolysate) in only 10 s of residence time, while preserving lipids in a solid biofuels intermediate. These solids recovered after FH of microalgae have the same fatty acid profiles as the original biomass (Jose Luis Garcia-Moscoso et al., 2013; Garcia-Moscoso et al., 2015; Teymouri, Kumar, et al., 2017). Applying this method to the wet algal biomass offers an environmentally-benign technique to extract phosphates in the hydrolysate while enhancing the quality of the biofuels intermediates for biofuels/bioproducts downstream processing.

Conversely, mineralization is a technique to precipitate specific elements from an aqueous medium such as algae hydrolysate. Conceptually, it is driven from the earth-mimetic mineral precipitation (deposits) phenomena. In other words, imitating the natural mechanism of the earth to form insoluble minerals at appropriate conditions (Takeshi Itakura, Sasai, & Itoh; Sasai, Matsumoto, & Itakura, 2011). This process could be either at hydrothermal conditions (hydrothermal mineralization, HTM) or atmospheric pressure (atmospheric precipitation, AP) based on the desired target products (e.g. hydroxyapatite (HAp) or dittmarite). The HTM technique has been applied for resource recovery (B, F, P, As, Sb, Cr, and Nd) and polluted water detoxification in the last decade (T. Itakura, Imaizumi, Sakita, Sasai, & Itoh, 2009; T. Itakura, Imaizumi, Sasai, & Itoh, 2008, 2009; T. Itakura, Sasai, & Itoh, 2004, 2005, 2006a, 2006b, 2007; Sasai et al., 2011).

In this study, the extracted *Scenedesmus* sp. microalgae nutrients (phosphorus and nitrogen) via FH process, were recovered through two different precipitation/mineralization pathways (Figure 19) to produce HAp and dittmarite by the addition of calcium (Ca) and magnesium (Mg) as mineralizers via the HTM and AP processes, respectively. Ca and Mg are essential micronutrients in algal cultivation due to their vital role in microalgae cell wall structure and chlorophyll molecule (Esakkimuthu, Krishnamurthy, Govindarajan, & Swaminathan, 2016). Therefore, these are partly available in the algal hydrolysate. The addition of extra mineralizer (Ca or Mg sources) help in meeting the stoichiometric ratio to precipitate HAp and dittmarite compounds.

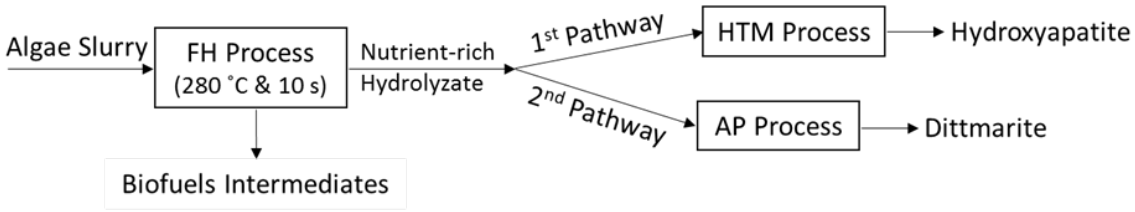

Figure 19. Schematic diagram of the proposed integrated pathways for nutrients recovery. FH: flash hydrolysis, HTM: hydrothermal mineralization, AP: atmospheric precipitation

HAp ($Ca_{10}(PO_4)6(OH)_2$) is the most thermodynamically stable calcium phosphate mineral at pH between 4 and 12 at normal temperatures (Koutsopoulos, 2002; Koutsoukos, Amjad, Tomson, & Nancollas, 1980). Its broad range of applications include synthetic bone, implant filling and coating, chromatography, corrosion resistant materials, drug delivery as well as catalytic activity (Azzaoui et al., 2014; Ferraz, Monteiro, & Manuel, 2004; Kano et al., 1994; Mori, Hara, Mizugaki, Ebitani, & Kaneda, 2003, 2004; Mossaad, Starr, Patil, & Riman, 2010; Sebti, Tahir, Nazih, & Boulaajaj,

2001; Sebti, Tahir, Nazih, Saber, & Boulaajaj, 2002; Song, Shan, & Han, 2008). HAp production has been conducted under a variety of physical and chemical conditions (Mehdi Sadat-Shojai, Khorasani, Dinpanah-Khoshdargi, & Jamshidi, 2013). However, most studies have been performed on mixtures of pure model compounds rather than applied to the actual phosphate and calcium rich aqueous streams (Mehdi Sadat-Shojai et al., 2013). Dittmarite, on the other hand, is the monohydrate form of magnesium ammonium phosphate (MAP – $MgNH_4PO_4 \cdot H_2O$) salt. The hexahydrate form is known as struvite; however, in this study dittmarite and MAP may use interchangeably. MAP precipitates where phosphate and ammonium-rich streams are introduced to alkaline conditions. Its application includes swine wastewaters (Md M. Rahman, Liu, Kwag, & Ra, 2011; Suzuki et al., 2007), urine waste (B. Liu, Giannis, Zhang, Chang, & Wang, 2013), beverage wastewater (Foletto, Santos, Mazutti, Jahn, & Gündel, 2013), landfill leachate (D. Kim, Ryu, Kim, Kim, & Lee, 2007), poultry manure (Yetilmezsoy & Sapci-Zengin, 2009), industrial wastewater (Tunay, Kabdasli, Orhon, & Kolcak, 1997), anaerobic digester effluents (Münch & Barr, 2001; Turker & Celen, 2007), and synthetic wastewater (Kofina & Koutsoukos, 2005). This white crystalline compound is considered a promising slow-release fertilizer for crops (Bhuiyan, Mavinic, & Koch, 2008) and recently as a nutrients source for algal cultivation (Barbera et al., 2017; R. W. Davis et al., 2015; Moed, Lee, & Chang, 2015).

Phosphate recovery in the form of HAp and dittmarite from the complex ionic/cationic algal hydrolysate with high organic content has never been studied before. The proposed integrated FH-HTM/AP processes have the potential to be applied in algae processing for on-site nutrients and biofuels intermediate recovery. Due to better heat

integration, this will improve the energy utilization during process stages, resulting in final product price reduction. Unlike a recent study by Griffin *et al.*, the HAp precipitated from the algae hydrolysate using FH-HTM pathway conducted at a relatively lower temperature (280 ˚C compare to 350 ˚C), the product was not mixed with any other type of solid compounds. Not to mention that particular method was only applicable for a special microalgal species that has been cultivated in a calcium-rich medium (Roberts et al., 2015). A related point to consider is the one-hour hydrothermal reaction in the current study is in contrast to couple of hours/days (J. Liu et al., 2003; F. Ren, Leng, Ding, & Wang, 2013; Yan, Li, Deng, Zhuang, & Sun, 2001) of residence time.

The objectives of this study are to (1) investigate the feasibility of HAp and MAP precipitation from the phosphate-rich algal hydrolysate through integrated FH-HTM and FH-AP processes, (2) evaluate the effect of seed inoculation on the nutrients removal and precipitates' property and structure in both pathways, (3) determine the effect of temperature, Mg/PO_4 molar ratio, and the reaction time on the phosphate removal in the FH-AP process, (4) characterize all solid and liquid phases in each step including the original *Scenedesmus* sp. microalgae, hydrolysate from FH, phosphate-depleted aqueous phase (after HTM/AP reactions), in addition to the recovered precipitates, (5) assess the structure, morphology, and crystallinity of the precipitates.

4.2. Materials and methods

4.2.1. Microalgae strain and characterization

Scenedesmus sp. microalgae which was cultivated in the biomass research laboratory (BRL) at Old Dominion University using the modified BG-11 in the photobioreactors, was used to for this study. Upon harvesting, algae biomass was freeze

dried and stored in an airtight container at a temperature below –20 ˚C until use. Elemental and proximate analyses in addition to the inorganic elemental composition were performed to fully characterize the algal biomass. Thermo Finnigan Flash EA 1112 elemental analyser (ThermoFisher Scientific, Waltham, MA) was used to determine the C, H, and N content of the freeze dried microalgae. 2,5-bis(5-tert-butyl-benzoxazol-2-yl) thiophene (BBOT) standard (certified number 202147–10/03/2015, ThermoFisher Scientific, Cambridge, UK) was used as a standard. Approximately, 1 mg of solid sample was placed in a 5×9 mm tin capsule (CE Elantech, Inc., Lakewood, NJ) for combustion in a furnace at 950 ˚C. The oven temperature was at 65 ˚C and the flow of the helium carrier gas was 100 mL/min. Each experiment was conducted in triplicate and the reported values are the average (± standard deviations). Inorganic elemental composition was measured using X-ray fluorescence (XRF) spectroscopy (Bruker S4 Pioneer, Bruker Corp., Billerica, MA). In order to determine proximate analysis (including ash, moisture, volatile, fixed carbon), thermogravimetric analyser (TGA) (TGA-50H, Shimadzu Corporation) was used and the method has been explained elsewhere (Roberts et al., 2015). Major elements (C, N, and P) of the initial biomass have been tracked in every stage along the process. Lipid content of the microalgae and the biofuels intermediates were measured gravimetrically, using the Bligh-Dyer method. Soxhlet extraction was carried out for 24 h with 2:1 (v/v) chloroform:methanol solvent, followed by drying and weighing the extracted lipids (Bligh & Dyer, 1959). Phosphate analysis was conducted using concentrated nitric acid-sulfuric acid digestion (House, 2012) followed by the modified ascorbic acid spectrophotometric method using UV–visible spectrophotometer (Varian, Cary 50 Conc) (Bettin, 2013).

4.2.2. Integrated FH-HTM method

In order to extract phosphate and other nutrients from the raw *Scenedesmus* sp. microalgae, 25 runs of FH experiment were conducted, all at 280 ˚C and 10 s of residence time to make sure adequate amount of hydrolysate was collected (Jose Luis Garcia-Moscoso et al., 2013). Detailed description of the FH process on various feedstocks and in different conditions could be found in our previous studies (Barbera et al., 2016; Jose Luis Garcia-Moscoso et al., 2013; Garcia-Moscoso et al., 2015; Sandeep Kumar et al., 2014; Talbot et al., 2016; Teymouri, Kumar, et al., 2017). After each FH run, the dark green solid-liquid mixture of products were separated by a Fisher Scientific accuSpinTM 400 centrifugal device. Biofuels intermediates were then stored for lipid analysis as explained earlier. All collected algae hydrolysate from different runs were filtered, homogenized, and while some were kept in the refrigerator at 2 ˚C for MAP precipitation experiments, the rest was freeze dried to be used for HAp experiments. Shimadzu TOC/TN analyser (TOC-V_{CSN}, Shimadzu) equipped with an ASI-V auto sampler was used to analyse the total organic carbon (TOC) and total nitrogen (TN) content in the hydrolysate before and after each reaction. The hydrolysate mixture was subjected to a digestion step as explained previously, followed by an ascorbic acid spectrophotometer method for the total and dissolved phosphate determination. Ammonia content was measured with high range (0.4-50.0 mg/L NH_3-N) Hach standard kits using salicylate method and Hach DR 2800 spectrophotometer. Atomic absorption spectrophotometry (AA-87000, Shimadzu) and Dionex ICS-5000 AAA-Direct ion chromatography instrument (ThermoFisher Scientific) equipped with the Dionex IonPacTM CS16 column

and a guard column were used to measure the calcium and magnesium content of the hydrolysate before and after the reactions respectively.

Followed by FH, a 27 mL stainless steel reactor designed by HIP Company (High Pressure Equipment Co.) was applied to continue with the HTM process. A thermocouple (P/N: TJ36-CAXL-116G-6, Omega Engineering, Inc.) and a 3000 psi pressure gauge (Omega Engineering, Inc.) were connected through a taper seal cross (P/N: 10-24AF4, High Pressure Equipment Co.) to monitor pressure and temperature. A fluidized sand bath (SBS-4, Techne) connected to a temperature/air flow controller (TC-9D, Techne) was used as the heat source for the reactor. The prime advantage of using a fluidized sand bath is to reduce the preheating time to < 5 min to reach the desired reaction temperature. In order to prepare the reaction media, approximately 5 g of freeze dried hydrolysate were dissolved in 250 mL Milli-Q water. This amount helped in recovering and collecting a sufficient amount of precipitate as a product of HTM. Calcium hydroxide ($Ca(OH)_2$) was added as a mineralizer to achieve a stoichiometric molar ratio of Ca/PO_4 = 1.67 for HAp ($Ca_{10}(PO_4)_6(OH)_2$) precipitation.

All HTM reactions were conducted at 280 ˚C and 1 h of residence time, which excludes preheating and cooling time. It is worth noting that this is the same temperature that the FH hydrolysate is received, which would eliminate the need of additional heating and pressurization. The control experiments were performed to investigate the nutrients removal in the absence of mineralizer. The effect of seed inoculation was also investigated by the addition of 30 mg of pure HAp (hydroxyapatite, reagent grade, Sigma-Aldrich) as seeding material to promote crystallization. Experiments were done in seven replicates in order to collect enough precipitates required for analysis. After each

experiment, the reactor was cooled down to room temperature within 2 min. The samples were centrifuged followed by filtration (0.22 µm mixed cellulose esters membrane, Merck Millipore Ltd.) of supernatant hydrolysate to collect all precipitates. TOC/TN, phosphate and ammonia analysis were done on the hydrolysate before and after each experiment to calculate the nutrients removal. The collected precipitates were freeze dried for storage. These samples were characterized by X-Ray Diffraction (XRD, MiniFlex II Desktop X-Ray Diffractometer, Rigaku Corp.) in the range of 10 to 70º (2θ/θ) with the scan speed of 2 º/min at 30 kV and 15 mA followed by the peak analysis using Rigaku PDXL software (version 1.8.0.3). Elemental analysis was performed as previously explained, to determine the carbon and nitrogen content in the precipitates. Chemical functional groups were analyzed using a Fourier Transform Infrared Spectroscopy (FTIR) (IR Prestige-21, Shimadzu) for 256 scans over a range of 400-4000 cm^{-1} and a resolution of 4 cm^{-1}. Thermal properties of the precipitated powder was also investigated using TGA in an inert atmosphere (30 mL/min) using platinum crucibles in the temperature range of 25–1200 ˚C with 10 ˚C/min temperature ramping and a 4 h temperature hold at 500 ˚C.

4.2.3. Integrated FH-AP method

For This alternative pathway provides opportunity to recover both phosphate and ammonium. These experiments were performed in ambient conditions to form MAP according to Eq. 8 (Doyle & Parsons, 2002):

$$Mg^{2+} + NH_4^{+} + PO_4^{3-} + xH_2O \rightarrow MgNH_4PO_4.x(H_2O) \quad (8)$$

Table 13 shows three different variables and three different levels that were selected in order to investigate the effect of each parameter on the phosphate removal

process. A random set of experimental conditions were designed using Matlab R2014b program (section 4.3.2, Table 16). Results are the average values of the duplicate experiments (± standard deviations).

Table 13. Variables and levels used in the AP process.

Variables	Level 1	Level 2	Level 3
Mg:PO_4 molar ratio	1:1	1.5:1	2:1
Temperature (˚C)	20	30	40
Reaction time (min)	60	120	180

In each experiment, 500 mL of hydrolysate was transferred into a 1 L Erlenmeyer flask with a stirring magnet to agitate with the speed of 350 rpm. Fisher Scientific Isotemp hotplate was used to maintain the desired temperature. During the process, a thermometer (Measurement Specialties 4600) was used to monitor the reaction temperature. Similarly, pH was continuously monitored and set at a value of 9 (by addition of NaOH 1 N) as the optimum conditions for struvite precipitation (Demeestere, Smet, Van Langenhove, & Galbacs, 2001; Doyle & Parsons, 2002; J. Wang, Burken, & Zhang, 2006; G. L. Zang et al., 2012). The molar concentration of the magnesium in the algal hydrolysate is much lower compared to that of phosphate and ammonium (0.28 compare to 1.67 and 1.71 mmol respectively). In order to maintain different magnesium ratios as per Table 13, $MgCl_2$ (reagent grade, Fischer Scientific) was added. Pure struvite (Alfa Aesar) were used in order to evaluate the effect of seed inoculation (D. Kim et al., 2007). After each reaction, the hydrolysate containing the precipitates was vacuum

filtered using Whatman 47 mm glass microfiber filters and the separated solids were oven dried at 45 ˚C. The obtained powder was characterized by means of EA, XRD, FTIR, and TGA. Figure 20 demonstrates the overall process pathways and product analyses methods used in this study.

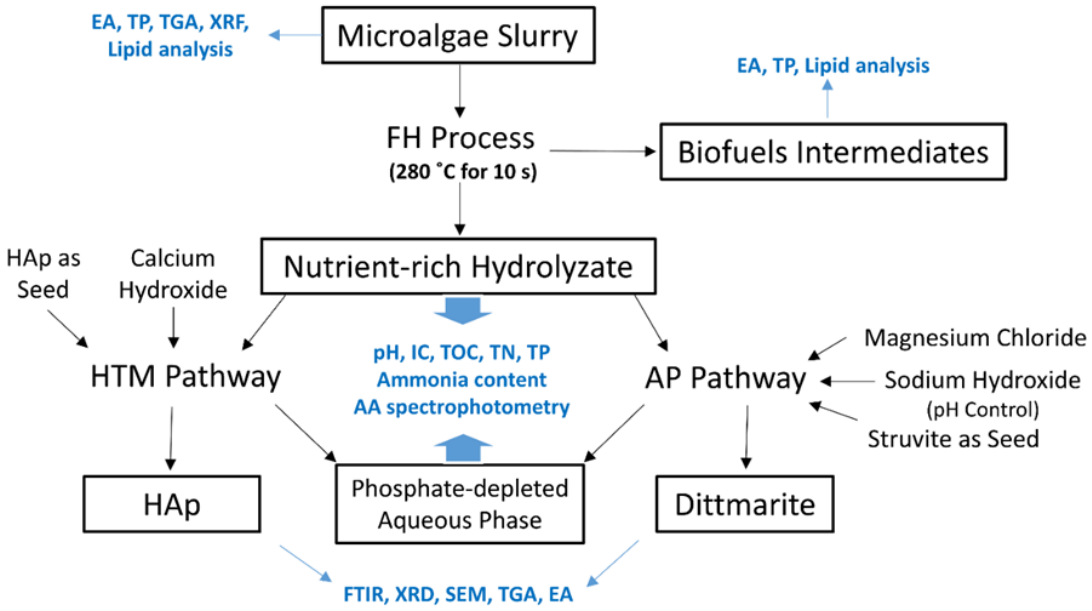

Figure 20. Schematic diagram of the phosphate recovery pathways (black) and products analyses (blue). All analyses were performed in duplicate unless otherwise stated.

4.3. Results and discussion

The ultimate and proximate analysis of the algal biomass is summarized in Table 14. The proximate analysis is a measure of the ash and moisture content of the algal biomass. The elemental composition of the organic fraction of a biomass including carbon, nitrogen, hydrogen, and oxygen (by difference) is measured through ultimate analysis (Biller et al., 2012b). Magnesium and calcium content of the *Scenedesmus* sp. microalgae measures as 0.1 ± 0.0 and 1.8 ± 0.1 respectively.

Table 14. *Scenedesmus* sp. microalgae ultimate and proximate analysis. Ultimate analysis is provided on an ash free dry weight percent. *Oxygen and others' percentage was calculated based on the difference (C + H + N + O + others = 100).

Ultimate Analysis	wt% (± Standard Deviation)[1]	Proximate Analysis	wt% (± Standard Deviation)[2]
Carbon	49.1 ± 0.3	Fixed Carbon	12.2 ± 0.2
Nitrogen	7.3 ± 0.1	Volatile	68.1 ± 0.1
Hydrogen	7.1 ± 0.1	Moisture	6.5 ± 0.3
Oxygen and Others*	36.5	Ash	13.2 ± 0.1
Total	100 ± 0.5	Total	100 ± 0.7

[1] Ultimate analysis values are the average of triplicate experiments.
[2] Proximate analysis values are the average of duplicate experiments.

The lipids content of the harvested microalgae was 16.1 ± 0.3 wt% (values are dry basis and the average of duplicate experiments ± standard deviations) which is comparable to literature data (Jose Luis Garcia-Moscoso et al., 2013; J.-Y. Lee et al., 2010). However, this number raised to 42.7 ± 0.7 wt% in the biofuels intermediates after being subjected to the FH process which is again in agreement with our previous study (Teymouri, Kumar, et al., 2017). This increase in the lipid content in addition to ash diminution and nitrogen content reduction has made these energy-rich biofuels intermediates an attractive feedstock for fuel production. Extensive analysis in this regard could be found in our previous studies (Jose Luis Garcia-Moscoso et al., 2013; Garcia-Moscoso et al., 2015).

4.3.1. HTM pathway

As stated earlier, a control experiment was done under the same reaction conditions as the HTM experiment (in duplicate) in the absence of the mineralizer (calcium hydroxide) as the baseline correction for the nutrients removal. No significant phosphorus and nitrogen removal were observed. However, the ammonium concentration increased from 37.9 ± 0.6 to 117.6 ± 4.1 mg/L ($\geq$ 3 times increase) which might be due to the decomposition of organic nitrogen compounds (e.g. soluble peptides and amino acids) in the algal hydrolysate to ammonia under HTM conditions (Saqib Sohail Toor, Rosendahl, & Rudolf, 2011). Negligible amount of precipitates were observed on the surface of 0.45 μm filter, which might be as a result of the reactions between organic molecules with hydroxyl, aldehyde, and carboxyl groups and also among each other through aldol condensation or esterification (G. Yu, Zhang, Schideman, Funk, & Wang, 2011). Results from TOC analysis demonstrated 20.9 ± 1.6 wt% reduction in the total carbon content, which could be attributed to the decarboxylation of organic carbon to carbon dioxide (CO_2) under HTM conditions (G. Yu et al., 2011).

Table 15 shows the results of the experiments conducted with and without seed inoculation and weight percentage of nutrients removal from the algal hydrolysate. It has been reported that seeding has promoted crystallization as well as increasing the crystalline particles sizes (H. Jang & Kang, 2002). Materials that have similar properties to the precipitates, are more effective seed crystals (H. Jang & Kang, 2002). However, the amount of seeding material does not have significant effect on the crystal growth rates (Koutsopoulos & Dalas, 2000). Both calcium and phosphate removal is slightly higher in the experiment implemented in the absence of seed inoculation; however, the XRD,

FTIR, and TGA analysis revealed that the composition of precipitates is different which is discussed later.

Table 15. The effect of seed on the nutrients removal in the algal hydrolysate at 280 ˚C and 1 h of reaction time (results are the average of duplicate experiments ± standard deviations).

	pH		**Nutrients Removal (wt%)**			
	Initial	Final	Carbon	Nitrogen	Phosphate	Calcium*
Experiment without seed inoculation	5.6	7.8	26.1 ± 1.1	6.2 ± 2.5	98.9 ± 0.3	92.3 ± 0.5
Experiment with seed inoculation	5.6	7.4	32.3 ± 2.6	9.1 ± 1.0	97.0 ± 0.4	85.8 ± 1.4

*Including external calcium source addition.

4.3.1.1. HAp characterization

Synthetic hydroxyapatite production covers a wide range of temperatures depending on the production methods (mechanical, hydrothermal, sol-gel, wet precipitation, phase transition, biomimetic deposition, and electro-deposition) (Mehdi Sadat-Shojai et al., 2013), pH of 8–12, and yields particle sizes from 15 nm to 2 μm (Mossaad et al., 2010). Among all available methods, hydrothermal synthesis of hydroxyapatite has gained high interest due to the ability to transform the HAp characteristics by raising the temperature (Mossaad et al., 2010; M. Sadat-Shojai, 2009; Mehdi Sadat-Shojai et al., 2013; Mehdi Sadat-Shojai, Khorasani, & Jamshidi, 2012). The process conditions of HTM are favorable for its integration to FH, since the algal hydrolysate from FH results in a hot, compressed liquid which can be directly fed into the HTM process. Figure 21 presented the results from the XRD analysis of the precipitated material as well as commercial HAp for comparison. Powder from the experiment

without any seed inoculation corresponds to whitlockite (WH, $Ca_{18}Mg_2(HPO_4)_2(PO_4)_{12}$) (DB-card# 01-070-2064, ICSD# 6190). Although, WH is the second major component of hard tissue after HAp, its formation mechanism and its contribution to our body is still not clear due to production of intermediate phases that usually transform to HAp in the pH between 7 and 8 as the most stable calcium phosphate crystal thermodynamically (H. L. Jang et al., 2014; Koutsoukos et al., 1980). It has also been reported that the presence of magnesium inhibits the formation of apatite to the benefit of WH formation (Lagier & Baud, 2003). Microalgae contain magnesium as the central atom of chlorophyll (Jeffrey & Wright, 1987; Küpper, Küpper, & Spiller, 1996) which most of it was extracted in the hydrolysate (Teymouri, Kumar, et al., 2017). Furthermore, in the pH range of reaction for the algal hydrolysate (Table 15), HPO_4^{2-} is the predominant phosphate species in the aqueous solution, which made the condition in favor of WH (Oladoja, Ololade, Adesina, Adelagun, & Sani, 2013). Jang *et al.* reported that WH and tricalcium phosphate (TCP) are closely related and many researchers have been using them interchangeably (H. L. Jang et al., 2014). Although the precipitates have been identified (XRD data) as single WH phase; in order to address the issue, the corresponding peaks in terms of intensity and position from the XRD pattern, were compared to pure standard TCP (Sigma-Aldrich, P/N= 900205). Thus, the possibility for TCP excluded. On the other hand, results originated from the experiment inoculating pure HAp as seeding material, identified HAp (DB-card# 01-076-0694, ICSD# 34457) as the main phase in the precipitates, while only a few peaks corresponded to WH, suggesting its presence as the secondary phase.

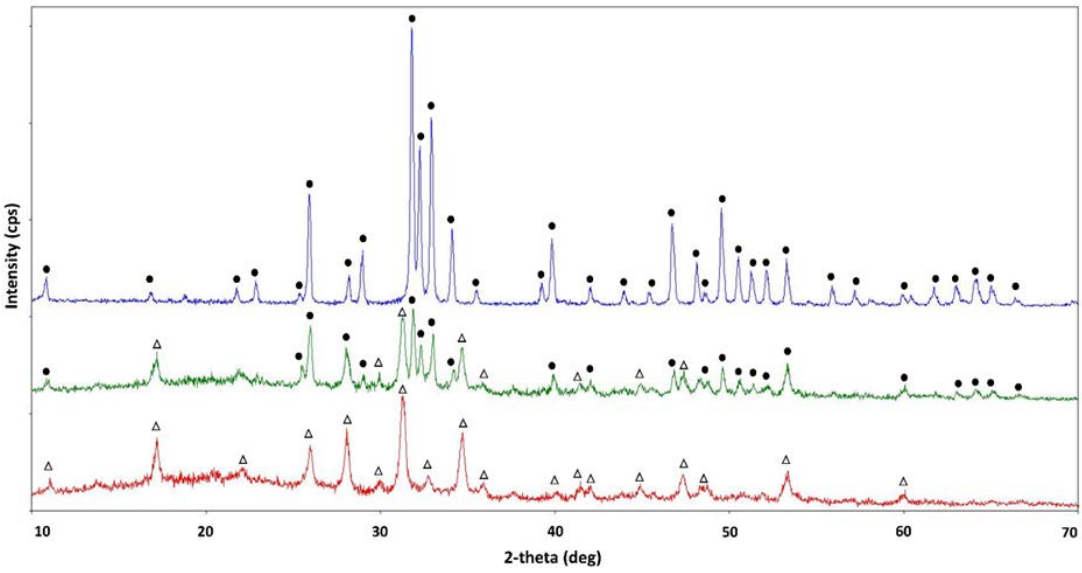

Figure 21. X-ray diffraction patterns for pure HAp (blue), precipitates in the presence (green) and absence (red) of seeding material. Peaks with triangle corresponds to WH and peaks with circles corresponds to HAp.

There are studies that highlighted the significant role of seeding material to promote crystallization by reducing reaction time (induction time), increasing mechanical strength, and producing larger crystals in different substances as well as HAp (Grover, Kim, & Ryall, 2002; D. Kim et al., 2007; Nancollas & Mohan, 1970; Tsuru, Ruslin, Maruta, Matsuya, & Ishikawa, 2015; J. Wang et al., 2006). Nancollas *et al.* reported that macroscopic amounts of HAp could be crystallized on the HAp seeds without the formation of any intermediate phases (Koutsoukos et al., 1980). Therefore, by the addition of seed crystals to the solution, the prolonged primary nuclei stage was eliminated and direct crystal growth occurred. In other words, the phase transformation proceeds without the induction period, resulting in much lower reaction time (Boskey & Posner, 1973). However, crystal growth was not the only precipitation pathway and small amounts of new nuclei formed as well (Boskey & Posner, 1973). This will significantly

increase the recovery rate of HAp production compared to the prior studies that synthesized HAp in hydrothermal conditions in 3–120 h of residence time (Mehdi Sadat-Shojai et al., 2013). Not to mention, they have all reported HAp production from pure chemicals rather than any actual phosphate-rich media such as algal hydrolysate.(Mehdi Sadat-Shojai et al., 2013)

In order to further confirm the results from XRD analysis on the precipitates, FTIR was performed on both the powder as recovered and their ashes (Figure 22) after combustion at 575 ˚C overnight to remove all organic carry-overs on the precipitates. Generally, no phase change from HAp to other calcium phosphate minerals occurs in the aforementioned combustion temperature (Gibson, Rehman, Best, & Bonfield*, 2000). The precipitates revealed recognizable absorption bands for HAp. As expected in the FTIR absorption spectrum, all peaks originated from the organic carry-over of the algal hydrolysate such as 1557 cm^{-1} (C-O), 2868, 2928, and 2959 cm^{-1} (C-H), were disappeared in their related ashes. Peaks observed at 548 and 602 cm^{-1}, 961 cm^{-1}, and 1013 cm^{-1} are due to PO_4^{3-} ν_4, ν_1, and ν_3 vibrations and are presented in both powder (with and without seed inoculation) and their ashes as well. The peak observed at 1082 cm^{-1} in the ash from precipitates in the presence of seed, matches the peak originated from the PO_4^{3-} ν_3 in the pure hydroxyapatite. However, there is a slight shift in the same peak position (1064 cm^{-1}) for the ash from the precipitates without any seeding material. Peaks revealed at 1418 and 1447 cm^{-1}, indicate the presence of CO_3^{2-} in the lattice. This confirms the formation of non-stoichiometric B-type (PO_4) carbonate substituted HAp (Roberts et al., 2015; Shu, Yanwei, Hong, Zhengzheng, & Kangde, 2005). Both anionic and cationic substitution is possible due to HAp general structure and has been reported

to improve its applications as biomaterials (Roberts et al., 2015). The absorption at 872 could have been as a result of HPO_4^{2-} in the powder (Destainville, Champion, Bernache-Assollant, & Laborde, 2003). The absorption taking place at 854 cm^{-1} is due to the P-OH stretching which might be an indicator of the presence of WH (Eilliot, 1994). This peak has been used previously to distinguish between WH and TCP since their XRD pattern also very similar (H. L. Jang et al., 2014). The peak presented at 631 cm^{-1} and in the range of 3500-3800 cm^{-1}, proved the presence of water in the HAp lattice, but there are no such peaks in the spectrum of TCP (Destainville et al., 2003; Theophanides, 2012).

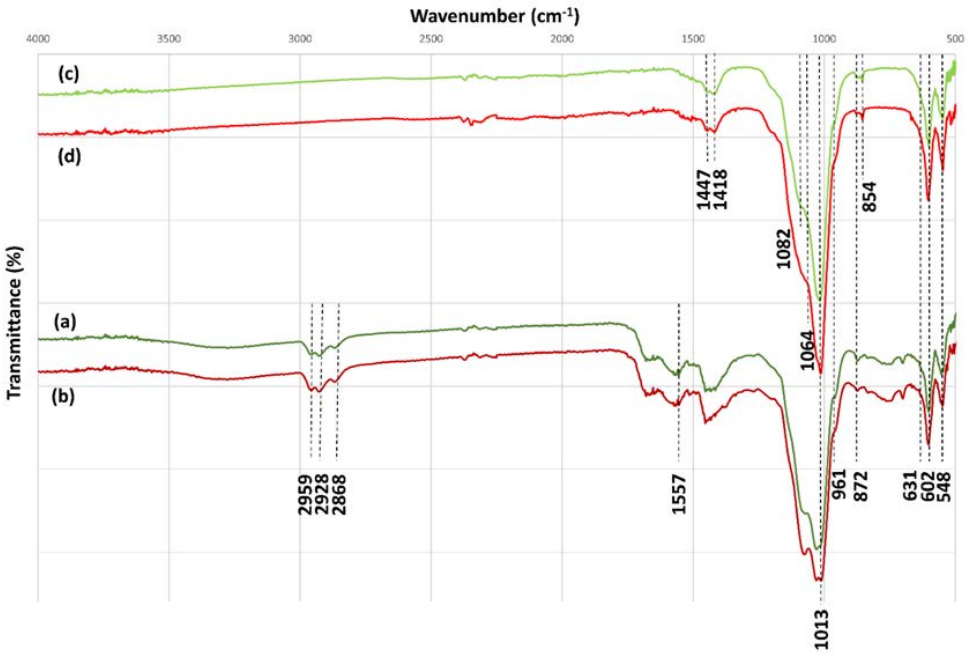

Figure 22. FTIR Spectrum of precipitates with (a) and without (b) seed inoculation and their corresponding ashes (c) and (d) respectively.

The results from the TGA are shown in Figure 23. The percentage weight loss in the range of 350-500 ˚C corresponds to water desorption in the lattice (Diallo-Garcia et al., 2011) followed by organic losses. The significant weight reduction illustrated at 500 ˚C (vertical line) is due to the 2-hour exposure of the powder at that temperature for

complete organic matter removal. There was not any other significant weight loss in the sample precipitated with seed inoculation, which follows a similar pattern in the pure HAp. There are two additional minor weight losses around 800 ˚C and 1150 ˚C in precipitates without seeding material which is mostly originated from dehydration of the internal WH structure ($HPO_4^{2-} \leftrightarrow P_2O_7^{4-} + H_2O$) (Diallo-Garcia et al., 2011; Gopal, Calvo, Ito, & Sabine, 1974; H. L. Jang et al., 2014).

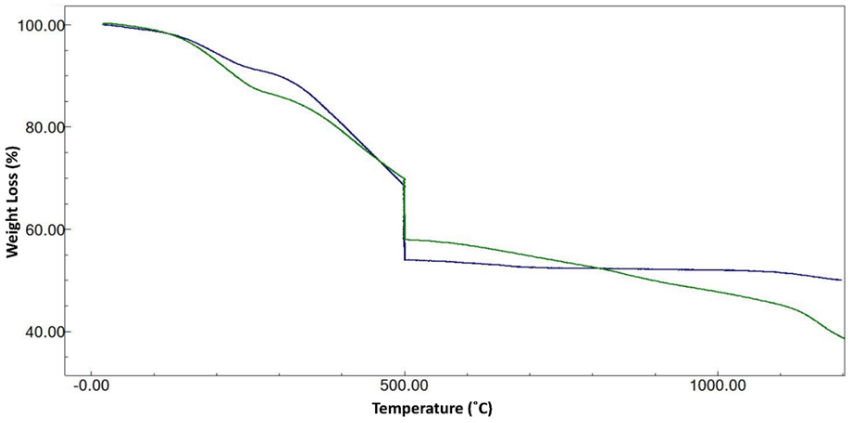

Figure 23. TGA analysis on the hydroxyapatite precipitates in the presence (blue line) and absence (green line) of seed.

The morphology of the combusted precipitates in addition to the commercial HAp seed are presented in the Figure 24. As observed, precipitation in the absence of seeds (Figure 24c), resulted in irregularly shaped particles, while, in the reaction in the presence of seeding material (Figure 24b), larger particles were collected with the same spherical shape as the initial seeds. Although, there are still small irregular particles which might be due to the new nuclei formation. Application of seeding material could help in controlling the morphology and size of the particles (Mehdi Sadat-Shojai et al., 2013).

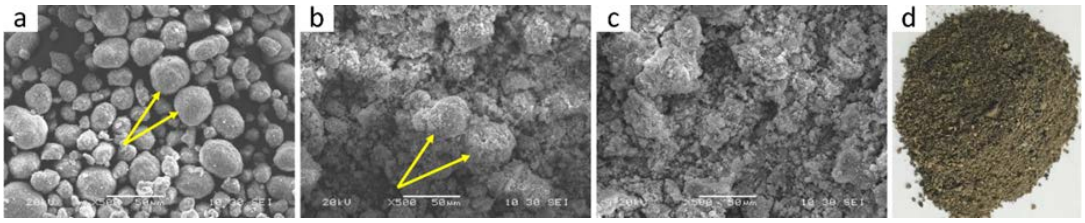

Figure 24. SEM analysis of (a) seeding material (pure HAp), (b) powder precipitated in the presence of seed, (c) powder precipitated without seed, and (d) actual substituted-HAp precipitate. Arrows pointed out the similar spherical morphologies.

4.3.2. AP pathway

In order to investigate the need of seed inoculation in MAP precipitation, one of the designed experimental conditions (20 ˚C, Mg/PO_4 molar ratio of 2, and 1 h of reaction time) were selected and the effect of seeding material on nutrients removal as well as precipitates were evaluated. Analysis on the hydrolysate for the experiments performed without seed, showed a phosphate and ammonium removal of 65.3 ± 0.1 wt% and 39.0 ± 1.2 wt% (compare with 65.9 ± 0.9 wt% and 29.0 ± 3.2 wt%), respectively. However, their XRD spectra were totally different which is in agreement with the literature. A recent study on the effect of various seeding materials such as quartz, granite, and pure struvite on the struvite precipitation, stated that pure struvite not only significantly increased the phosphate removal, but also improved the settling characteristics of precipitates by producing larger particles which is a favorable parameter in the industry (J. Wang et al., 2006). Kim *et al.* also reported that the addition of pre-formed struvite, enhanced the phosphate and ammonium removal by increasing the crystal growth mechanism rather than the crystal nucleation (D. Kim et al., 2007). This resulted in the reduction of the induction time (time needed for nucleation occurrence). Therefore, the MAP precipitation process in this study was performed using pure struvite

as seeding material (D. Kim et al., 2007; J. Wang et al., 2006). MAP can precipitate in a wide range of pH (7.0–11.5) (R. Kumar & Pal, 2015; Md Mukhlesur Rahman et al., 2014). The optimum pH has been reported as 9 where it shows its lowest solubility in the reaction medium.(Demeestere et al., 2001; J. Wang et al., 2006; G. L. Zang et al., 2012) Mg^{2+}:NH_4^+:PO_4^{3-} molar ratio is another factor that directly affects the precipitation process. Although, various ratios such as 1:1:1, 1.5:1:1, 1:1.3:1, 1.6:1:1, 1.2:3:1, and 1:2:1 have been used (R. Kumar & Pal, 2015; Md Mukhlesur Rahman et al., 2014), many researchers have preferred the stoichiometry molar ratio of 1:1:1, which is the most favorable condition in industrial-scale studies when operational cost due to chemical consumption must be reduced. Temperature and pH increase has been reported to reduce the induction time in the precipitation process (Abbona, Lundager Madsen, & Boistelle, 1982); however, there is a steady increase in its solubility with temperature until 50 ˚C. Above 64 ˚C the structure of MAP crystals change (Doyle & Parsons, 2002), therefore in the majority of studies, room temperature was preferred, which is in agreement with our study (Bouropoulos & Koutsoukos, 2000; Kofina & Koutsoukos, 2005; G. L. Zang et al., 2012). The effect of parameters (Mg/PO_4 molar ratio, temperature, and reaction time) on the phosphate removal was plotted in the Figure 25. All results are based on the average values of duplicate experiments (Table 16).

Table 16. Phosphate removal (wt%) in the all performed experiments at various conditions (results are the average of duplicate experiments ± standard deviations).

Run	Mg/PO_4 Molar Ratio	Temperature, ˚C	Reaction time, min	Phosphate Removal, wt%
1	1.5:1	40 ˚C	120	25.0 ± 0.6
2	1.5:1	40 ˚C	60	32.0 ± 0.6

3	1:1	40 ˚C	120	27.6 ± 0.9
4	2:1	40 ˚C	180	47.3 ± 1.1
5	1:1	40 ˚C	60	14.9 ± 3.2
6	2:1	20 ˚C	120	67.1 ± 0.1
7	1.5:1	20 ˚C	120	63.6 ± 0.3
8	1.5:1	20 ˚C	180	57.1 ± 0.2
9	1.5:1	20 ˚C	60	42.3 ± 1.6
10	2:1	20 ˚C	60	65.8 ± 0.9
11	1:1	20 ˚C	180	53.7 ± 0.8
12	2:1	20 ˚C	180	57.3 ± 4.1
13	1:1	30 ˚C	180	43.1 ± 0.1
14	1:1	30 ˚C	60	31.7 ± 0.6
15	2:1	30 ˚C	120	52.1 ± 0.1
16	1.5:1	30 ˚C	180	42.6 ± 0.9
17	2:1	30 ˚C	180	60.6 ± 3.3
18	1:1	30 ˚C	120	30.5 ± 0.5
19	1.5:1	30 ˚C	60	47.2 ± 0.1
20	2:1	30 ˚C	60	58.0 ± 0.1

Among all selected conditions in Table 16, the most phosphate removal occurred for run 6 and 10 at 20 ˚C and Mg/PO_4 molar ratio of 2, in the range of 65.8–67.1 wt%. A control experiment with no magnesium chloride addition was conducted at the same condition of run 6 (Table 16). It demonstrated almost no phosphate removal validating the role of the mineralizer for the phosphate removal via MAP formation. Nonetheless, there are several other magnesium compounds other than magnesium chloride (e.g. magnesium hydroxide, brine, seawater, magnesite, magnesia) that could be used for MAP precipitation; however, evaluating the effect of each mineralizer on the overall nutrients removal as well as precipitates' characteristics is beyond the scope of this study (Doyle &

Parsons, 2002; Gunay, Karadag, Tosun, & Ozturk, 2008; B. Liu et al., 2013; Prabhu & Mutnuri, 2014).

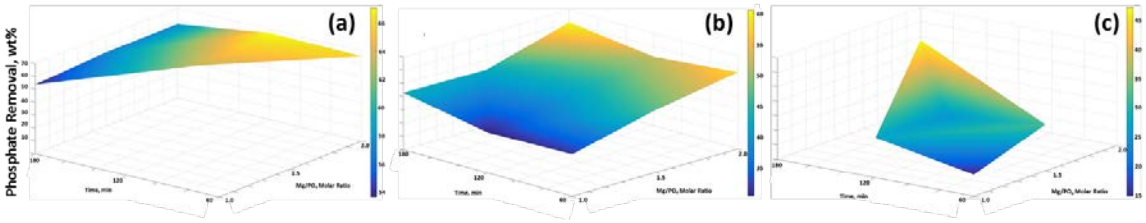

Figure 25. The effect of Mg/PO4 molar ratio and retention time at (a) 20 ˚C, (b) 30 ˚C, and (c) 40 ˚C on the phosphate removal in the algal hydrolysate. Statistical data has been provided in the Table 16.

4.3.2.1. Dittmarite characterization

Although in experiments performed with and without seed inoculation, phosphate removal in the hydrolysate was similar, the precipitated material had different characteristics as per the XRD spectra. In fact, no individual peak was detected for the precipitates obtained from the experiments conducted without seeding material suggesting the possibility for precipitation of the amorphous magnesium phosphate (AMP) (Crutchik & Garrido, 2011). On the other hand, precipitates from the experiments inoculating with seed material, no matter of their reaction conditions, revealed to be the monohydrate form of MAP known as dittmarite ($MgNH_4PO_4 \cdot H_2O$) (DB-card# 00-036-1491). Dittmarite is much more stable than the hexahydrate (struvite) form (having decomposition temperature around 220 ˚C) and its ammonium losses is negligible, in contrast with the hexahydrate which occur even at 35 ˚C (Bhuiyan et al., 2008; Bridger, Salutsky, & Starostka, 1962). Phosphorus content in dittmarite is higher than struvite (compare 19.9 wt% with 9.8 wt%), makes it more favorable as a slow-release fertilizer

(Bhuiyan et al., 2008). However, in ambient temperature and high moisture environment, it hydrates to the hexahydrate MAP (struvite).

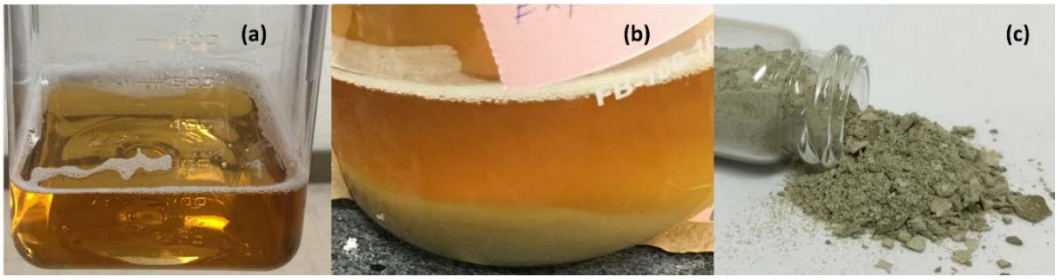

Figure 26. (a) Algal hydrolysate from FH (b) after the precipitation process (c) dry dittmarite precipitates.

Figure 27 compares the XRD patterns of pure struvite, precipitated dittmarite, and the amorphous powder at the run 6 conditions. The images of fresh algal hydrolysate before and after reaction and dittmarite precipitates are also displayed in the Figure 26.

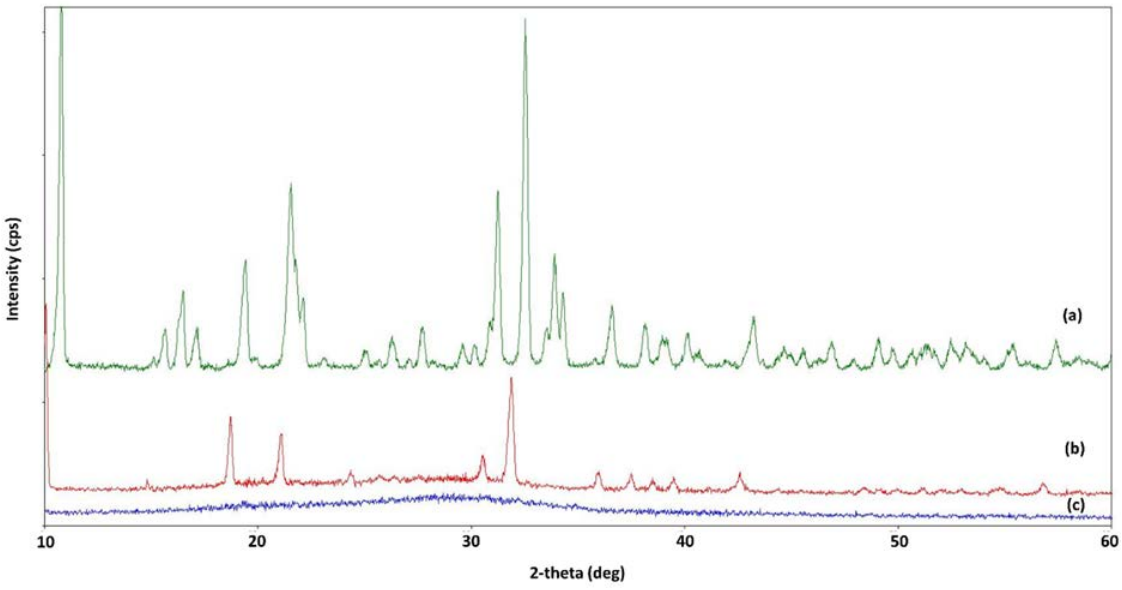

Figure 27. X-ray diffraction patterns for (a) pure MAP, (b) precipitated dittmarite in the presence of seeding material for run 6, and (c) the amorphous precipitates.

Figure 28 compares the FTIR spectra of the pure struvite, precipitated dittmarite, and the amorphous powder (without seeding). Peaks observed at 3415.9 cm^{-1} are due to the O-H and N-H stretching vibrations (presence of water of hydration). Peaks at 1651 cm^{-1} appeared as a result of bending H_2O vibrations. Absorption occurring at 1467.8, 1427.3, and 1103.3 cm^{-1} are caused by N-H bending vibrations in the NH_4^+ unit. Peaks at 1051.2, 968.3, 949, and 567 cm^{-1} originate from the ionic phosphate vibrations. The absorption taking place at 758 cm^{-1} is because of the N-H bond. Finally, the Mg-O bond resulted in the peak at 630.7 cm^{-1} (Chetankumar Kanubhai Chauhan, 2012; Chetan K Chauhan, Joseph, Parekh, & Joshi, 2008; Jueshi, Zhongyuan, Qian, & Qiulin, 2012). As illustrated by the FTIR spectrum, all major peaks in the pure struvite (as standard) also appeared in the precipitated dittmarite; however, there are few obvious differences in the spectrum of the amorphous powder such as missing peaks related to the NH_4^+ unit, suggesting the precipitation of the AMP (C. Qi, Zhu, Lu, Wu, & Chen, 2015).

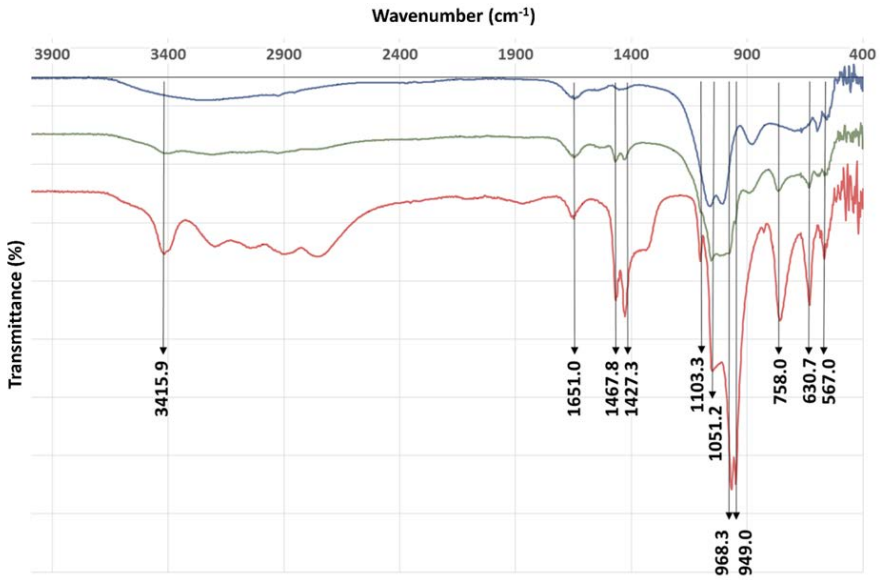

Figure 28. FTIR spectra of the pure struvite (red), precipitated dittmarite (green), and AMP precipitates.

Thermal properties of precipitates are demonstrated in the Figure 29. As expected, there was a significant weight loss in pure struvite compared to dittmarite due to the water of hydration. It has been confirmed here that dittmarite is more stable than both struvite and AMP and it decomposes around 220 ˚C which agrees with other studies (Bhuiyan et al., 2008; Md Mukhlesur Rahman et al., 2014). However, compared to pure struvite, there are some weight losses in the range of 300-500 ˚C for the precipitated powders mostly due to organic contents. Elemental analysis showed the presence of carbon and nitrogen as 7.5 ± 0.5 and 3.9 ± 0.2 wt% for precipitated dittmarite and 9.1 ± 0.2 and 1.7 ± 0.0 wt% for precipitated AMP respectively.

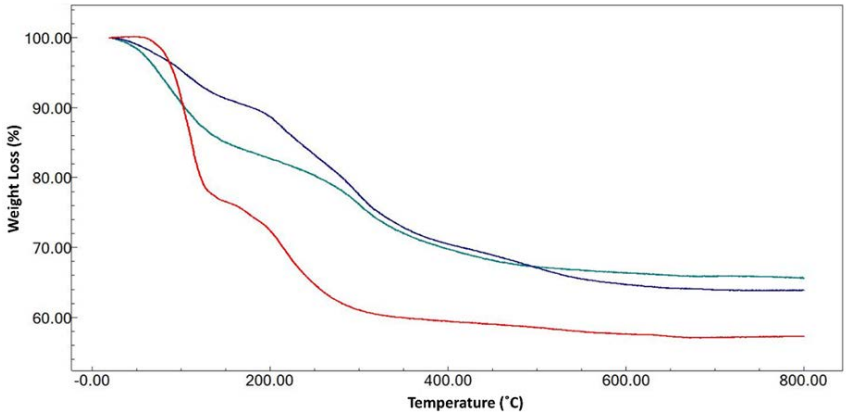

Figure 29. TGA analysis of dittmarite (blue), AMP precipitates (green), and pure struvite (red).

In order to appraise the morphology of the precipitates, SEM analysis was conducted on the pure struvite that inoculated as seed, dittmarite, and amorphous powder (Figure 30). It is obvious from the images, dittmarite particles precipitated in the presence of seed (pure struvite) has very similar morphology as the seed (plate/flake shape). The other precipitate (AMP) is a much smaller needle-like particle which is as an indicator of the nucleation stage rather than crystal growth.

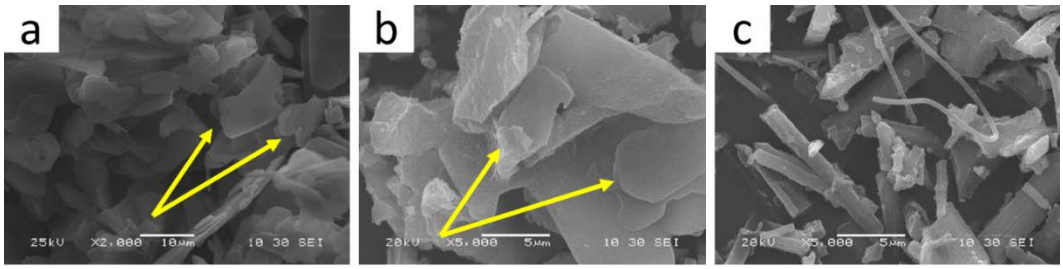

Figure 30. SEM analysis of (a) pure struvite (seeding material), (b) precipitated dittmarite, and (c) the amorphous powder. Arrows pointed out the similar flake shape morphologies.

To understand and compare the overall material balance of the integrated FH-HTM/AP processes, the C, N, & P elemental balance has been demonstrated in the Figure 31. The carbon and nitrogen content of the freeze dried microalgae feedstock are based on the ultimate analysis provided in the Table 14. As indicated, almost 80 wt% of the initial phosphorus in the algal biomass could be recovered as substituted-HAp, a valuable product, via FH-HTM integrated process, while approximately, 55.1 wt% of phosphorus and 3.7 wt% of nitrogen presented in the initial biomass, has been recovered as dittmarite through FH-AP pathway.

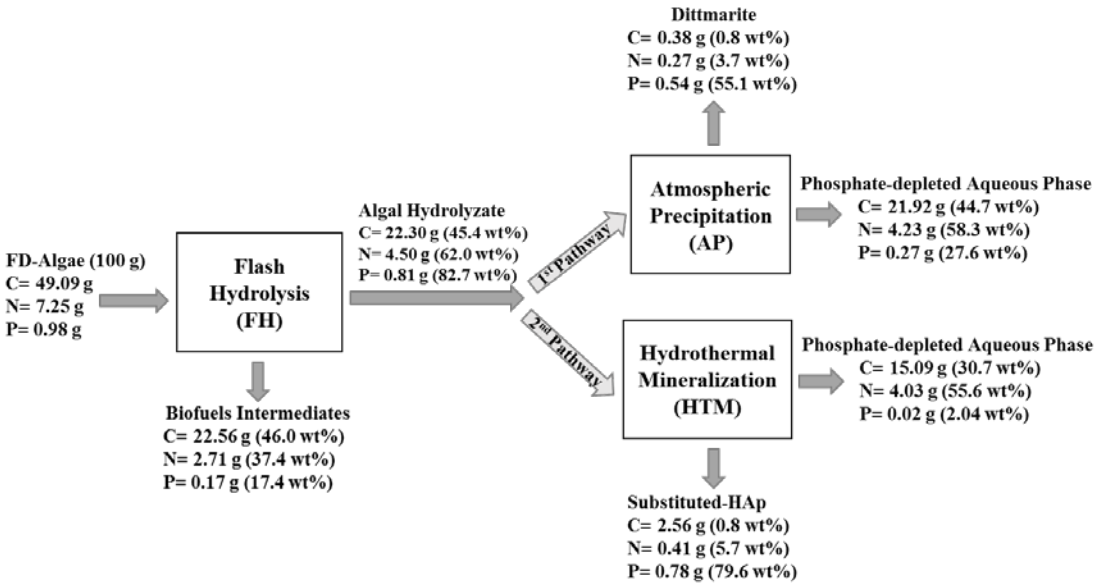

Figure 31. Overall C, N, & P elemental balance for the integrated FH-AP (1st pathway) and FH-HTM (2nd pathway) processes. Presented data are based on the actual experimental results and the unaccounted materials could be attributed to the processing loss and gasification. Weight percentages (wt%) for each element are based on the original freeze dried (FD) Scenedesmus sp. microalgae.

Based on the results of FH-HTM and FH-AP, it seems that it would be a viable option to integrate the entire process as shown in Figure 32 for algae to biofuels and bioproducts approach. It can be an on-site/on-farm process where almost 100% of algae components and water are utilized sustainably using a subcritical water-based green process. Another benefit of this innovative combined pathway is the potential to take advantage of HTM process in the favor of dittmarite production. As a result of HTM process, the concentration of ammonium in the aqueous phase will increase by a factor of 3. This will increase the productivity of dittmarite in the following AP process. This robust approach can be applicable to other phosphate-rich aqueous phase such as hydrothermal liquefaction's aqueous phase or any other wastewater streams (industrial,

swine, dairy, etc.) and will address the current nutrients management obstacles involved in all these processes. Introducing these products to the market, will remove several significant barriers to the economic viability of the microalgae-to-fuel industrialization.

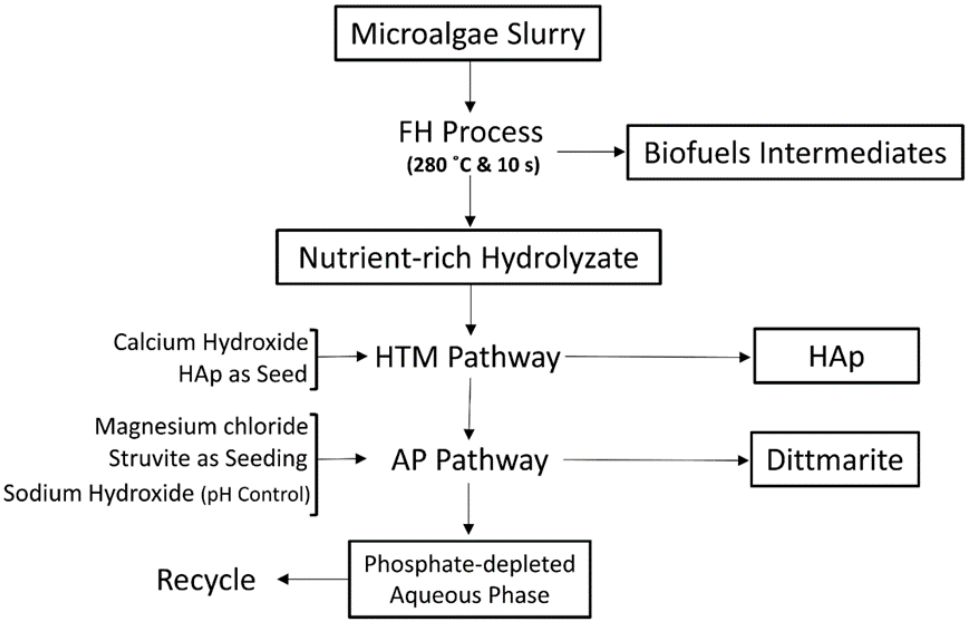

Figure 32. Schematic diagram of the proposed integrated FH-HTM-AP process.

4.4. Conclusions

In this study, two pathways were successfully applied to *Scenedesmus* sp. microalgae to recover phosphorus in forms of value added bioproducts. Spherical shaped carbonated hydroxyapatite precipitated through the integrated flash hydrolysis-hydrothermal mineralization (FH-HTM) process. The rapid mineralization (1 h vs. 3-120 h of previous studies) of phosphate with high yield (up to 80 wt% of the phosphorus present in microalgae) were achieved in this study. In another pathway, flake shaped dittmarite was recovered via atmospheric precipitation (FH-AP) process of algae

hydrolysate. The presence of seeding material played a crucial role in precipitates' composition and crystallinity in both pathways. These approaches could bring a promising solution for nutrients management in algae cultivation and production of value added bioproducts (HAp and dittmarite) while, simultaneously, enhancing the quality of biofuels intermediates as a feedstock in terms of ash diminution, nitrogen reduction, and lipid accumulation.

4.5. Acknowledgements

The authors would like to acknowledge the National Science Foundation (NSF) for the financial support of this study through the NSF CAREER Award #CBET-1351413, Dr. Wei Cao at Old Dominion University's Applied Research Center (Newport News, VA) for his assistance in the XRD and SEM analysis, Dr. Tarek Abdel-Fattah for the assistance in the XRF analysis, and Dr. Elena Barbera for her assistance in the MAP experiments.

CHAPTER 5

EFFECT OF REACTION TIME ON PHOSPHATE MINERALIZATION FROM MICROALGAE HYDROLYSATE

Note: The contents of this chapter have been published in the ACS Sustainable Chemistry & Engineering journal.

Teymouri, A., Stuart, B. J., & Kumar, S. (2017). Effect of Reaction Time on Phosphate Mineralization from Microalgae Hydrolysate. ACS Sustainable Chemistry & Engineering. doi:10.1021/acssuschemeng.7b02951.

The development of algal biorefineries is strongly associated with the nutrient management, particularly phosphorus, which is a limited mineral resource. Flash hydrolysis (FH) has been widely applied to a variety of algae species to fractionate its constituents. This chemical-free, subcritical water technique was used to extract more than 80 wt% of phosphorus available in the *Scenedesmus* sp. as water-soluble phosphates in the aqueous phase (hydrolysate). The phosphate-rich hydrolysate was subjected to the hydrothermal mineralization (HTM) process at 280 ˚C and 5–90 min of residence time to mineralize phosphates as allotropes of calcium phosphate such as hydroxyapatite (HAp) and whitlockite (WH). In the current study, the effect of reaction time on phosphate mineralization from the hydrolysate as well as the composition, structure and the morphology of the precipitates were studied. Calcium hydroxide and commercial HAp were used as the mineralizer and seeding material, respectively. More than 97 wt% of phosphate and almost 94 wt% of calcium were removed in the first 5 min of the HTM

process. Results revealed that as the HTM reaction time increased, calcium phosphate precipitates transformed from WH to carbonated HAp. The integration of the proposed mineralization process with FH can be a cost-effective pathway to produce sustainable, and high value phosphate-based bioproducts from algae. The application of HAp includes biomedical applications such as synthetic bone and implant filling, drug delivery, chromatography, corrosion resistance materials, catalytic activities and fertilizers.

5.1. Introduction

The US Department of Energy (DOE) has set up a target production of 60 billion gallons per year (BGY) of biofuels, which is equal to 30% of the US transportation fuels by 2030. Microalgae is a promising feedstock for the biofuels and bioproducts production. Numerous studies have been conducted to commercialize the process; however, due to a number of technical challenges such as microalgae species selection, large-scale productivity potential, resource availability, cultivation, harvesting, and chosen oil extraction technique, the development is far behind in industrial production.(Quinn & Davis, 2015; Su et al., 2017) Techno-economic analysis (TEA) and life cycle assessment (LCA) have pointed out considerable amount of costs associated with the nutrient (N & P) supply and recommends the production of value-added bioproducts to enhance the sustainability and cost-effectiveness of the overall process.(Shurtz, Wood, & Quinn, 2017) In addition to cost, availability of nutrients, particularly phosphorus, which is derived from an irreplaceable resource, has always been a major concern. A recent study by Shurtz *et al.* highlighted the 3.85 and 0.87 million metric tons (Mmt) of nitrogen and phosphorus requirement respectively, for the 10 BGY of renewable fuel production.(Shurtz et al., 2017) This amount is significant

comparing to the total 7.71 Mmt phosphate (P_2O_5) rock production in the US in 2015.(Jasinski, 2015) This will substantially affect the fertilizer market which may result in food cost increase. Furthermore, from the bioenergy point of view, phosphorus is toxic for automotive exhaust catalyst.(Zhang et al., 2016) Therefore, seeking a comprehensive method that could recover phosphorus content of microalgae in form of byproducts could facilitate the algal processing industry.

Flash hydrolysis (FH) has been widely applied as an environmentally benign process that capitalizes on the difference in reaction kinetics of algae components to extract nutrients in the aqueous phase (hydrolysate), while retaining the lipids in the solid phase known as biofuels intermediates. A variety of microalgae feedstocks have been tested through FH technique to extract nutrients.(Barbera et al., 2016; Barbera et al., 2017; Jose Luis Garcia-Moscoso et al., 2013; Garcia-Moscoso et al., 2015; Sandeep Kumar et al., 2014; Talbot et al., 2016; Teymouri, Kumar, et al., 2017) It has been shown that 280 ˚C and 10 s of residence time is the optimum condition regarding nutrients extraction efficiency.(Garcia-Moscoso et al., 2015) Applying this technique to *Scenedesmus* sp. slurry resulted in more than 80 wt% of phosphorus and 60 wt% of nitrogen present in the hydrolysate fraction. Our prior studies (Barbera et al., 2017; Teymouri, Kumar, et al., 2017) have demonstrated the feasibility of hydrolysate for direct nutrients recycling, which is suitable for a scenario where storage of algae hydrolysate is neither required nor available. However, direct recycling of nutrients is not a viable option whenever storage of nutrients (algae hydrolysate) for algae cultivation is envisioned. The organic compounds in the hydrolysate favors bacterial growth and makes it a nonviable option for the storage of this dilute aqueous stream. An alternative option is

to develop a process that can convert these nutrients to nonperishable high value bioproducts.

Hydrothermal mineralization (HTM) is a technique that has been conceptually driven from the earth-mimetic deposit phenomena and has been used to precipitate ions out of the aqueous phase. The method has been already applied for detoxification of water as well as resource recovery.(T. Itakura, Imaizumi, Sasai, et al., 2009; Sasai et al., 2011) Our previous study (Teymouri, Stuart, & Kumar, 2018) focused on integration of the FH and HTM or FH and AP (atmospheric precipitation) processes in order to recover phosphorus from algae hydrolysate in the form of products such as hydroxyapatite (HAp, $Ca_{10}(PO_4)_6(OH)_2$) and/or whitlockite (WH, $Ca_{18}Mg_2(HPO_4)_2(PO_4)_{12}$), and dittmarite (magnesium ammonium phosphate, MAP, $MgNH_4PO_4.H_2O$). This study provided a basis for further experimental studies to understand the mechanism of HAp formation and the effect of time on phosphate mineralization.

HAp is the most stable calcium orthophosphate at pH above 4 and has a variety of chemical and biomedical applications, including bone tissue regeneration, cell proliferation, drug delivery, implant coating, and catalytic activity.(Lovón-Quintana, Rodriguez-Guerrero, & Valença, 2017; Mori et al., 2003; Sopyan, Mel, Ramesh, & Khalid, 2007) HAp has been produced through methods such as chemical precipitation, electrospinning, electrospraying, solid state, microwave irradiation, self-propagating combustion, emulsion and microemulsion, surfactant assisted precipitation, chemical vapor, flux cooling, and hydrothermal processing.(Haider, Haider, Han, & Kang, 2017) Among these options, hydrothermal method is favored, due to the ability of producing a pure phase with high crystallinity(Jokić et al., 2011). The hydrothermal studies for HAp

production used a long reaction time (few hours to days), while using pure calcium and phosphorus containing compounds as reactants.(M.-L. Qi et al., 2017; Mehdi Sadat-Shojai et al., 2013) It is also theorized that HAp synthesis for biomedical application from natural reactants, such as microalgae hydrolysate has higher chance to get accepted by an organism in human body.(Felício-Fernandes & Laranjeira, 2000) On the other hand, WH is known as the second component in hard tissue after HAp.(H. L. Jang et al., 2014) Although studies on WH showed better bone regeneration compared to HAp,(H. L. Jang et al., 2016) its synthetic mechanism and role in the body has not yet been well understood. (H. L. Jang et al., 2015)

Our prior study (Ali Teymouri, 2017) has confirmed the recovery of almost 83 wt% of phosphorus from microalgae in the form of carbonate HAp and WH via the integrated FH-HTM process at 280 ˚C and 1 h of residence time. In the same study,(Ali Teymouri, 2017) we identified the significant role of seeding materials to promote crystallization in the precipitation process. To date, no study was carried out about the kinetics of HAp and WH under hydrothermal condition. However, few studies investigated HAp as well as WH formation through precipitation process at temperatures below 90 ˚C. Tomson and Nancollas suggested that octacalcium phosphate is the precursor to HAp precipitation at physiological pH.(TOMSON & NANCOLLAS, 1978) This idea was then supported by Liu *et al.* on the precipitation of HAp at pH between 10 and 11. They introduced following steps for HAp synthesis: transferring from octacalcium phosphate (OCP) to amorphous calcium phosphate (ACP) and then to calcium-deficient hydroxyapatite and HAp.(C. Liu, Huang, Shen, & Cui, 2001) Furthermore, it has been noted that HAp formation kinetics are initially controlled by

surface areas of the reactants, whereas the rate of formation is controlled by diffusion. (P. W. Brown & Fulmer, 1991) On the other hand, pure WH nanoparticles (without any intermediate phases) were precipitated in a ternary $Ca(OH)_2$–$Mg(OH)_2$–H_3PO_4 system under acidic condition (pH<4.2) with excess Mg^{2+} to impede the HAp growth.(H. L. Jang et al., 2014) Their study revealed that in the presence of Mg^{2+}, after reducing pH, HAp transformed into dicalcium phosphate dehydrate and then into WH. Although, none of the above studies are in hydrothermal conditions, they will still guide us through the possible HAp and WH production mechanisms.

The current study investigates the effect of HTM reaction time on the phosphate mineralization process and the chemistry of calcium phosphate precipitates. To this aim, we seek the following objectives: (1) evaluating phosphate and calcium removal from the aqueous phase after each HTM experiment, (2) characterizing liquid and solid phases associated with every stage of this study as well as the initial algal biomass, (3) assessing the composition, structure, thermal stability, crystallinity, and morphology of minerals precipitated at different reaction times. This is the first kind of study in which the kinetics of calcium phosphate precipitates from algae hydrolysate is being investigated. Understanding the kinetics of phosphate removal and the bioproducts formation pathways from the algae hydrolysate will lead to a smarter energy and material integration, resource utilization, as well as an efficient, reliable, and economic design of downstream processes in the algal biorefineries.

5.2. Materials and methods

5.2.1. Microalgae characterization

Scenedesmus sp. was cultivated in the Biomass Research Laboratory (BRL) at Old Dominion University using the BG-11 media as explained in our previous study. (Teymouri, Kumar, et al., 2017) Following harvesting, microalgae were freeze dried and stored in plastic airtight bottles at below –20 ˚C until the experiment. Microalgae were fully characterized by performing proximate and ultimate analysis using thermogravimetric analysis (TGA) (TGA-50H, Shimadzu Corporation) and Thermo Finnigan Flash EA 1112 automatic elemental analyzer (ThermoFisher Scientific, Waltham, MA), respectively. For ultimate analysis, 2,5-Bis(5-tert-butyl-benzoxazol-2-yl) thiophene (BBOT) standard (certified# 202147-10/03/2015, ThermoFisher Scientific, Cambridge, UK) were used as a standard. The EA combustion furnace was set at 950 ˚C while the oven was at 65 ˚C. Helium was used as a carrier gas with the flow of 100 mL/min. All experiments were conducted in triplicate and the reported values are the averages. Moisture and volatile analysis were calculated through a pyrolysis process using nitrogen flow. The temperature was ramped (10 ˚C/min) to 90 ˚C, then, was increased in a stepwise function (1 ˚C/min) to 110 ˚C. Again, the temperature was ramped (10 ˚C/min) to 800 ˚C and was increased in a stepwise function (1 ˚C/min) until 850 ˚C. Moisture and volatile content were then calculated based on zero weight losses at 100 and 850 ˚C, respectively. The sample was cooled down to 120 ˚C and after switching the flow to compressed air, ramped (10 ˚C/min) to 800 ˚C for the combustion process to calculate ash and fixed carbon. Finally, the sample entered the last stepwise function (1

˚C/min) to 850 ˚C and held until the derivative weight change was less than 0.01 wt%/min.

5.2.2. Experimental procedure

More than 10 FH experiments were performed at optimum conditions to collect enough hydrolysate for this study. Optimum conditions for maximum nutrient recovery, which were 280 ˚C and 10 s of residence time, was selected based on our previous studies.(Jose Luis Garcia-Moscoso et al., 2013; Garcia-Moscoso et al., 2015) Following each run, products were subjected to solid liquid separation using Fisher Scientific accuSpinTM 400 centrifuge and vacuum filtration. Biofuels intermediates that preserved most of the lipids, were stored at below −20 ˚C. Hydrolysate were analyzed for total organic carbon (TOC) and total nitrogen (TN) using Shimadzu TOC/TN analyzer (TOC-V_{CSN}, Shimadzu) equipped with an ASI-V auto sampler to ensure its homogeneity to be mixed and freeze-dried. Algal hydrolysate for HTM experiments were prepared by dissolving 6.6 g of freeze-dried hydrolysate powder in 350 mL Milli-Q water. Dionex ICS-5000 AAA-Direct Ion Chromatography (IC) instrument (Thermo Fisher Scientific) equipped with the Dionex IonPacTM CS16 column and a guard column was used to evaluate the dissolved phosphate before and after each HTM reaction. Atomic absorption spectrophotometry (AA-87000, Shimadzu) was used to detect calcium. A 27 mL custom designed stainless steel reactor from HIP Company (High Pressure Equipment Co.) was used for HTM reactions. Omega pressure gauge and thermocouple (P/N: TJ36-CAXL-116G-6, Omega Engineering, Inc.) were connected through a taper seal cross (P/N: 10-24AF4, High Pressure Equipment Co.) to the top of the reactor to continuously monitor pressure and temperature during the reaction (Figure 33).

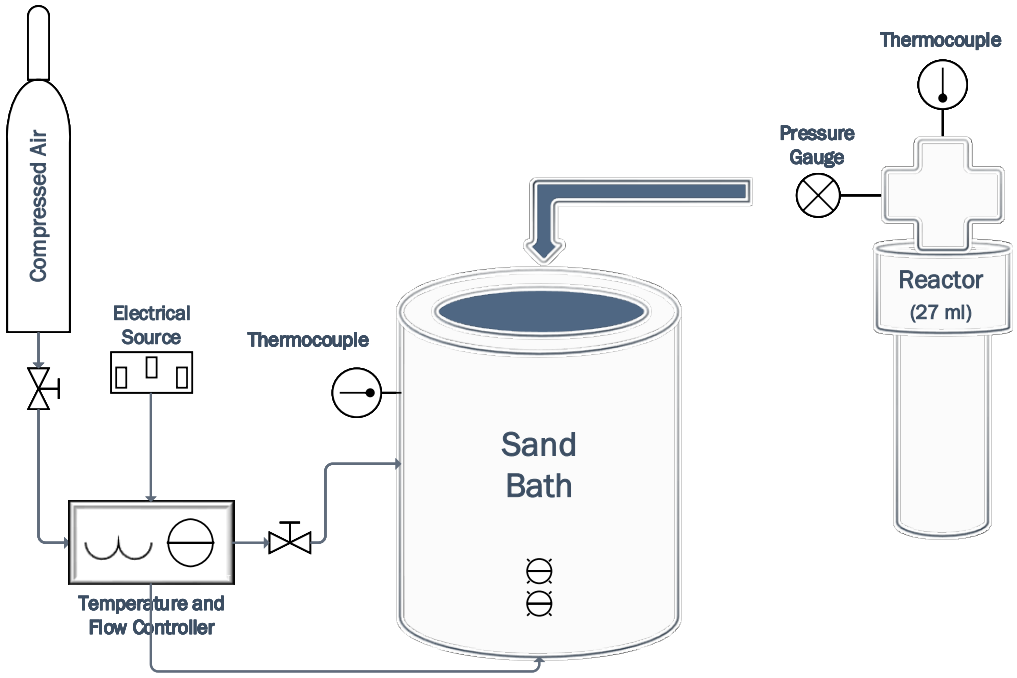

Figure 33. Schematic diagram of the experimental setup of the HTM reactor

Calcium hydroxide (equal to Ca/PO_4 molar ratio of 1.67 as a theoretical value for HAp precipitation) and 50 mg of commercial hydroxyapatite (reagent grade, Sigma-Aldrich) were added as mineralizer and seeding material, respectively. A Techne SBS-4 fluidized sand bath which equipped with a Techne TC-9D temperature and airflow controller was used as a heating source (Figure 33). HTM processes were conducted at 280 ˚C and 2000 psi. This temperature was selected because algae hydrolysate is the product of FH at 280 ˚C and it can be efficient for heat integration. Different residence times including 5, 15, 30, 45, 60, and 90 min were tested in duplicate in the HTM process. After each run, the reactor was allowed to cool down in a water bucket to room temperature in about 2–3 min and products were centrifuged and filtered (0.22 µm mixed cellulose esters membrane, Merck Millipore Ltd.) to collect precipitates for further characterization. Precipitates dried at 60 ºC were analyzed by X-ray diffraction (XRD,

MiniFlex II Desktop X-ray Diffractometer, Rigaku Corp.) in the range of 10 to 80 º (2θ/θ) with the scan speed of 2 º/min at 30 kV and 15 mA followed by the peak analysis using Rigaku PDXL software (version 1.8.0.3). TGA was used for studying the thermal stability of the precipitated mineral in temperature range of 25–1200 ˚C in nitrogen atmosphere with the flow rate of 30 mL/min in an alumina (Al_2O_3) sample holder. This included a steady temperature ramp of 10 ˚C/min until 500 ˚C, with a stepwise function (1 ˚C/min) at 90–110 ˚C, followed by 3 h hold at 500 ˚C. The heating continued the rate of 5 ˚C/min until reached 1200 ˚C and hold for an hour. The functional groups were evaluated by fourier transform infrared spectroscopy (FTIR) (IR Prestige-21, Shimadzu) with 256 scans over a range of 400–4000 cm-1 and a resolution of 4 cm^{-1}. Elemental characterization, elemental mapping, and morphology of the precipitated minerals were evaluated using scanning electron microscope (SEM- JEOL JSM-6060LV, Tokyo, Japan) featured with energy-dispersive X-ray spectroscopy (EDS, Thermo Electron NORAN System SIX). Aqueous phase was analyzed for phosphate and calcium as well as nitrogen and carbon content after each run. Figure 34 shows the overall process including analyses methods.

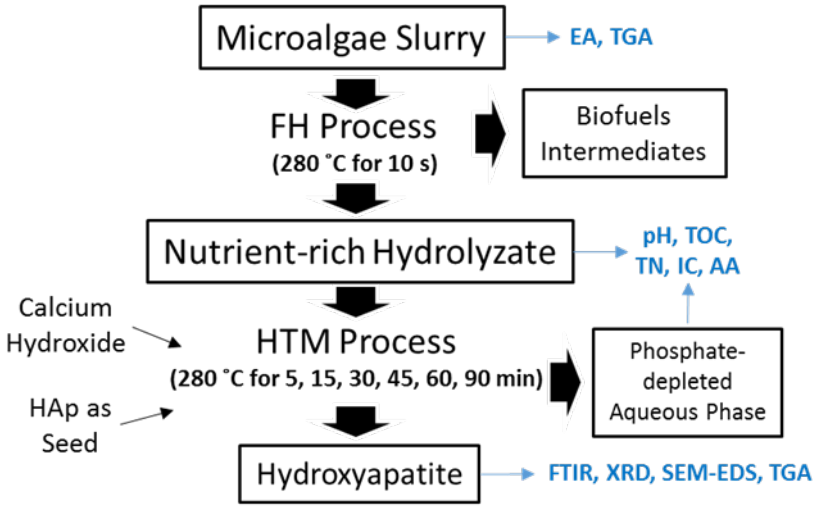

Figure 34. Schematic diagram of the overall process (black) and products analyses (blue). All analyses were performed in duplicate unless otherwise stated.

5.3. Results and discussion

Ultimate and proximate analysis of the *Scenedesmus* sp. microalgae harvested for this study is shown in Table 17.

Table 17. *Scenedesmus* sp. ultimate and proximate analysis. Ultimate analysis is provided on an ash free dry weight percent. *Oxygen was calculated based on the difference (C + H + N + O = 100).

Ultimate analysis	wt% (± Standard Deviation)	Proximate analysis	wt% (± Standard Deviation)
Carbon	49.1 ± 0.3	Moisture	6.5 ± 0.3
Nitrogen	7.3 ± 0.1	Ash	13.2 ± 0.1
Hydrogen	7.1 ± 0.1	Volatiles	68.1 ± 0.1
*Oxygen	36.5	Fixed carbon	12.2 ± 0.2

The reconstituted hydrolysate was analyzed for TOC, TN, phosphate, and calcium contents prior to HTM process. The results came up as 6670.0 ± 8.5, 1295.0 ± 9.9, 665.1 ± 3.9, and 34.4 ± 1.1 mg/L respectively. These data were used to evaluate the stoichiometric amount of mineralizer (calcium hydroxide) required to prepare Ca/PO_4 equal to 1.67 for HAp precipitation reaction. The high concentration of nitrogen is due to proteinaceous compounds such as peptides and amino acids extracted after FH process from algal biomass.(Jose Luis Garcia-Moscoso et al., 2013) The effect of amino acids and soluble peptides on the mineralization process of HAp is an important topic that is

still under debate.(H. Wang, 2004) However, at the HTM reaction conditions, they will all decompose to ammonia and other degradation products. (Garcia-Moscoso et al., 2015) Another important factor in the HAp synthesis from algal biomass is the usage of seeding material. It has been reported that seeding material could promote crystallization and the amount does not have a considerable effect on the crystal growth rate.(H. Jang & Kang, 2002; Koutsopoulos & Dalas, 2000) Similarly, Brown and Fulmer's research revealed that seeding with HAp accelerated the initial reaction for HAp formation.(P. W. Brown & Fulmer, 1991) The use of HAp seeds will result in stoichiometric crystalline HAp without the formation of precursor phases.(Inskeep & Silvertooth, 1988) Study conducted by Kubota *et al.* showed that the seed loading is a critical factor in controlling the crystal size distribution (CSD) in the crystallization of potassium alum. They also emphasized that the high concentration of seeds will eliminate the secondary nucleation phenomena in the cooling process.(Kubota, Doki, Yokota, & Sato, 2001) In addition, our preliminary results have also explained the crucial role of the seeding material for hydroxyapatite crystallization.(Ali Teymouri, 2017) Therefore, equal amount of commercial HAp (50 mg) was used for each experiment as seeding material.

Same analysis were done on the phosphate-depleted aqueous phase after each reaction to evaluate the nutrient removal kinetics. The following equation (Eq. 9) has been applied for each component's removal as weight percentage of its total concentration.

$$\text{removal of component } i \text{ (wt\%)} = [(C_{i,\,in} - C_{i,\,out}) / C_{i,\,in}] \times 100 \qquad (9)$$

where $C_{i,\,in}$ is the concentration of component *i* in the hydrolysate before HTM reactions, and $C_{i,\,out}$ is the concentration of component *i* after HTM reactions. The results revealed

that 97.1 ± 0.4 wt% of phosphate and 93.7 ± 0.3 wt% of calcium removed in the first 5 min of HTM process in forms of calcium phosphate precipitates. Both the rate and the extent of recovery in this study is much higher compared to similar studies. For instance, Yu *et al.* reached 74 or 92 wt% of phosphate removal after 2 or 4 h of reaction time in the form of HAp, respectively.(Y. Yu, Wu, & Clark, 2010) Results revealed by Chen *et al.* showed phosphate removal of 91.3 wt% after 24 h reaction as HAp.(X. Chen, Kong, Wu, Wang, & Lin, 2009) This is also confirmed by a review study performed by Shadat-Shojai *et al.* in which the majority of HAp formations occurred in 3–120 h of residence time excluding the production pathways (Mehdi Sadat-Shojai et al., 2013).

Carbon and nitrogen content of the aqueous phase have also reduced by 10.4 ± 0.6 wt% and 4.6 ± 1.3 wt% in the shortest (5 min) HTM reaction, respectively. Carbon reduction might be due to the decarboxylation or decarbonylation of organic carbon under hydrothermal conditions, (G. Yu et al., 2011) while degradation of proteinaceous compounds to ammonia might be the reason for nitrogen content reduction.(Saqib Sohail Toor et al., 2011) This could be the reason for the pH increase of the reaction media from 5.6 before HTM process to approximately 7.2 after the reaction. The precipitates recovered after each run were fully characterized. The precipitated minerals were compared with commercial HAp (as a reference) during XRD analysis (Figure 35) as well as the international center for diffraction data (ICDD) data bank in terms of peaks intensity and position via the Rigaku PDXL software. Precipitates were assigned as carbonated HAp (JCPDS# 01-076-0694) while the presence of WH (JCPDS# 01-070-2064) has been also observed as the secondry phase. Peaks related to WH have been

marked with dashed-line (Figure 35). Mg^{2+} and HPO_4^{2-} ions play a structural role in the WH formation and both are readily available in the algal hydrolysate (Eq. 10).

$$18Ca^{2+} + 2Mg^{2+} + 14PO_4^{3-} + 2H^{+} \rightarrow Ca_{18}Mg_2(HPO_4)_2(PO_4)_{12} \quad (10)$$

Mg^{2+} is one of the essential microalgae nutrients due to its role in chlorophyll molecule and algal cell wall while the later anion is the major phosphate species in the slightly acidic pH range (5.6) of the hydrolysate.(Esakkimuthu et al., 2016) It has also been reported that the presence of magnesium in the reaction solution impedes the formation of HAp in the favor of WH (J. C. Elliott, 2013).

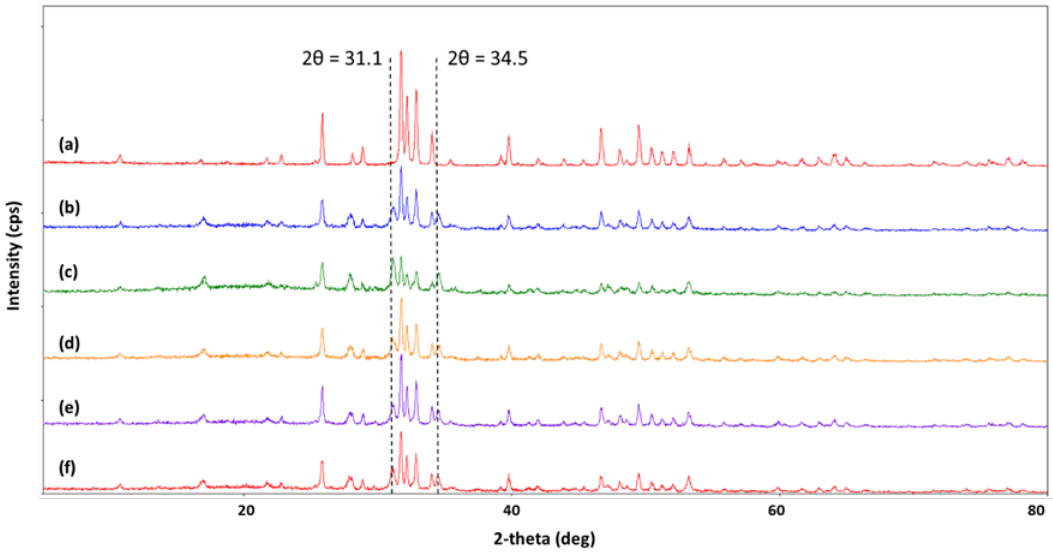

Figure 35. X-ray diffraction patterns for (a) commercial HAp, and HTM experiments conducted at 280 ˚C and reaction times of (b) 90 min, (c) 60 min, (d) 45 min, (e) 30 min, (f) 15 min. Peaks that are marked with dashed-line at 2θ = 31.1 and 34.5 identified as WH.

Figure 36 shows the FTIR spectra of all the precipitates. The HAp and WH related peaks as well as peaks due to the organic carryovers from the carbon-rich

hydrolysate were observed. Peaks revealed in the range of 2860–2960 cm^{-1} (C–H stretch), 1668 cm^{-1} (C=C stretch), 1588 cm^{-1} (C–C) originated from organic and aromatic compounds carryovers. Peaks at 1087, 1038, 1013 cm^{-1} (PO_4–ν_3), 960 cm^{-1} (PO_4–ν_1), 564 cm^{-1} (PO_4–ν_4), 602 cm^{-1} (PO–ν_4), 476 cm^{-1} (PO_2–δ), observed in all precipitates as well as the commercial HAp. However, the sharp small peaks at 634 cm^{-1} (OH^-) detected only in commercial HAp. Absence of the (OH^-) peak, which is as a result of the water associated with the HAp lattice, confirmed the formation of substituted HAp by XRD analysis. Peaks observed at 1383 cm^{-1} (CO_3–ν_3), 1445 cm^{-1} (CO_3^{2-}) are indication for non-stoichiometric B–type carbonate substitution in the HAp lattice (Roberts et al., 2015; Shu et al., 2005). It has been reported that ionic and cationic substitutions have improved the biomedical properties of HAp (Roberts et al., 2015). Some recent studies have shown that carbonate substitution in HAp structure enhances the biocompatibility characterization and bone regeneration.(Shen et al., 2017; Szcześ, Hołysz, & Chibowski) Peaks relevant to the OH^- group in the lattice are observed in the range of 3500–3600 cm^{-1}. These peaks are a result of water in the HAp lattice and were not observed in the spectrum of TCP (tricalcium phosphate).(Destainville et al., 2003; Theophanides, 2012) The small sharp peak observed at 880 cm^{-1} might be a result of either HPO_4^{2-} or CO_3^{2-} in the calcium deficient HAp.(Berzina-Cimdina & Borodajenko, 2012; F. Ren et al., 2013) The intensity of this peak dropped as the reaction time in the HTM process increased and almost disappeared for the precipitates from the 90 min experiment indicating the conversion to the stoichiometric HAp. This has been confirmed with the EDS analysis explained later.

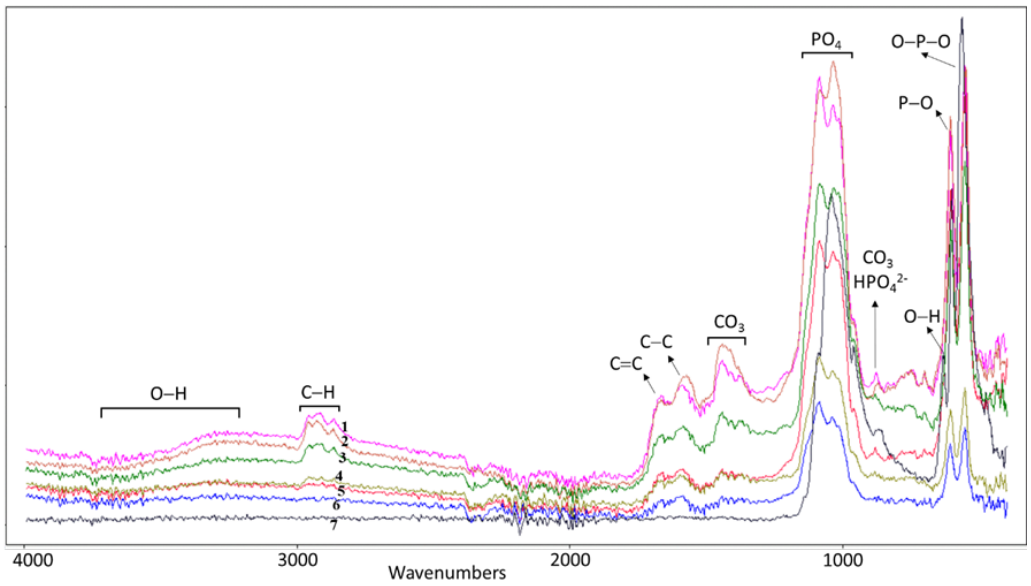

Figure 36. FTIR spectrum of precipitates recovered after 5 min (#5), 15 min (#6), 30 min (#1), 45 min (#4), 60 min (#2), and 90 min (#3) of residence time in the HTM process and their comparison with the commercial HAp (#7).

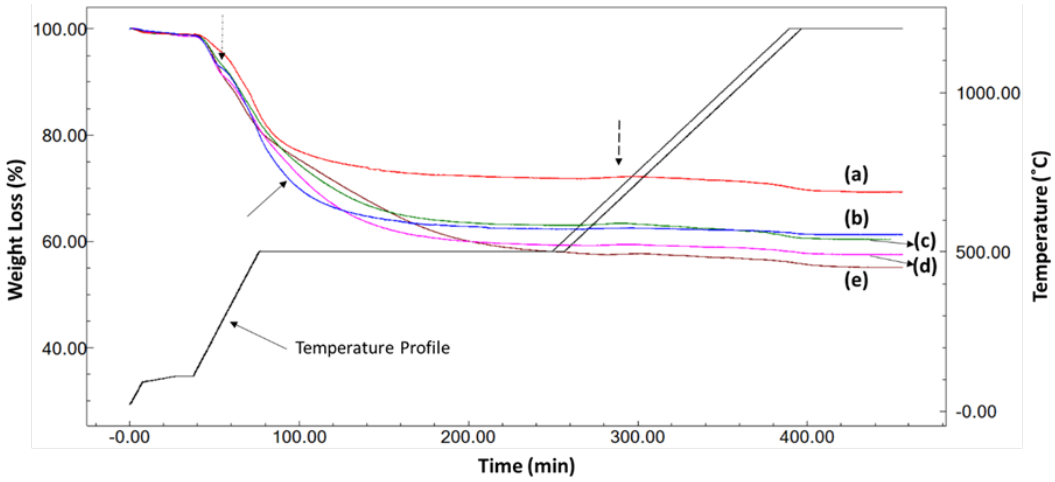

Figure 37. TGA patterns for HTM experiments conducted at 280 ˚C and reaction times of (a) 5 min, (b) 90 min, (c) 15 min, (d) 45 min, (e) 30 min. Black line indicates the TGA temperature profile.

Figure 37 indicates the TGA of samples. As observed, there are similar trends for all precipitated powder including a minor weight loss near 110 ˚C due to the moisture content and a major weight loss up to 500 ˚C, which is related to residual organic matter from the carbon-rich algal hydrolysate.(Felício-Fernandes & Laranjeira, 2000) Powder obtained after 90 min reaction time has relatively, higher weight loss up to 500 ˚C (solid arrow in Figure 37b). This might be due to higher carbonate in the HAp lattice that has reduced its thermal stability.(Felício-Fernandes & Laranjeira, 2000) There was also a notable change in the weight loss rate for the same sample as well as the powder related to the 45 min HTM process, which are marked with a dot arrow near 270 ˚C. This change might correspond to the detachment of adsorbed water followed by the loss of the water in the lattice.(Diallo-Garcia et al., 2011; Felício-Fernandes & Laranjeira, 2000) In all samples there were weight gain at around 600 ˚C which had inverse relation with the residence time of the HTM process. This might be a result of hydroxyl ions uptake into the lattice of hydroxyapatite during the crystallization process.(Gross, Gross, & Berndt, 1998) Another weight loss started around 1150 ˚C for all precipitates, which could have originated from the HAp dihydroxylation. Overall, precipitates from the HTM process after 90 min of reaction time had less than 1.0% weight loss in the range of 500–1200 ˚C which is similar to commercial HAp thermal stability. These findings were in agreement with prior results that by increasing the HTM reaction time, precipitates predominately formed HAp rather than WH. This hypothesis was further supported through the elemental composition of the recovered powder using EDS analysis (Table 18). Presence of magnesium and carbon have been observed as they are required for the WH and carbonated HAp formation, respectively. However, the amount of magnesium was the lowest (0.26 wt%) in the minerals recovered after 90 min of reaction time. In addition,

Ca/P molar ratio for the precipitated powder matched the ratio of Ca/P = 1.67 in HAp. The small amount of Mg^{2+} might be due to the incorporation of this cation in the structure of HAp lattice.(Felício-Fernandes & Laranjeira, 2000) Low magnesium content (< 1wt%) could be substituted in HAp without structural changes.(Fadeev, Shvorneva, Barinov, & Orlovskii, 2003) This is the case for HAp in human bone as well.(H. L. Jang et al., 2016) Figure 38 demonstrates the two-dimensional elemental mapping of the minerals recovered after 90 min of HTM process. The results indicate the ubiquitous presence of the carbon, calcium, magnesium, phosphorus, and oxygen elements in the precipitates. The uniform distribution of magnesium in the HAp lattice is in agreement with prior studies.(Roberts et al., 2015) This uniformity also applies to the Ca and P elements of HAp composition. This would contribute to the good bone osseointegration of HAp particles for biomediacal applications.(Q. Wei et al., 2015)

Table 18. Quantitative results from the EDS analysis of precipitates in various retention times.

HTM Reaction Time, min	C, wt%	O, wt%	Mg, wt%	P, wt%	Ca, wt%	Ca/P Mol. Ratio
15	ND	35.40	0.58	14.75	36.41	1.91
30	5.56	34.60	1.62	14.78	30.49	1.59
45	18.66	31.99	1.02	11.27	25.10	1.72
90	ND	39.07	0.26	16.73	36.24	1.67

ND: Not detected. The carbon peaks were observed in the EDS pattern; however, the corresponding peak was overlapped by the oxygen peak.

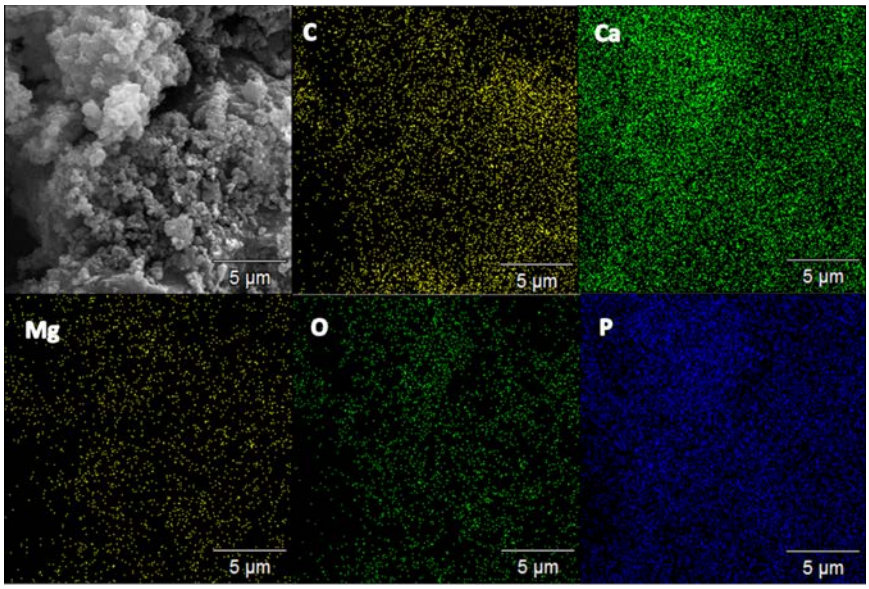

Figure 38. Elemental mapping of carbon, calcium, phosphorus, oxygen, and magnesium of precipitated minerals after 90 min of HTM process.

Morphology of the precipitates recovered after each experiment was analyzed through SEM analysis (Figure 39). As the HTM reaction time increased, small spherical particles of HAp (seeding material) became larger and changed to flat agglomerates. These morphologies are similar to the Palazzo *et al.* study in which calcium deficient HAp (CDHA) precipitated in the presence of amino acids.(Palazzo et al., 2009)

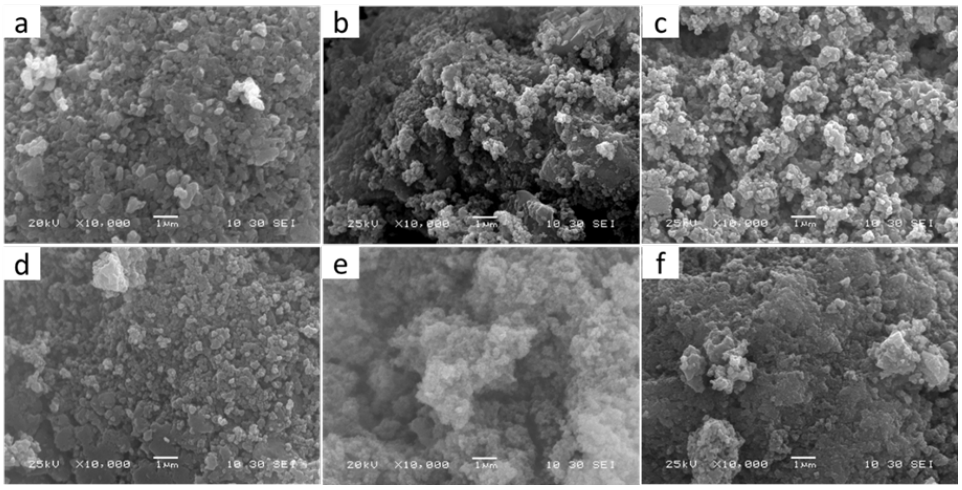

Figure 39. SEM images of commercial HAp used as seeding material (a), and the precipitated material after 15 min (b), 30 min (c), 45 min (d), 60 min (e), and 90 min (f) of HTM process. All images have the same 10,000× magnification.

Overall, the results from this study showed that phosphate and calcium removal from the algal hydrolysate mainly occurred in the first 5 min of reaction time. Based on the XRD, FTIR, and EDS analysis, calcium phosphate minerals were discovered to be a mixture of WH and carbonated HAp. However, as the reaction time increased, HAp tended to be the predominant species. This was confirmed by the Ca/P ratio of 1.67 (equal to HAp ratio) for the minerals of experiment performed at 90 min of residence time. Theses precipitates followed similar thermal behavior as the pure commercial HAp, which was used as a control. In addition, magnesium was detected through EDS analysis to be minimally incorporated through the HAp lattice.

5.4. Conclusions

This work investigates the effect of phosphate removal from the *Scenedesmus* sp. microalgae hydrolysate in the forms of HAp and WH through the integrated FH-HTM process. Majority of phosphate and calcium removal from the hydrolysate occurred in the first 5 min of reaction; however, by tuning the reaction time, calcium phosphate minerals transformed from WH to carbonated HAp with the Ca/P molar ratio of 1.67 after 90 min of residence time. The morphology of particles changed from small spherical in seeding material to larger flat agglomerates. Overall, 80 wt% of phosphorus in the microalgae was recovered in the forms of WH and HAp, which could be used for biomaterials applications.

5.5. Acknowledgments

The authors acknowledge the financial supports of this work by National Science Foundation (NSF) through the NSF CAREER Award CBET-1351413 and NSF PFI: AIR TT Grant 1640593 and Dr. Wei Cao at Applied Research Center (Newport News, VA) for the assistance with the XRD and SEM-EDS analysis.

CHAPTER 6

EVALUATION OF LIPID EXTRACTABILITY AFTER FLASH HYDROLYSIS OF ALGAE

Note: the contents of this chapter have been submitted to be published in the journal of Fuels. To the date of this dissertation the status of the manuscript was under review.

Teymouri, A.; Adams, K.; Dong, T.; Stuart, B.; Kumar, S., Evaluation of Lipid Extractability after Flash Hydrolysis of Algae. *Fuel Journal* 2017, manuscript id: JFUE-D-17-04622, (under review).

Microalgae is identified as a promising feedstock for producing renewable liquid transportation fuels. However, lipids extraction from microalgae for downstream processing to biofuels is one of the important challenges for an algal based biorefinaries. In this study, flash hydrolysis (FH) of microalgae has been proposed as a chemicals-free technique to fractionate algae components (proteins and lipids) and enhance its lipids extractability. To this aim, FH process was performed on three different algal species (*Scenedesmus* sp., *Nannochloropsis* sp., and *Chlorella vulgaris*) at 280 ˚C and 10 s of residence time. Following FH, in addition to the nutrients rich hydrolysate, approximately, 40 wt% of solids containing almost all (>90 wt%) the lipids termed as biofuels intermediates (BI), were recovered. Kinetics study on lipids extractability from the BI as well as their lipid profile analyses were conducted for each algal species. The results showed that the FH process had significantly enhanced the lipids extractability from the BI compared to the respective raw algal species. For all three algae species, lipid yields from BI were higher than that of the raw algae. Lipid yields of *Chlorella vulgaris*

in first 15 min were more than five times higher (52.3 ± 0.8 vs. 10.7 ± 0.9 wt%) than that of raw algae during n-hexane based solvent extraction. The kinetics of lipids extractability followed a zero-order reaction rate for all wet raw microalgae and the BI of *Scenedesmus* sp., while the BI recovered from the other two algal species determined as a second-order reaction. Comparison of fatty acids profiles of the extracted lipids indicated the contribution of FH process in saturating fatty acids. Subsequent to lipids extraction, a conventional hydrothermal liquefaction (HTL) was performed at 350 ºC and 1 h to compare the biocrude yields from raw versus BI of *Chlorella vulgaris* microalgae. The results showed that the biocrude yields from the BI and its quality significantly enhanced post FH than that of raw algae.

6.1. Introduction

Efforts to reduce fossil fuel consumption have been attempted around the world with the aims of mitigating negative environmental harms such as air and water pollution, establishing energy independence, and inspiring innovation in alternative fuels development. The dependence on fossil fuels is heavily ingrained into society, while alternative energy only accounts for less than 10% of the global energy supply according to the United States Department of Energy ("U.S. energy consumption by energy source," 2017). Outstanding biological photosynthetic carbon assimilation potential is one of the main reasons that algal biomass is being considered as a clean fuel and bioproducts source (Lieve M. L. Laurens et al., 2017). There are over thousands of species of algae, but their basic composition consist of mainly proteins, lipids, and carbohydrates (Keymer, Ruffell, Pratt, & Lant, 2013). In particular, microalgae can accumulate lipids up to 20-50 wt%, which have high interest for a variety of bioproducts in food, cosmetics,

and pharmaceutical industries (X. Ren et al., 2017) in addition to its biofuels potential. The algae to biofuels production process has had much success from pilot to large scale operation, but equally as many obstacles that prevent it from becoming competitive with conventional fossil fuels. One of the scientific challenges of algal biofuels commercialization includes lipid extractability from algae cells (Hannon, Gimpel, Tran, Rasala, & Mayfield, 2010). Lipid extraction methods are a key to the biofuels/bioproducts quality and yield from algae. The conventional oil extraction steps include breaking the algae cell walls, freeing the oil, and separating the oil out of the oil cake (Tao Dong, Knoshaug, Pienkos, & Laurens, 2016; Ramesh, 2013). There are multiple technologies for lipid extraction from microalgae that are categorized under solvent extractions (Folch, Bligh and Dyer method), mechanical approaches (expeller press, bead beating, ultrasonic-assisted, microwave), and solvent-free methods (osmotic pressure, isotonic, enzyme-assisted) (Ranjith Kumar, Hanumantha Rao, & Arumugam, 2015). Choice of oil extraction typically depends on moisture content, quantity to be treated, quality of end-product, extraction efficiency, safety aspects, and cost economics (Ramesh, 2013). Three methods including expeller, supercritical CO_2 fluid extraction, and hexane extraction seem to be the most viable for industrial scale (Hannon et al., 2010; Ramesh, 2013). Among the three, hexane has been used in the most applications of oil extraction (Suganya & Renganathan, 2012). It has high stability, low greasy residual effects, and low corrosiveness(Erickson, 2015; Suganya & Renganathan, 2012). It has less toxicity compared to chloroform and methanol (Tao Dong, Eric P. Knoshaug, Philip T. Pienkos, et al., 2016). In addition, it is apolar (water immiscible) with low latent heat of boiling that makes it possible to be separated through low energy separation recovery methods (Chemat, 2017; Tao Dong, Eric P. Knoshaug, Philip T. Pienkos, et al.,

2016). However, it has a poor extractability efficiency compared to chlorinated solvents (i.e. chloroform) (Balasubramanian, Yen Doan, & Obbard, 2013). Techno-economic analyses (TEA) has shown that costs involved for lipid extraction with hexane is the second largest operational cost (R. Davis et al., 2012). Therefore, there is persistently strong demands for novel pretreatment methods of feedstock resulting in the overall improvement of the hexane extraction process. Alternative to lipid extraction approach, hydrothermal liquefaction (HTL) of microalgae feedstock can directly convert the lipids into a biocrude oil, which is then subjected to further upgradation to fuel (López Barreiro et al., 2013). Many efforts have been made to optimize the process in terms of enhancing the biocrude yields (Chan et al., 2017; Guo, Yeh, Song, Xu, & Wang, 2015; Sheehan & Savage, 2017). However, high nitrogen contents in HTL biocrude causes catalyst poisoning during downstream processing for liquid hydrocarbons/transportation fuels (Duan & Savage, 2011). Production of high amounts of NO_x emissions in the downstream processing originating from nitrogenous compounds in proteins and chlorophyll content of microalgae is another serious challenge that this process needs to overcome (Duan & Savage, 2011; López Barreiro et al., 2013).

Flash hydrolysis is a chemical-free subcritical water-based continuous process that fractionates microalgae components in a short residence time of 10 s. Our previous studies have shown multiple advantages of using FH process for microalgae in terms of nutrient management either in forms of recycling or bioproducts formation (Ali Teymouri, 2017; Barbera et al., 2016; Barbera et al., 2017; Jose Luis Garcia-Moscoso et al., 2013; Garcia-Moscoso et al., 2015; Sandeep Kumar et al., 2014; Talbot et al., 2016; Teymouri, Kumar, et al., 2017; Teymouri, Stuart, & Kumar, 2017) while protecting the

lipids in solids. It was reported that 24-52 wt% (depending upon algal species) of the solid residue, known as biofuels intermediates (BI) are recovered after FH with diminished ash and nitrogen content (Jose Luis Garcia-Moscoso et al., 2013). We have also demonstrated that more than 90 wt% of total lipids available in the raw microalgae has been retained in the biofuels intermediates (BI) after FH process (Jose Luis Garcia-Moscoso et al., 2013; Garcia-Moscoso et al., 2015). The previous SEM images (Jose Luis Garcia-Moscoso et al., 2013) of BI have shown its globular condensed appearance after the FH treatment. It has indicated that the process affected the physical dimensions of the particles to a smaller size. However, it is not clear if the FH process adversely affected the lipids extractability from the BI due to reduced solvent accessibility or entrapping oil after the recondensation process. Thus, it is worth studying the lipid extraction efficiency from these BI particles (Tao Dong, Eric P. Knoshaug, Philip T. Pienkos, et al., 2016).

This study aimed to investigate the lipid extraction efficiency after the FH process and feasibility of producing biocrude from the BI via HTL. The main objectives of this study were to (i) conduct a kinetics study on the lipids extractability from the BI of three common algal species (*Scenedesmus* sp., *Nannochloropsis* sp., and *Chlorella vulgaris*), (ii) analyze the fatty acids profile of extracted lipids and compare it with that of extracted from untreated algae, (iii) produce biocrude from the BI using HTL and compare the yield and biocrude quality with biocrude produced via direct HTL (no FH) of microalgae.

6.2. Material and methods

6.2.1. Algae strain and characterization

For the lipid extraction experiment, three microalgae species including *Scenedesmus* sp., *Nannochloropsis* sp., and *Chlorella vulgaris* (*Chlorella v.*) was

selected. They are known as the most promising candidates for biofuels production due to their lipid productivity and growth rate (Tao Dong, Eric P. Knoshaug, Philip T. Pienkos, et al., 2016; Lieve M. L. Laurens et al., 2017). *Chlorella v.* were purchased from Arizona Center for Algae Technology and Innovation (AzCATI), *Nannochloropsis* sp. microalgae was received from Sandia National Laboratory (SNL), and *Scenedesmus* sp. was cultivated in a raceway open pond near Spring Grove, Virginia (Talbot et al., 2016). All samples were freeze dried at arrival and stored at -20 ℃ until application. In order to collect an adequate amount of BI for experiments, multiple FH tests were performed on each microalgae species at the FH optimum conditions of 280 ℃ and 10 s of residence time as explained in our previous studies (Garcia-Moscoso et al., 2015; Teymouri, Kumar, et al., 2017). Followed by FH, products were centrifuged (Fisher Scientific accuSpinTM 400) and vacuum filtered (1.5 µm, Whatman 47 mm glass microfiber filters) to separate the lipid rich BI from the hydrolysate. The recovered BI from each algal species was then subjected to freeze drying and stored at -20 ℃ until application. All microalgae samples and their respective BI were subjected to ash analysis using National Renewable Energy Laboratory (NREL) method (Van Wychen & Laurens, 2013) followed by elemental analysis. Thermo Finnigan Flash EA 1112 elemental analyzer (ThermoFisher Scientific, Waltham, MA) with 2,5-Bis (5-tert-butylbenzoxazol-2-yl) thiophene (BBOT) standard (certified no. 202147-10/03/2015, ThermoFisher Scientific, Cambridge, UK) were used to characterize the elemental composition of algal biomass (Jose Luis Garcia-Moscoso et al., 2013).

6.2.2. Experimental setup and procedure

6.2.2.1. Total lipid yield and FAME composition

To evaluate the lipid extraction performance of the microalgae feedstock, two critical factors including lipid yields and FAME profile needed to be considered (Halim et al., 2011). First, the total extractable lipid was recovered after the FH to evaluate if FH can improve lipid yield. 0.35 g of dry biomass was fed into a glass tube and 4 ml of Deionized (DI) water was added to the tube to fully soak the dry biomass at 4 ℃ overnight to mimic conditions after wet flash hydrolysis as well as algal ponds. To assist the oil extraction (specific free fatty acid, FFA), 0.5 wt% of sulfuric acid was added to reduce the pH. 3 ml of hexane was then added to the tube and a magnetic stir bar was added to stir the biomass on a multi-position magnetic plate. The extraction was carried out for 2 h on the magnetic plate. Tubes were vortexed for 30 s, every 30 min to improve the extraction. After the extraction, the tubes were centrifuged at 2000 g for 10 min for phase separation. Then, the upper phase was moved to a preweighted glass tube. The solvent was evaporated in a vacuum oven at 40 ℃ overnight (T. Dong, Van Wychen, Nagle, Pienkos, & Laurens, 2016). The experiment was carried out in triplicate. The oil yield calculated from the following equation (Eq. 11):

$$\text{Oil yield (wt\%)} = \text{extracted oil (g)} / \text{starting biomass (g)} \times 100\% \quad (11)$$

6.2.2.2. Lipid extraction kinetics

To better understand the lipid extraction process, a lipid kinetic study was conducted. Lipid yields represent extraction efficiency and is measured through the following equation (Eq. 12):

Lipid yields = extracted lipid (g) / dried algae (g) × 100 (12)

To perform the lipid extraction experiments, 1 g of raw algae or BI were added to 20 ml of Milli-Q water (EMD Millipore, Milli-Q Direct 16 water purification system) to make a homogenous slurry in a 250 ml Erlenmeyer flask sealed with a rubber stopper to avoid evaporation. This is to imitate the algae slurry after cultivation processes such as flocculation and avoid the energy intensive drying stage; although moisture content of more than 5 wt% is known to decrease the extraction efficiency (Suganya & Renganathan, 2012). A 20 ml of n-hexane 85% (Fisher Chemical, high-resolution gas chromatography) was added to the same flask and placed on magnetic stir plates (Fisher Scientific Isotemp) for mixing with magnetic stir rods at 350 rpm at room temperature of approximately 25 ℃. Experiments were done in duplicate for 15, 30, 60, 90, 120, 180, and 240 minutes of extraction time for both raw and BI of algae. After mixing for designated time, the resulting mixture was transferred into 50 ml centrifuge tubes. Each individual flask was rinsed 3 times with 1 ml aliquots of the same n-hexane solvent to recover all lipids to the tube and was centrifuged for 10 min at 2000 g. The supernatant was removed after filtration using 0.2 µm nylone syringe filters (Fisherbrand, cat no. 09-719-006) and placed in pre-weighed glass vials. Solvent was removed by placing glass vials in oven at 55 ºC for 48 h until all solvent had evaporated, and then, weighed for recovered lipids. For long term lipids storage, glass vials were covered with Parafilm and transferred to a freezer at -20 ºC for further analysis.

The quantified amount of extracted lipid of each feedstock provided us with adequate data to model the mass transfer of lipid molecules from wet algal slurry to the

solvent medium. Following the simplified reaction was assumed to perform the kinetics study:

Lipid in algae slurry + solvent → lipid extracted in solvent (13)

The detail mass transfer of lipid through water and solvent layers were discussed elsewhere (Tao Dong, Eric P. Knoshaug, Philip T. Pienkos, et al., 2016; Halim, Danquah, & Webley, 2012). The reaction order and reaction rate constant (k) were calculated by fitting the experimental data obtained from lipid extraction experiments as explained in our prior study (Garcia-Moscoso et al., 2015). Briefly, we plotted C_t (for zeroth order), ln C_t (first order), $1/C_t$ (second order) versus extraction time, where C_t was the lipid available in the algae at time t. The reaction rate constant was obtained from the slope of the plotted graph whose linearity was the best fit.

6.2.2.3. Hydrothermal liquefaction

For the HTL process, 6.1 g of each feedstock: freeze dried raw and BI of the *Chlorella v.* microalgae, were added to 60 ml of Milli-Q water resulting in 9.4 ± 0.0 (± standard deviation) and 9.5 ± 0.0 wt% solid content, respectively. The experiments were carried out in duplicate (for each feedstock) at 350 ℃ and 1 h of residence time using a 31.5 ml stainless steel cylindrical reactor (High Pressure Equipment Co.) equipped with pressure gauge (Omega Engineering, Inc.) and thermocouple (P/N: TJ36-CAXL-116G-6, Omega Engineering, Inc.) to monitor the pressure and temperature throughout the experiment. A fluidized sand bath (SBS-4, Techne) was used as a heating source equipped with a temperature and flow controller (TC-9D, Techne). After the completion of the reaction, the reactor was quenched in cold water for 5 min and left at room temperature for ~ 60 min to equilibrate. Products were then transferred to a 50 ml

centrifuge tube. The reactor was rinsed with 20 ml of dichloromethane (in 3 ml portions) and transferred to the same centrifuge tube. The mixture was then vortexed (3000 rpm for 1 min) and centrifuged (2000 g for 1 min) which resulted in separation of aqueous fractions (on top) from the mixture of solids and organics (on the bottom). The aqueous phase was removed, filtered using 1.5 µm glass microfiber filters (Whatman), and transferred to preweighed vials. The solids and organic fraction were separated with 0.45µm glass microfiber filters (Whatman) using vacuum filtration. The solid phase was oven dried at 65 ℃ for 24 h. The organic phase was transferred to preweighed vials and the dichloromethane was evaporated to dryness by flowing ultrapure nitrogen gas over the tubes for approximately 8 h to calculate biocrude yield. All products including biocrude, aqueous phase, and solid residue were analysed for gravimetric yield and elemental composition (gases were not accounted for).

Algal biomass (raw and BI), solid residue (char) formed after HTL process, and biocrude were subjected to EA as explained in section 2.1, while total organic carbon/total nitrogen (TOC/TN) analyser (TOC-VCSN, Shimadzu) equipped with an ASI-V auto sampler were used for the recovered aqueous phase. Following equations were used to calculate the wt% of yield and elemental distribution:

$$\text{Yield (wt \%)} = \text{mass of product fraction (g)} / \text{mass of alga (g)} \times 100\% \quad (14)$$

$$\text{Elemental distribution (\%)} = (\text{mass of element in product fraction/mass of element in alga}) \times 100\% \quad (15)$$

Heating value of the biocrudes were estimated based on empirical formula such as Dulong’s formula:

$$(\text{HHV(MJ/kg)} = 0.3383C + 1.422 -(H–O/8) \quad (16)$$

where, C, H, and O are the elemental percentages of the biocrude that were measured through elemental analysis (R. Wei et al., 2017). Thermogravimetric analysis (TGA) of crude oil was performed using TGA-50H (Shimadzu Corporation) from 25 ºC to 900 ºC in 50 ml/min nitrogen gas flow at 10 ºC/min to estimate the boiling point range (Biller & Ross, 2011b; W.-T. Chen et al., 2014).

Cetane number (CN) is a measurement of the quality of diesel fuel that considers ignition delay time and combustion quality (Stansell, Gray, & Sym, 2012). CN for this study was estimated using models from the work of Stansell et al. (Stansell et al., 2012), who used a combination of models from the work of Lapuerta et al. (Lapuerta, Rodríguez-Fernández, & de Mora, 2009) and Tong et al. (Tong, Hu, Jiang, & Li, 2011). CNs were calculated using the following equations where n is carbon number and db is double bond number:

For Saturated SFAs:

$$CN = -107.71 + 31.126n - 2.042n^2 + 0.499n^3 \quad (17)$$

For MUFAs:

$$CN = 109 - 9.292n + 0.354n^2 \quad (18)$$

For PUFAs:

$$CN = -21.157 + (7.965 - 1.785db + 0.235db^2)n - 0.099n^2 \quad (19)$$

CN for the specific biodiesel/FAME is given by the following equation where CN_i is cetane number of each class and m_i is mass percentage of each FAME in the biodiesel:

$$CN = 1.068\ S\ (CN_i m_i) - 6.747 \quad (20)$$

6.3. Results and discussion

The elemental composition of all three microalgae species were presented in the Table 19. As demonstrated, FH process resulted in biofuels intermediates with higher percentages of carbon and hydrogen, but with reduced nitrogen content. BI of *Chlorella v.* showed approximately, 80 wt% less ash compared to the original untreated microalgae. This was similar to our prior study on *Nannochloropsis gaditana* (Teymouri, Kumar, et al., 2017), which denotes the potential of FH as a treatment process for high ash feedstocks.

Table 19. Microalgae characterization (raw/untreated and biofuels intermediates) used for this study. All values are wt% (± standard deviation).

Algae Species	Treatment	Carbon	Nitrogen	Hydrogen	Ash
***Scenedesmus* sp.**	Raw	49.1 ± 0.3	7.3 ± 0.1	7.1 ± 0.1	4.5 ± 0.7
	BI	55.5 ± 0.3	6.7 ± 0.3	7.6 ± 0.1	n/a
***Nannochloropsis* sp.**	Raw	46.8 ± 0.2	7.9 ± 0.0	7.4 ± 0.1	11.0 ± 0.0
	BI	61.8 ± 0.4	7.0 ± 0.3	8.4 ± 0.0	n/a
Chlorella v.	Raw	52.9 ± 0.7	2.8 ±0.9	7.9 ± 0.7	2.5 ± 0.6
	BI	68.3 ± 0.2	2.6 ± 0.1	10.2 ± 0.0	0.5 ± 0.0

n/a: Not analyzed.

On the other hand, data from the total non-polar lipid (fatty acids) yield (Table 20) revealed that total extracted amounts were significantly higher after the FH process. It increased about 2 and 3 times for *Scenedesmus* sp. and *Nannochloropsis* sp. respectively.

Table 20. Total fatty acid yield of raw and BI microalgae selected for this study.

Algae Species	Lipid yield	
	Raw	BI
Scenedesmus sp.	1.4 ± 0.2	2.9 ± 0.1
Nannochloropsis sp.	3.0 ± 0.1	8.6 ± 0.1

To evaluate the lipid extraction process from the wet algal biomass, lipid yields from raw and BI of each algae species were compared from 15–240 min of extraction time (Figure 40).

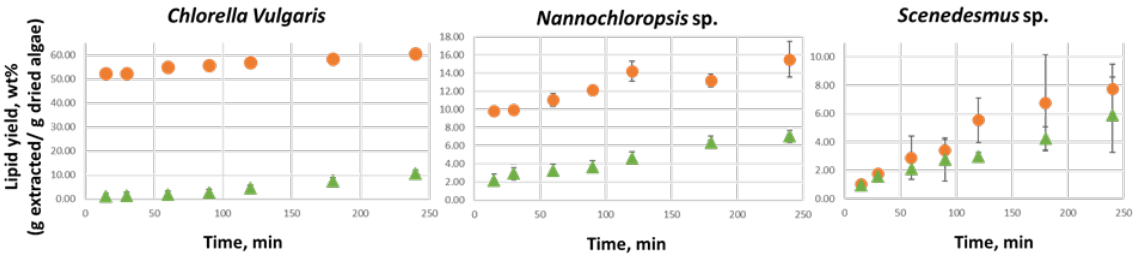

Figure 40. Lipid yields comparison of raw (green triangles) and biofuels intermediates/BI (orange dots) of *Chlorella v.* (left) *Nannochloropsis* sp. (center), and *Scenedesmus* sp. (right), over time. Error bars are the standard deviations.

Figure 40 shows, for all microalgae species and in all extraction times, BI of each microalgae produced higher lipid yields compared to raw/untreated algae. This difference in yields, proportionally increased as the total lipid content of algal biomass increased. In

other words, the FH process had substantial effect on lipid extractability of high lipid content microalgae such as *Chlorella v.* The lipid yields wt% of BI of *Chlorella v.* after 15 min extraction is more than 5 times higher than that of raw algae after 4 h of extraction time (52.3 ± 0.8 vs. 10.7 ± 0.9 wt%). This is approximately a 16-fold reduction in the extraction time in addition to the higher lipid yields. Table 21 presents the average lipid yields values of performed experiments for all three algal species including standard deviations. Many other studies have also investigated the effect of pretreatment methods on the extraction efficiency of biomass (S. Y. Lee, Cho, Chang, & Oh, 2017). A parametric study on lipid extraction after dilute acid pretreatment was conducted by impact of biochemical composition on susceptibility of algal biomass to acid-catalyzed pretreatment for sugar and lipid recovery (T. Dong et al., 2016). Cravotto *et al.* reported 50-500% increase in the lipid yield and up to 10-fold reduction in extraction time using combined effects of temperature, ultrasound, and microwave (Cravotto et al., 2008).

Table 21. Lipid yields values of performed experiments for all algal species (*Scenedesmus* sp., *Nannochloropsis* sp., and *Chlorella v.*) including standard deviations. Results are the average of duplicate experiments (± standard deviation)

	Chlorella v.		***Nannochloropsis* sp.**		***Scenedesmus* sp.**	
Time	Raw	BI	Raw	BI	Raw	BI
15	1.1 ± 0.1	52.3 ± 0.8	2.9 ± 0.2	9.8 ± 0.1	1.0 ± 0.3	1.0 ± 0.1
30	1.5 ± 0.6	52.4 ± 0.6	2.9 ± 0.1	9.9 ± 0.1	1.6 ± 0.1	1.8 ± 0.1
60	1.9 ± 0.3	55.2 ± 0.2	3.3 ± 0.2	11.1 ± 0.7	2.1 ± 0.8	2.9 ± 1.5

90	2.7 ± 1.1	55.9 ± 1.4	3.7 ± 0.0	12.2 ± 0.1	2.8 ± 1.5	3.4 ± 0.8
120	4.5 ± 1.0	56.9 ± 2.7	4.6 ± 0.5	14.2 ± 1.1	3.0 ± 0.3	5.6 ± 1.6
180	7.5 ± 0.8	58.6 ± 2.0	6.4 ± 1.4	13.2 ± 0.7	4.3 ± 0.8	6.8 ± 3.4
240	10.7 ± 0.9	60.8 ± 2.6	7.0 ± 1.6	15.5 ± 2.0	5.9 ± 2.7	7.8 ± 1.7

The rate constant (k) and reaction order of the lipid extractability of the three algal biomass are reported in the Table 22. The correlation factors (r^2) ranged between 0.9091 and 0.975. All algal species followed the zero-order reaction rate. This is different from the first-order kinetics of lipid extraction from wet algal biomass that was previously reported by Halim *et al.* studies (Halim et al., 2012; Halim et al., 2011).

Table 22. Reaction orders and constants (k) of the three algal species.

Algae species		**Reaction order**	**Reaction constant, k**	**Correlation factor, r^2**
***Scenedesmus* sp.**	Raw	0	0.022	0.9737
	BI	0	0.0325	0.9612
***Nannochloropsis* sp.**	Raw	0	0.0256	0.9091
	BI	2	0.0027	0.9411
Chlorella v.	Raw	0	0.043	0.975

	BI	2	0.0021	0.9485

On the other hand, we observed different behavior for the lipid extraction from BI of the three algal species. The susceptibility of biomass to pretreatment can be significantly affected by its biochemical composition (T. Dong et al., 2016). As presented in the Table 22, lipid extraction from the BI of *Scenedesmus* sp. followed a zero-order reaction rate, while this changed to a second-order reaction rate for the BI of *Nannochloropsis* sp. and *Chlorella v.* For the raw biomass, the extraction constant increased as the lipid content increased. However, there are multiple factors affecting the k value such as agitation/mixing of the algal biomass, ratio of organic solvent to dried microalgae, and the extraction temperature (Halim et al., 2012).

In order to verify whether the FH process might have affected the quality of extracted lipids, the FAME profile of the raw and BI for each microalga were compared and reported in the Table 23.

Table 23. Fatty acid compositions (w/w) of oils extracted from raw and biofuels intermediates (BI) of *Scenedesmus* sp., *Nannochloropsis* sp., and *Chlorella v.* microalgae. Values are weight percentage (wt%) of each fatty acid with respect to the total FAME identified. FAME with content less than 0.5% was not shown.

	***Scenedesmus* sp.**		***Nannochloropsis* sp.**		***Chlorella v.***	
	raw	BI	raw	BI	raw	BI
Total FAME	5.4 ±0.1	7.6 ±0.1	10.9 ±0.2	12.9 ±0.5	28.3 ±0.1	62.8 ±0.0
C16:0	24.4	38.3	15.8	29.9	24.4	25.7

C16:1	13.1	15.0	27.2	42.1	4.4	4.5
C16:2	3.0	1.9	0.5	0.4	2.4	2.3
C16:3	10.2	5.4	0.3	0.7	6.0	5.4
C16:4	1.5	0.6	0.0	0.0	2.0	1.7
C18:0	2.2	3.6	0.2	0.5	1.4	1.5
C18:1	10.6	14.2	3.6	5.9	23.6	23.8
C18:2	7.9	3.9	2.3	1.8	20.0	19.8
C18:3	22.0	6.8	0.1	0.1	14.0	12.4
C20:0	0.6	1.1	0.0	0.0	0.0	0.0
C20:3	0.0	0.0	1.4	0.4	0.0	0.0
C20:4	0.0	0.0	6.1	1.9	0.0	0.0
C20:5	0.0	0.0	38.1	9.1	0.0	0.0

The BI recovered after FH process showed 40.7, 18.3, and 121.9 wt% higher FAME content for *Scenedesmus* sp., *Nannochloropsis* sp., and *Chlorella v.*, respectively. This was expected due to the cell wall hydrolysis capability of subcritical water (Tao Dong, Eric P. Knoshaug, Philip T. Pienkos, et al., 2016). FFA is easier to be extracted from aqueous environment than bipolar phospholipids and FFA is a preferred biofuel precursor as well (Tao Dong et al., 2017). Moreover, phospholipids are known to be hydrolyzed to FFA under the FH condition (Levine et al., 2010). Lipid extracted from the BIs of microalgae demonstrated higher saturated fatty acids compared to raw biomass, which *Nannochloropsis* sp. owned the highest change from 16 to 30.4 wt% and *Chlorella v.* possessed the lowest change from 25.8 to 27.2 wt% of total fatty acids identified.

These saturated fatty acids are the most useful ones for biodiesel production (Steriti, Rossi, Concas, & Cao, 2014). Poly unsaturated fatty acids (PUFA) such as C16:4, C18:3, C20:3-5 are decreasing in the extracted lipids from the BI compared to the raw algae feedstock. This is desirable since PUFA are known to be responsible for the poor volatility, the low oxidation stability, and the direction towards gum formation in some oilseed-derived biodiesel (Halim et al., 2012).

Cetane number for diesel fuel in the United States is regulated at ≥ 40 and much higher in the European Union (EU) at ≥ 51 (Lapuerta et al., 2009). All algae species for this study pass regulations for the US and some for the EU. It is important to note that in the cases of all algae species, *Nannochloropsis* sp., *Scenedesmus* sp., and *Chlorella v.*, the biofuels intermediate have a higher CN number with an 18%, 15 % and 2% CN increase from raw algae to biofuel intermediate, respectively (Table 24). For biofuel intermediates, the species with the smallest percentage of unsaturated FA, *Scenedesmus* sp. yielded the higher CN although CN values were in the same range. Stansell et al. (Stansell et al., 2012) reported CN of algae species by class which can be compared to species used in this study. Eustigmatophycea, Cryptophycae, and Trebaouxiophycae the classes of *Nannochloropsis* sp., *Scenedesmus* sp., and *Chlorella v.* had cetane numbers of 52.3, 45.6 and 46.3, respectively. CNs calculated from biodiesel produced from this experiment suggest that biodiesel produced from biofuels intermediates result in a higher quality fuel and that all biodiesel produced (from raw algae/biofuel intermediates) exceeds regulations from U.S., making them a promising candidate for biodiesel usage.

Table 24. Cetane numbers of raw and biofuels intermediates (BI) of three algal species used in this study.

Algae species	**Treatment**	**CN**
Nannochloropsis sp.	Raw	44.9
Nannochloropsis sp.	BI	52.9
Scenedesmus sp.	Raw	46.1
Scenedesmus sp.	BI	53.0
Chlorella v.	Raw	49.1
Chlorella v.	BI	49.9

As stated earlier, in order to further confirm the enhanced lipid extractability of BI recovered after FH process, a typical HTL experiment was performed on both raw and BI of *Chlorella v.* microalgae. Figure 41 revealed weight percentage of product yields after the HTL process. As demonstrated, the biocrude yield from the HTL experiment of the raw algae is 43.3 wt%. This is similar to the Brown *et al.* study that conducted HTL on *Nannochloropsis* sp. with the same lipid content at the same conditions (T. M. Brown, Duan, & Savage, 2010). It is expected that microalgae with various biochemical compositions resulted in different biocrude yields (Sheehan & Savage, 2017). However, no similar studies on the biocrude yields from the HTL process on the post-algae hydrolysis residue were found.

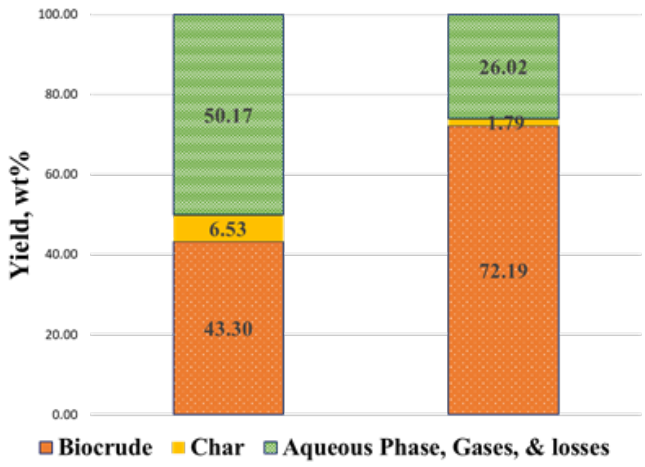

Figure 41. Comparison of HTL product yields at 350 ºC and 1 h reaction time for untreated (left bar) and BI (right bar) of *Chlorella v.* microalgae.

HTL on the BI of *Chlorella v.* produced 72.2 wt % of biocrude, which is about 66.7 wt% higher yield compared to the raw/untreated microalgae. Furthermore, lesser amount of char and aqueous phase were observed. The biocrude yield of BI as a feedstock, is much higher compared to many recent studies, which are in the range of 50-60 wt% (Chiaramonti, Prussi, Buffi, Rizzo, & Pari, 2017). The biocrude yield and composition depends on the loading concentration, temperature, residence time, and the use of catalyst (Chiaramonti et al., 2017). In addition, the quality of the recovered biocrude were always a matter of concern. The results from elemental analysis were shown in the Table 25. As indicated in Table 25, the H/C atomic ratio improved from 1.55 in the biocrude recovered from the raw algae to 1.74 for the biocrude yield from HTL of BI. The N/C atomic ratio also improved to a lower value of 0.016 (about 50% reduction). The oxygen content of the biocrude had a marginal decrease of 0.2 wt%, which is probably the reason for higher heating value of biocrude yield from the BI

feedstock (Table 25) (R. Wei et al., 2017). This HHV value is higher than prior studies which ranged between 33–39 MJ/kg (Anastasakis & Ross, 2011; Biller & Ross, 2011b).

Table 25. Elemental composition of the biocrude obtained through hydrothermal liquefaction of *Chlorella v.* microalgae. All Values are weight percentage ±standard deviation. The total values are slightly (<1 wt%) above 100, since all elements are the averages of measured values.

Feedstock	C (wt%)	N (wt%)	H (wt%)	O (wt%)	H/C	N/C	HHV (MJ/kg)
Chlorella v. - raw	76.6 ±0.3	2.8 ±0.0	9.9 ±0.1	10.9 ±0.4	1.55	0.031	38.1
Chlorella v. - BI	76.9 ±0.4	1.4 ±0.0	11.2 ±0.1	10.7 ±0.0	1.74	0.016	40.0

In order to evaluate the boiling point distribution of the biocrudes, TG analysis was performed. Results from TGA were plotted in the Figure 42. This process can be interpreted as a miniature distillation (W.-T. Chen et al., 2014).

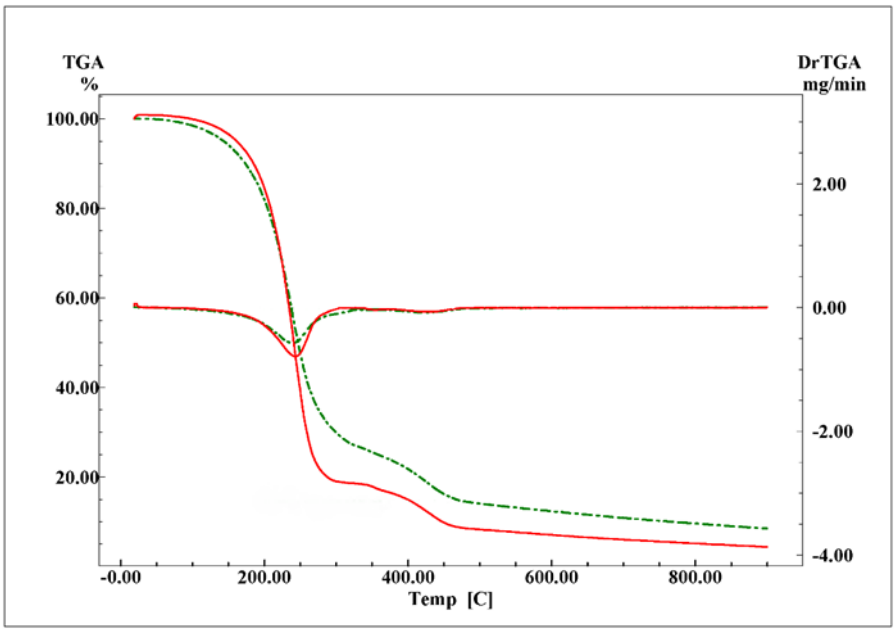

Figure 42. TGA comparison of biocrude recovered after hydrothermal liquefaction of raw (green) and biofuels intermediates, BI, (red) of *Chlorella v.* The peaks in derivative graph for raw and BI biocrude happened at 239.5 and 243.3 ºC respectively.

The detailed comparison of biocrudes boiling point distribution is reported in Table 26. Biocrude yield from the HTL experiment of BI showed higher weight loss in the overall process under inert environment (96.4 wt% compared to 91.5 wt%). This verifies the higher presence of volatiles and less amount of ash and residues in the biocrude. Losses below 120 ℃ were due to drying of water and any remained solvent. Distillation of biocrude obtained from the BI feedstock showed lower fractions in all ranges above 300 °C. This, however, contributes to higher fraction (65.7 wt%) distilled between 200 and 300 °C, which is the range for jet fuel and diesel oil.

Table 26. Boiling point distribution of the biocrudes (wt%).

Distillate range, ℃	**Typical application of the coke oil (W.-T. Chen et al., 2014)**	**Raw algae biocrude**	**BI biocrude**
20-110	Bottle gas and chemicals	2.1	1.2
110-200	Gasoline	15.8	14.9
200-300	Jet fuel, fuel for stoves, and diesel oil	52.2	65.7
300-400	Lubricating oil for engines, fuel for ships, and machines	8.1	3.9
400-550	Lubricants and candles, fuel for ships	8.6	7.3
550-700	Fuel for ships, factories, and central heating	2.3	1.6
700-800	Asphalt and roofing	1.2	0.8
800-900	Residues	1.1	0.8

Another way to compare biocrude obtained from raw *Chlorella v.* and its BI, is the CNH elemental balance alongside the process (Figure 43). As illustrated, solid residues are much less when BI is subjected to the HTL process. This is partially, due to the FH contribution to the ash diminution in the BI macro-molecules (Teymouri, Kumar, et al., 2017). Another interesting merit of the FH process prior to the regular HTL, is the capability to extract nutrients in the forms of amino acids and soluble peptides in the hydrolysate (Garcia-Moscoso et al., 2015). This integration significantly reduced the

nutrients, particularly nitrogen content in the biocrude. Comparing elemental balance in the Figure 43, biocrude obtained from the raw algae (section a) carried up to 42.6 wt% of the total nitrogen content of the original microalgae, versus only 12.3 wt% of that in the biocrude obtained from BI (section b). Nitrogen content reduction in the biocrude is desirable to minimize the amount of NO_x formation during the combustion and to move forward with the upgrading process (Anastasakis & Ross, 2011; G. Yu et al., 2011).

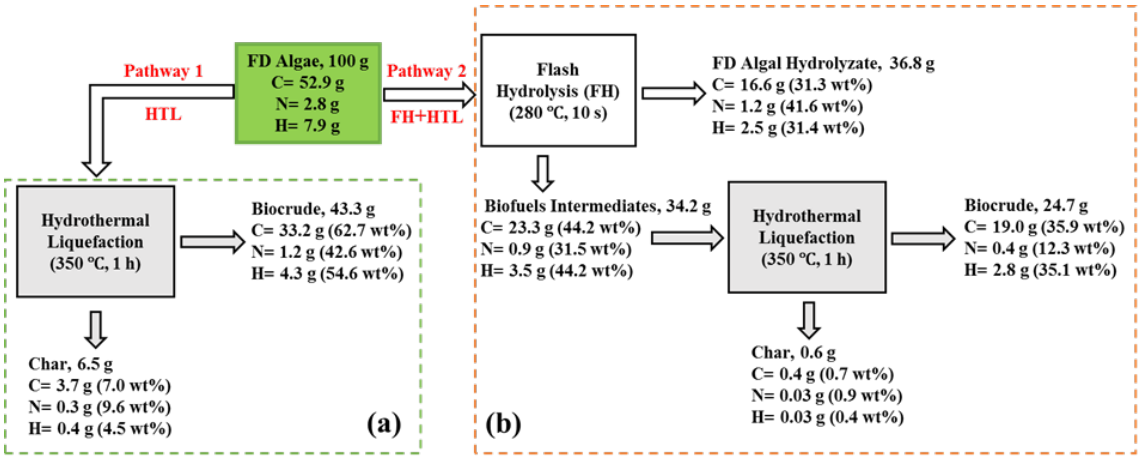

Figure 43. CNH elemental balance and product yields after hydrothermal liquefaction of raw *Chlorella v.* Microalgae (a) and its BI (b). CNH weights (g) in every stage is based on the total input weight of each element in the original freeze dried (FD) algae. Weight percentages (wt%) shown in the parenthesis calculated as: grams of the element recovered in that stage / grams of that element initially entered the system. CNH values regarding gas and aqueous phase is excluded.

Although, the overall biocrude yield in the HTL of the untreated algae is higher, it is worth considering the higher quality of biocrude obtained from the HTL of BI, in addition to all other potential bioproducts recovered from the algal hydrolysate (Barbera et al., 2017; Jose Luis Garcia-Moscoso et al., 2013; Garcia-Moscoso et al., 2015;

Sandeep Kumar et al., 2014). Finally, a life cycle assessment (LCA) and techno-economic analysis (TEA) is recommended to value the scalability of this study.

6.4. Conclusions

This study investigated the effect of flash hydrolysis (FH) process on the lipid extractability of three microalgae species including *Scenedesmus* sp., *Nannochloropsis* sp., and *Chlorella vulgaris*. Results revealed that FH process significantly improved the lipid extraction of wet algal biomass by both reducing the extraction time and increasing the yield. Kinetics studies' results indicated that wet extraction of untreated algal biomass followed a zero-order reaction rate; however, biofuels intermediates (BI) that recovered from FH at 280 ℃ and 10 s, followed a second-order rate (BI of *Scenedesmus* sp. exceptionally followed zeroth order). Fatty acid profile comparison of raw and BI of each microalga showed the contribution by FH by increasing the percentage of saturated FAMEs in the profile. Biocrude yield via hydrothermal liquefaction (HTL) of *Chlorella v.* BI was higher (72.2 wt%) compared to the raw algae (43.3 wt%). It contained less amount of nitrogen, oxygen, and higher H/C ratio. TGA results also implied that the wt% of jet fuel and diesel range distillate increased in the BI of *Chlorella v.*

6.5. Acknowledgments

The authors would like to acknowledge Dr. Ryan Davis at Sandia National Laboratories for providing the *Nannochloropsis* sp. biomass used for this study and the National Science Foundation (NSF) for the financial support of this work through the NSF CAREER Award# 1351413 and PFI: AIR TT Grant# 1640593.

CHAPTER 7

RECOMMENDATIONS FOR FUTURE WORKS

In this study, hydrothermal processing techniques such as flash hydrolysis were applied on microalgae feedstock to extract macro-nutrients such as phosphorus and nitrogen in the hydrolysate, while preserving the lipids in the solid fraction known as biofuels intermediates. The nutrient-rich hydrolysate either recycled for algal cultivation or converted to value-added bioproducts such as amino acids, peptides, hydroxyapatite, and dittmerite. While this research has provided useful applications regarding nutrients management in algal processing, several opportunities for extending the scope of this research remain to discuss in future as follows:

In chapter 2 of this dissertation, flash hydrolysis was used to solubilize peptides and arginine in the hydrolysate as two high value bioproducts in the algae processing, while lipids were preserved in the biofuels intermediates. The effects of temperature and residence time on the yield of both bioproducts were investigated. However, it is suggested that this process further be optimized for maximum yields of sugar from the microalgae.

In chapter 3, the viability of FH process for a lipid-rich, high-ash marine microalgae was evaluated. Due to the promising results in applying this hydrothermal technique for nutrients extraction on algal biomass, it is suggested to investigate the effect of FH process on the nutrients removal efficiency from other feedstocks such as sewage sludge. This will direct this process to a whole new industry and potentially provide funding opportunities from wastewater treatment industries.

Through chapter 4 of this study, dittmarite and hydroxyapatite were produced from *Scenedesmus* sp. microalgae through the FH-HTM and FH-AP pathways. These integrated approaches could be applied to any phosphate or/and nitrogen rich medium such as municipal, agricultural, and industrial wastewater streams to remove nutrients in forms of valuable products. It is suggested to further expand this study to a pilot plant scale targeting waste streams in dairy industries that are usually very rich in phosphorus. The synthesized HAp through this study can be evaluated for catalytic applications such as biocrude upgradation after the HTL process. In addition, the biomedical applications of HAp synthesis from the microalgae worth studying since the HAp is originated from a natural source and is expected to have higher chance to get accepted by the human organisms. On the other hand, the integrated FH-AP process resulted in a dittmerite synthesis from an algal biomass. However, the phosphate removal was about 67 wt% and has the potential to be improved. It is highly recommended to evaluate the effect of pH (in the range of 7–11) and different mineralizers on the nutrient removal percentage from the hydrolysate to increase the process efficiency.

In chapter 5, the effect of reaction time on the calcium phosphate minerals were investigated. Although, it was demonstrated that after 90 min of reaction time synthetic HAp had the Ca/P molar ratio of 1.67 (same as the theoretical HAp), the effect of hydrothermal reaction temperature was never considered. It is recommended to continue this study to determine the effect of temperature on the structure of the precipitate HAp. Moreover, since nano range HAp particles have higher interest due to their wider biomedical applications, using organic modifiers such as ethylenediamminetetraacetic

acid (EDTA, $C_{10}H_{16}N_2O_8$) is highly recommended to precipitate HAp nanoparticles with controlled structure.

Chapter 6 evaluated the effect of FH process on the lipid extractability of three algal species. The higher yields and the premium quality of the biocrude obtained from the HTL of biofuels intermediates compared to the untreated microalgae was also demonstrated. However, the reaction conditions of HTL process was selected based on a typical HTL conditions and definitely have the potential to be optimized for higher biocrude yield, lower nitrogen content, and higher H/C ratio. In order to value this study a comprehensive Aspen plus modeling that includes techno-economic analysis is suggested to simultaneously take into account all processes based on the actual experimental data and calculated kinetics from this study. Furthermore due to the significant health benefits of omega-3 fatty acids and thus their high demand and marketability, similar research could be performed to evaluate the effect of FH process on the extractability of eicosapentaenoic acid (EPA, 20:5) and docosahexaenoic acid (DHA, 22:6) in a lipid-rich microalgae. It is also suggested that an efficient cultivation system developed to address the global need for omega-3 fatty acids through efficient growth of lipid-rich algal biomass. There are many other potential markets for high value bioproducts from microalgae such as astaxanthin. A comprehensive study can target astaxanthin-rich microalgae such as *Haematococcus* sp. to increase its cultivation efficiency or optimize its extraction from the wet algal biomass with techniques such as FH. Providing all these multiple pathways will enhance the algal biomass commercialization potential as a sustainable feedstock for feed and fuel.

REFERENCES

Abbona, F., Lundager Madsen, H. E., & Boistelle, R. (1982). Crystallization of two magnesium phosphates, struvite and newberyite: Effect of pH and concentration. *Journal of Crystal Growth, 57*(1), 6-14. doi:http://dx.doi.org/10.1016/0022-0248(82)90242-1

Abdelmoez, W., Nakahasi, T., & Yoshida, H. (2007). Amino acid transformation and decomposition in saturated subcritical water conditions. *Industrial & Engineering Chemistry Research, 46*(16), 5286-5294.

Ahmad, A. L., Yasin, N. H. M., Derek, C. J. C., & Lim, J. K. (2011). Microalgae as a sustainable energy source for biodiesel production: A review. *Renewable and Sustainable Energy Reviews, 15*(1), 584-593. doi:http://dx.doi.org/10.1016/j.rser.2010.09.018

Ali Teymouri, B. S., Sandeep Kumar. (2017). *Kinetics of phosphate precipitation from the nutrients-rich algal hydrolyzate*. Paper presented at the The 253rd ACS National Meeting, San Francisco, California. https://ep70.eventpilot.us/web/page.php?page=Session&project=ACS17SPRING&id=2658421

Anastasakis, K., & Ross, A. B. (2011). Hydrothermal liquefaction of the brown macro-alga Laminaria Saccharina: Effect of reaction conditions on product distribution and composition. *Bioresour Technol, 102*(7), 4876-4883. doi:https://doi.org/10.1016/j.biortech.2011.01.031

Arakawa, T., Tsumoto, K., Kita, Y., Chang, B., & Ejima, D. (2007). Biotechnology applications of amino acids in protein purification and formulations. *Amino acids, 33*(4), 587-605.

Azzaoui, K., Lamhamdi, A., Mejdoubi, E. M., Berrabah, M., Hammouti, B., Elidrissi, A., . . . Al-Deyab, S. S. (2014). Synthesis and characterization of composite based on cellulose acetate and hydroxyapatite application to the absorption of harmful substances. *Carbohydrate Polymers, 111*, 41-46. doi:http://dx.doi.org/10.1016/j.carbpol.2014.04.058

Balasubramanian, R. K., Yen Doan, T. T., & Obbard, J. P. (2013). Factors affecting cellular lipid extraction from marine microalgae. *Chemical Engineering Journal, 215*(Supplement C), 929-936. doi:https://doi.org/10.1016/j.cej.2012.11.063

Barbera, E., Sforza, E., Kumar, S., Morosinotto, T., & Bertucco, A. (2016). Cultivation of Scenedesmus obliquus in liquid hydrolysate from flash hydrolysis for nutrient recycling. *Bioresour Technol, 207*, 59-66. doi:http://dx.doi.org/10.1016/j.biortech.2016.01.103

Barbera, E., Teymouri, A., Bertucco, A., Stuart, B. J., & Kumar, S. (2017). Recycling Minerals in Microalgae Cultivation through a Combined Flash Hydrolysis–Precipitation Process. *ACS Sustainable Chemistry & Engineering, 5*(1), 929-935. doi:10.1021/acssuschemeng.6b02260

Becker, E. W. (2007a). Micro-algae as a source of protein. *Biotechnology Advances, 25*(2), 207-210. doi:http://dx.doi.org/10.1016/j.biotechadv.2006.11.002

Becker, E. W. (2007b). Micro-algae as a source of protein. *Biotechnol Adv, 25*(2), 207-210. doi:10.1016/j.biotechadv.2006.11.002

Benemann, J. R., Weissmann, J. C., Koopman, B. L., & Oswald, W. J. (1977). Energy production by microbial photosynthesis. *Nature, 268*(5615), 19-23.

Berzina-Cimdina, L., & Borodajenko, N. (2012). Research of calcium phosphates using Fourier transform infrared spectroscopy *Infrared Spectroscopy-Materials Science, Engineering and Technology*: InTech.

Bettin, F. (2013). Treating urban wastewaters with microalgae: batch and continuous flow experiments and preliminary process design.

Bhuiyan, M. I. H., Mavinic, D. S., & Koch, F. A. (2008). Thermal decomposition of struvite and its phase transition. *Chemosphere, 70*(8), 1347-1356. doi:http://dx.doi.org/10.1016/j.chemosphere.2007.09.056

Bi, Z., & He, B. B. (2013). Characterization of Microalgae for the Purpose of Biofuel Production. *Transactions of the ASABE, 56*(4), 1529-1539.

Biller, P., & Ross, A. B. (2011a). Potential yields and properties of oil from the hydrothermal liquefaction of microalgae with different biochemical content. *Bioresour Technol, 102*(1), 215-225. doi:http://dx.doi.org/10.1016/j.biortech.2010.06.028

Biller, P., & Ross, A. B. (2011b). Potential yields and properties of oil from the hydrothermal liquefaction of microalgae with different biochemical content. *Bioresour Technol, 102*(1), 215-225. doi:10.1016/j.biortech.2010.06.028

Biller, P., & Ross, A. B. (2014). Pyrolysis GC–MS as a novel analysis technique to determine the biochemical composition of microalgae. *Algal Research, 6*, 91-97. doi:10.1016/j.algal.2014.09.009

Biller, P., Ross, A. B., Skill, S. C., Lea-Langton, A., Balasundaram, B., Hall, C., . . . Llewellyn, C. A. (2012a). Nutrient recycling of aqueous phase for microalgae cultivation from the hydrothermal liquefaction process. *Algal Research-Biomass Biofuels and Bioproducts, 1*(1), 70-76. doi:DOI 10.1016/j.algal.2012.02.002

Biller, P., Ross, A. B., Skill, S. C., Lea-Langton, A., Balasundaram, B., Hall, C., . . . Llewellyn, C. A. (2012b). Nutrient recycling of aqueous phase for microalgae cultivation from the hydrothermal liquefaction process. *Algal Research, 1*(1), 70-76. doi:http://dx.doi.org/10.1016/j.algal.2012.02.002

Bligh, E. G., & Dyer, W. J. (1959). A rapid method of total lipid extraction and purification. *Canadian journal of biochemistry and physiology, 37*(8), 911-917.

Boskey, A. L., & Posner, A. S. (1973). Conversion of amorphous calcium phosphate to microcrystalline hydroxyapatite. A pH-dependent, solution-mediated, solid-solid conversion. *The Journal of Physical Chemistry, 77*(19), 2313-2317. doi:10.1021/j100638a011

Bouropoulos, N. C., & Koutsoukos, P. G. (2000). Spontaneous precipitation of struvite from aqueous solutions. *Journal of Crystal Growth, 213*(3–4), 381-388. doi:http://dx.doi.org/10.1016/S0022-0248(00)00351-1

Bridger, G. L., Salutsky, M. L., & Starostka, R. W. (1962). Micronutrient Sources, Metal Ammonium Phosphates as Fertilizers. *Journal of Agricultural and Food Chemistry, 10*(3), 181-188. doi:10.1021/jf60121a006

Brown, P. W., & Fulmer, M. (1991). Kinetics of Hydroxyapatite Formation at Low Temperature. *Journal of the American Ceramic Society, 74*(5), 934-940. doi:10.1111/j.1151-2916.1991.tb04324.x

Brown, T. M., Duan, P., & Savage, P. E. (2010). Hydrothermal Liquefaction and Gasification of Nannochloropsis sp. *Energy & Fuels, 24*(6), 3639-3646. doi:10.1021/ef100203u

Caleb Talbot, J. G.-M., Hannah Drake, and Sandeep Kumar. (2016). Cultivation of Microalgae Using Flash Hydrolysis Nutrients Recycle. *Algal Research*.

Canter, C. E., Blowers, P., Handler, R. M., & Shonnard, D. R. (2015). Implications of widespread algal biofuels production on macronutrient fertilizer supplies: Nutrient demand and evaluation of potential alternate nutrient sources. *Applied Energy, 143*, 71-80. doi:10.1016/j.apenergy.2014.12.065

Chakinala, A. G., Brilman, D. W., van Swaaij, W. P., & Kersten, S. R. (2009). Catalytic and non-catalytic supercritical water gasification of microalgae and glycerol. *Industrial & Engineering Chemistry Research, 49*(3), 1113-1122.

Chan, Y. H., Quitain, A. T., Yusup, S., Uemura, Y., Sasaki, M., & Kida, T. (2017). Optimization of hydrothermal liquefaction of palm kernel shell and consideration of supercritical carbon dioxide mediation effect. *The Journal of Supercritical Fluids*. doi:https://doi.org/10.1016/j.supflu.2017.06.007

Chauhan, C. K. (2012). Growth and characterization of struvite and related crystals.

Chauhan, C. K., Joseph, K., Parekh, B., & Joshi, M. (2008). Growth and characterization of struvite crystals. *Indian Journal of Pure & Applied Physics, 46*(7), 507.

Chemat, S. (2017). *Edible Oils: Extraction, Processing, and Applications*: CRC Press.

Chen, C.-Y., Yeh, K.-L., Aisyah, R., Lee, D.-J., & Chang, J.-S. (2011). Cultivation, photobioreactor design and harvesting of microalgae for biodiesel production: a critical review. *Bioresour Technol, 102*(1), 71-81.

Chen, W.-T., Zhang, Y., Zhang, J., Yu, G., Schideman, L. C., Zhang, P., & Minarick, M. (2014). Hydrothermal liquefaction of mixed-culture algal biomass from wastewater treatment system into bio-crude oil. *Bioresour Technol, 152*(Supplement C), 130-139. doi:https://doi.org/10.1016/j.biortech.2013.10.111

Chen, X., Kong, H., Wu, D., Wang, X., & Lin, Y. (2009). Phosphate removal and recovery through crystallization of hydroxyapatite using xonotlite as seed crystal. *Journal of Environmental Sciences, 21*(5), 575-580. doi:http://dx.doi.org/10.1016/S1001-0742(08)62310-4

Chiaramonti, D., Prussi, M., Buffi, M., Rizzo, A. M., & Pari, L. (2017). Review and experimental study on pyrolysis and hydrothermal liquefaction of microalgae for biofuel production. *Applied Energy, 185*(Part 2), 963-972. doi:https://doi.org/10.1016/j.apenergy.2015.12.001

Chisti, Y. (2007). Biodiesel from microalgae. *Biotechnology Advances, 25*(3), 294-306. doi:http://dx.doi.org/10.1016/j.biotechadv.2007.02.001

Correll, D. L. (1998). The Role of Phosphorus in the Eutrophication of Receiving Waters: A Review. *Journal of Environmental Quality, 27*(2). doi:10.2134/jeq1998.00472425002700020004x

Council, N. R. (2012). *Sustainable Development of Algal Biofuels in the United States*. Washington, DC: The National Academies Press.

Cravotto, G., Boffa, L., Mantegna, S., Perego, P., Avogadro, M., & Cintas, P. (2008). Improved extraction of vegetable oils under high-intensity ultrasound and/or microwaves. *Ultrasonics Sonochemistry, 15*(5), 898-902. doi:https://doi.org/10.1016/j.ultsonch.2007.10.009

Crutchik, D., & Garrido, J. M. (2011). Struvite crystallization versus amorphous magnesium and calcium phosphate precipitation during the treatment of a saline industrial wastewater. *Water Science and Technology, 64*(12), 2460-2467. doi:10.2166/wst.2011.836

Davis, R., Fishman, D., Frank, E. D., Wigmosta, M. S., Aden, A., Coleman, A. M., . . . Wang, M. Q. (2012). *Renewable diesel from algal lipids: an integrated baseline for cost, emissions, and resource potential from a harmonized model*. Retrieved from

Davis, R. E., Fishman, D. B., Frank, E. D., Johnson, M. C., Jones, S. B., Kinchin, C. M., . . . Wigmosta, M. S. (2014). Integrated Evaluation of Cost, Emissions, and Resource Potential for Algal Biofuels at the National Scale. *Environmental Science & Technology, 48*(10), 6035-6042. doi:10.1021/es4055719

Davis, R. W., Siccardi Iii, A. J., Huysman, N. D., Wyatt, N. B., Hewson, J. C., & Lane, T. W. (2015). Growth of mono- and mixed cultures of Nannochloropsis salina and Phaeodactylum tricornutum on struvite as a nutrient source. *Bioresour Technol, 198*, 577-585. doi:http://dx.doi.org/10.1016/j.biortech.2015.09.070

Dean, A. P., Sigee, D. C., Estrada, B., & Pittman, J. K. (2010). Using FTIR spectroscopy for rapid determination of lipid accumulation in response to nitrogen limitation in freshwater microalgae. *Bioresource Technology, 101*(12), 4499-4507. doi:http://dx.doi.org/10.1016/j.biortech.2010.01.065

Demeestere, K., Smet, E., Van Langenhove, H., & Galbacs, Z. (2001). Optimalisation of Magnesium Ammonium Phosphate Precipitation and Its Applicability to the Removal of Ammonium. *Environmental Technology, 22*(12), 1419-1428. doi:10.1080/09593332208618177

Demirbas, A., & Fatih Demirbas, M. (2011). Importance of algae oil as a source of biodiesel. *Energy Conversion and Management, 52*(1), 163-170. doi:http://dx.doi.org/10.1016/j.enconman.2010.06.055

Destainville, A., Champion, E., Bernache-Assollant, D., & Laborde, E. (2003). Synthesis, characterization and thermal behavior of apatitic tricalcium phosphate. *Materials Chemistry and Physics, 80*(1), 269-277. doi:http://dx.doi.org/10.1016/S0254-0584(02)00466-2

Diallo-Garcia, S., Laurencin, D., Krafft, J.-M., Casale, S., Smith, M. E., Lauron-Pernot, H., & Costentin, G. (2011). Influence of Magnesium Substitution on the Basic Properties of Hydroxyapatites. *The Journal of Physical Chemistry C, 115*(49), 24317-24327. doi:10.1021/jp209316k

Dong, T., Fei, Q., Genelot, M., Smith, H., Laurens, L. M. L., Watson, M. J., & Pienkos, P. T. (2017). A novel integrated biorefinery process for diesel fuel blendstock production using lipids from the methanotroph, Methylomicrobium buryatense. *Energy Conversion and Management, 140*(Supplement C), 62-70. doi:https://doi.org/10.1016/j.enconman.2017.02.075

Dong, T., Knoshaug, E. P., Davis, R., Laurens, L. M. L., Van Wychen, S., Pienkos, P. T., & Nagle, N. (2016). Combined algal processing: A novel integrated biorefinery process to produce algal biofuels and bioproducts. *Algal Research, 19*(Supplement C), 316-323. doi:https://doi.org/10.1016/j.algal.2015.12.021

Dong, T., Knoshaug, E. P., Pienkos, P. T., & Laurens, L. M. L. (2016). Lipid recovery from wet oleaginous microbial biomass for biofuel production: A critical review. *Applied Energy, 177*, 879-895. doi:http://dx.doi.org/10.1016/j.apenergy.2016.06.002

Dong, T., Van Wychen, S., Nagle, N., Pienkos, P. T., & Laurens, L. M. L. (2016). Impact of biochemical composition on susceptibility of algal biomass to acid-catalyzed pretreatment for sugar and lipid recovery. *Algal Research, 18*(Supplement C), 69-77. doi:https://doi.org/10.1016/j.algal.2016.06.004

Doyle, J. D., & Parsons, S. A. (2002). Struvite formation, control and recovery. *Water Research, 36*(16), 3925-3940. doi:http://dx.doi.org/10.1016/S0043-1354(02)00126-4

Duan, P., & Savage, P. E. (2011). Catalytic hydrothermal hydrodenitrogenation of pyridine. *Applied Catalysis B: Environmental, 108-109*(Supplement C), 54-60. doi:https://doi.org/10.1016/j.apcatb.2011.08.007

Eboibi, B. E., Lewis, D. M., Ashman, P. J., & Chinnasamy, S. (2014). Effect of operating conditions on yield and quality of biocrude during hydrothermal liquefaction of halophytic microalga Tetraselmis sp. *Bioresour Technol, 170*(Supplement C), 20-29. doi:https://doi.org/10.1016/j.biortech.2014.07.083

Eilliot, J. (1994). Structure and Chemistry of the Apatite and other Calcium Orthophosphate: Elsevier, Amsterdam.

Elliott, D. C., Hart, T. R., Neuenschwander, G. G., Rotness, L. J., Roesijadi, G., Zacher, A. H., & Magnuson, J. K. (2013). Hydrothermal processing of macroalgal feedstocks in continuous-flow reactors. *ACS Sustainable Chemistry & Engineering, 2*(2), 207-215.

Elliott, D. C., Hart, T. R., Schmidt, A. J., Neuenschwander, G. G., Rotness, L. J., Olarte, M. V., . . . Holladay, J. E. (2013). Process development for hydrothermal liquefaction of algae feedstocks in a continuous-flow reactor. *Algal Research, 2*(4), 445-454.

Elliott, J. C. (2013). *Structure and chemistry of the apatites and other calcium orthophosphates* (Vol. 18): Elsevier.

Erickson, D. R. (2015). *Practical handbook of soybean processing and utilization*: Elsevier.

Esakkimuthu, S., Krishnamurthy, V., Govindarajan, R., & Swaminathan, K. (2016). Augmentation and starvation of calcium, magnesium, phosphate on lipid production of Scenedesmus obliquus. *Biomass and Bioenergy, 88*, 126-134. doi:http://dx.doi.org/10.1016/j.biombioe.2016.03.019

Esteban, M. B., Garcia, A. J., Ramos, P., & Marquez, M. C. (2008). Kinetics of amino acid production from hog hair by hydrolysis in sub-critical water. *Journal of Supercritical Fluids, 46*(2), 137-141. doi:DOI 10.1016/j.supflu.2008.04.008

Esteban, M. B., García, A. J., Ramos, P., & Márquez, M. C. (2008). Kinetics of amino acid production from hog hair by hydrolysis in sub-critical water. *The Journal of Supercritical Fluids, 46*(2), 137-141. doi:http://dx.doi.org/10.1016/j.supflu.2008.04.008

Fadeev, I. V., Shvorneva, L. I., Barinov, S. M., & Orlovskii, V. P. (2003). Synthesis and Structure of Magnesium-Substituted Hydroxyapatite. *Inorganic Materials, 39*(9), 947-950. doi:10.1023/a:1025509305805

Felício-Fernandes, G., & Laranjeira, M. C. M. (2000). Calcium phosphate biomaterials from marine algae. Hydrothermal synthesis and characterisation. *Química Nova, 23*, 441-446.

Ferraz, M., Monteiro, F., & Manuel, C. (2004). Hydroxyapatite nanoparticles: a review of preparation methodologies. *Journal of Applied Biomaterials and Biomechanics, 2*(2), 74-80.

Foletto, E. L., Santos, W. R. B. d., Mazutti, M. A., Jahn, S. L., & Gündel, A. (2013). Production of struvite from beverage waste as phosphorus source. *Materials Research, 16*, 242-245.

Garcia-Moscoso, J. L., Obeid, W., Kumar, S., & Hatcher, P. G. (2013). Flash hydrolysis of microalgae (Scenedesmus sp.) for protein extraction and production of biofuels intermediates. *Journal of Supercritical Fluids, 82*(0), 183-190. doi:DOI 10.1016/j.supflu.2013.07.012

Garcia-Moscoso, J. L., Obeid, W., Kumar, S., & Hatcher, P. G. (2013). Flash hydrolysis of microalgae (Scenedesmus sp.) for protein extraction and production of biofuels intermediates. *The Journal of Supercritical Fluids, 82*, 183-190. doi:http://dx.doi.org/10.1016/j.supflu.2013.07.012

Garcia-Moscoso, J. L., Teymouri, A., & Kumar, S. (2015). Kinetics of Peptides and Arginine Production from Microalgae (Scenedesmus sp.) by Flash Hydrolysis.

Industrial & Engineering Chemistry Research, 54(7), 2048-2058. doi:10.1021/ie5047279

Garcia Alba, L., Torri, C., Fabbri, D., Kersten, S. R. A., & Brilman, D. W. F. (2013). Microalgae growth on the aqueous phase from Hydrothermal Liquefaction of the same microalgae. *Chemical Engineering Journal, 228*, 214-223. doi:http://dx.doi.org/10.1016/j.cej.2013.04.097

Gençer, E., & Agrawal, R. (2016). A commentary on the US policies for efficient large scale renewable energy storage systems: Focus on carbon storage cycles. *Energy Policy, 88*, 477-484. doi:http://dx.doi.org/10.1016/j.enpol.2015.11.003

Gibson, I. R., Rehman, I., Best, S. M., & Bonfield*, W. (2000). Characterization of the transformation from calcium-deficient apatite to β-tricalcium phosphate. *Journal of Materials Science: Materials in Medicine, 11*(12), 799-804. doi:10.1023/a:1008905613182

Giordano, M., Kansiz, M., Heraud, P., Beardall, J., Wood, B., & McNaughton, D. (2001). Fourier transform infrared spectroscopy as a novel tool to investigate changes in intracellular macromolecular pools in the marine microalga Chaetoceros muellerii (Bacillariophyceae). *Journal of Phycology, 37*(2), 271-279. doi:DOI 10.1046/j.1529-8817.2001.037002271.x

Glansdorff, N., & Xu, Y. (2006). Microbial arginine biosynthesis: pathway, regulation and industrial production *Amino acid biosynthesis~ pathways, regulation and metabolic engineering* (pp. 219-257): Springer.

Gollakota, A. R. K., Kishore, N., & Gu, S. (2017). A review on hydrothermal liquefaction of biomass. *Renewable and Sustainable Energy Reviews*. doi:https://doi.org/10.1016/j.rser.2017.05.178

Gopal, R., Calvo, C., Ito, J., & Sabine, W. K. (1974). Crystal Structure of Synthetic Mg-Whitlockite, Ca18Mg2H2(PO4)14. *Canadian Journal of Chemistry, 52*(7), 1155-1164. doi:10.1139/v74-181

Gouveia, L., & Oliveira, A. C. (2009). Microalgae as a raw material for biofuels production. *Journal of industrial microbiology & biotechnology, 36*(2), 269-274.

Griffiths, M. J., & Harrison, S. T. (2009). Lipid productivity as a key characteristic for choosing algal species for biodiesel production. *Journal of Applied Phycology, 21*(5), 493-507.

Gross, K. A., Gross, V., & Berndt, C. C. (1998). Thermal Analysis of Amorphous Phases in Hydroxyapatite Coatings. *Journal of the American Ceramic Society, 81*(1), 106-112. doi:10.1111/j.1151-2916.1998.tb02301.x

Grover, P. K., Kim, D.-S., & Ryall, R. L. (2002). The effect of seed crystals of hydroxyapatite and brushite on the crystallization of calcium oxalate in undiluted human urine in vitro: implications for urinary stone pathogenesis. *Molecular Medicine, 8*(4), 200-209.

Gunay, A., Karadag, D., Tosun, I., & Ozturk, M. (2008). Use of magnesit as a magnesium source for ammonium removal from leachate. *Journal of Hazardous*

Materials, 156(1–3), 619-623. doi:http://dx.doi.org/10.1016/j.jhazmat.2007.12.067

Guo, Y., Wang, S., Huelsman, C. M., & Savage, P. E. (2013). Products, pathways, and kinetics for reactions of indole under supercritical water gasification conditions. *The Journal of Supercritical Fluids, 73*, 161-170.

Guo, Y., Yeh, T., Song, W., Xu, D., & Wang, S. (2015). A review of bio-oil production from hydrothermal liquefaction of algae. *Renewable and Sustainable Energy Reviews, 48*(Supplement C), 776-790. doi:https://doi.org/10.1016/j.rser.2015.04.049

Haider, A., Haider, S., Han, S. S., & Kang, I.-K. (2017). Recent advances in the synthesis, functionalization and biomedical applications of hydroxyapatite: a review. *RSC Advances, 7*(13), 7442-7458.

Halim, R., Danquah, M. K., & Webley, P. A. (2012). Extraction of oil from microalgae for biodiesel production: A review. *Biotechnology Advances, 30*(3), 709-732. doi:https://doi.org/10.1016/j.biotechadv.2012.01.001

Halim, R., Gladman, B., Danquah, M. K., & Webley, P. A. (2011). Oil extraction from microalgae for biodiesel production. *Bioresour Technol, 102*(1), 178-185. doi:https://doi.org/10.1016/j.biortech.2010.06.136

Handler, R. M., Shonnard, D. R., Kalnes, T. N., & Lupton, F. S. (2014). Life cycle assessment of algal biofuels: Influence of feedstock cultivation systems and conversion platforms. *Algal Research, 4*, 105-115. doi:http://dx.doi.org/10.1016/j.algal.2013.12.001

Hannon, M., Gimpel, J., Tran, M., Rasala, B., & Mayfield, S. (2010). Biofuels from algae: challenges and potential. *Biofuels, 1*(5), 763-784.

Harman-Ware, A. E., Morgan, T., Wilson, M., Crocker, M., Zhang, J., Liu, K., . . . Debolt, S. (2013). Microalgae as a renewable fuel source: fast pyrolysis of Scenedesmus sp. *Renewable Energy, 60*, 625-632.

Hecky, R., & Kilham, P. (1988). Nutrient limitation of phytoplankton in freshwater and marine environments: a review of recent evidence on the effects of enrichment. *Limnology and Oceanography, 33*(4), 796-822.

House, C. D. (2012). Standard methods for the examination of water and wastewater. *American Public Health Association Publisher. Washington, DC, 1496p*.

Hu, Z., Zheng, Y., Yan, F., Xiao, B., & Liu, S. (2013). Bio-oil production through pyrolysis of blue-green algae blooms (BGAB): product distribution and bio-oil characterization. *Energy, 52*, 119-125.

Huerlimann, R., de Nys, R., & Heimann, K. (2010). Growth, lipid content, productivity, and fatty acid composition of tropical microalgae for scale-up production. *Biotechnol Bioeng, 107*(2), 245-257. doi:10.1002/bit.22809

Inskeep, W. P., & Silvertooth, J. C. (1988). Kinetics of hydroxyapatite precipitation at pH 7.4 to 8.4. *Geochimica et Cosmochimica Acta, 52*(7), 1883-1893. doi:http://dx.doi.org/10.1016/0016-7037(88)90012-9

Itakura, T., Imaizumi, H., Sakita, T., Sasai, R., & Itoh, H. (2009). Precipitation removal and recovery of Cr(VI) from aqueous solution under hydrothermal condition. *Nippon Seramikkusu Kyokai Gakujutsu Ronbunshi/Journal of the Ceramic Society of Japan, 117*(1371), 1199-1202.

Itakura, T., Imaizumi, H., Sasai, R., & Itoh, H. (2008). Chromium and phosphorous recovery from polluted water by hydrothermal mineralization. *WIT Transactions on Ecology and the Environment, 109*, 781-788. doi:10.2495/WM080791

Itakura, T., Imaizumi, H., Sasai, R., & Itoh, H. (2009). Phosphorus mineralization for resource recovery from wastewater using hydrothermal treatment. *Nippon Seramikkusu Kyokai Gakujutsu Ronbunshi/Journal of the Ceramic Society of Japan, 117*(1363), 316-319.

Itakura, T., Sasai, R., & Itoh, H. Detoxification of wastewater containing As and Sb by hydrothermal mineralization.

Itakura, T., Sasai, R., & Itoh, H. (2004). *Resource recovery from Nd-Fe-B permanent magnet by hydrothermal treatment.* Paper presented at the Second International Conference on Waste Management and the Environment, Rhodes.

Itakura, T., Sasai, R., & Itoh, H. (2005). Precipitation recovery of boron from wastewater by hydrothermal mineralization. *Water Research, 39*(12), 2543-2548. doi:10.1016/j.watres.2005.04.035

Itakura, T., Sasai, R., & Itoh, H. (2006a). Arsenic recovery from water containing arsenite ions by hydrothermal mineralization. *Chemistry Letters, 35*(11), 1270-1271. doi:10.1246/cl.2006.1270

Itakura, T., Sasai, R., & Itoh, H. (2006b). A novel recovery method for treating wastewater containing fluoride and fluoroboric acid. *Bulletin of the Chemical Society of Japan, 79*(8), 1303-1307. doi:10.1246/bcsj.79.1303

Itakura, T., Sasai, R., & Itoh, H. (2007). Detoxification of antimonic contaminated water and precipitation recovery of antimony by mineralization under hydrothermal condition. *Chemistry Letters, 36*(4), 524-525. doi:10.1246/cl.2007.524

Jang, H., & Kang, S.-H. (2002). Phosphorus removal using cow bone in hydroxyapatite crystallization. *Water Research, 36*(5), 1324-1330. doi:http://dx.doi.org/10.1016/S0043-1354(01)00329-3

Jang, H. L., Jin, K., Lee, J., Kim, Y., Nahm, S. H., Hong, K. S., & Nam, K. T. (2014). Revisiting Whitlockite, the Second Most Abundant Biomineral in Bone: Nanocrystal Synthesis in Physiologically Relevant Conditions and Biocompatibility Evaluation. *ACS Nano, 8*(1), 634-641. doi:10.1021/nn405246h

Jang, H. L., Lee, H. K., Jin, K., Ahn, H.-Y., Lee, H.-E., & Nam, K. T. (2015). Phase transformation from hydroxyapatite to the secondary bone mineral, whitlockite. *J. Mater. Chem. B, 3*(7), 1342-1349. doi:10.1039/c4tb01793e

Jang, H. L., Zheng, G. B., Park, J., Kim, H. D., Baek, H.-R., Lee, H. K., . . . Nam, K. T. (2016). In Vitro and In Vivo Evaluation of Whitlockite Biocompatibility: Comparative Study with Hydroxyapatite and β-Tricalcium Phosphate. *Advanced Healthcare Materials, 5*(1), 128-136. doi:10.1002/adhm.201400824

Jasinski, S. M. (2015). Minerals Yearbook, Phosphate Rock. from United States Geological Survey https://minerals.usgs.gov/minerals/pubs/commodity/myb/

Jeffrey, S. W., & Wright, S. W. (1987). A new spectrally distinct component in preparations of chlorophyll c from the micro-alga Emiliania huxleyi (Prymnesiophycease). *Biochimica et Biophysica Acta (BBA) - Bioenergetics, 894*(2), 180-188. doi:http://dx.doi.org/10.1016/0005-2728(87)90188-5

Johansson, T. B. (1993). *Renewable energy: sources for fuels and electricity*: Island press.

Johnson, E. A., Liu, Z., Salmon, E., & Hatcher, P. (2013). One-Step Conversion of Algal Biomass to Biodiesel with Formation of an Algal Char as Potential Fertilizer. In J. W. Lee (Ed.), *Advanced Biofuels and Bioproducts* (pp. 695-705): Springer New York.

Jokić, B., Mitrić, M., Radmilović, V., Drmanić, S., Petrović, R., & Janaćković, D. (2011). Synthesis and characterization of monetite and hydroxyapatite whiskers obtained by a hydrothermal method. *Ceramics International, 37*(1), 167-173. doi:http://dx.doi.org/10.1016/j.ceramint.2010.08.032

Jones, D. B. (1941). *Factors for converting percentages of nitrogen in foods and feeds into percentages of proteins*: US Department of Agriculture Washington, DC.

Jueshi, Q., Zhongyuan, L., Qian, L., & Qiulin, Z. (2012). Rapid Synthesis of Dittmarite by Microwave-Assisted Hydrothermal Method. *Advances in Materials Science and Engineering, 2012*.

Kano, S., Yamazaki, A., Otsuka, R., Ohgaki, M., Akao, M., & Aoki, H. (1994). Application of hydroxyapatite-sol as drug carrier. *Bio-medical materials and engineering, 4*(4), 283-290.

Karty, J. (2014). *Organic Chemistry : Principles and Mechanisms with Access*. New York: W. W. Norton & Company.

Keymer, P., Ruffell, I., Pratt, S., & Lant, P. (2013). High pressure thermal hydrolysis as pre-treatment to increase the methane yield during anaerobic digestion of microalgae. *Bioresour Technol, 131*(Supplement C), 128-133. doi:https://doi.org/10.1016/j.biortech.2012.12.125

Kim, D., Ryu, H.-D., Kim, M.-S., Kim, J., & Lee, S.-I. (2007). Enhancing struvite precipitation potential for ammonia nitrogen removal in municipal landfill leachate. *Journal of Hazardous Materials, 146*(1–2), 81-85. doi:http://dx.doi.org/10.1016/j.jhazmat.2006.11.054

Kim, K. H., Choi, I. S., Kim, H. M., Wi, S. G., & Bae, H.-J. (2014). Bioethanol production from the nutrient stress-induced microalga Chlorella vulgaris by enzymatic hydrolysis and immobilized yeast fermentation. *Bioresour Technol, 153*, 47-54.

Knothe, G. (2010). Biodiesel and renewable diesel: a comparison. *Progress in energy and combustion science, 36*(3), 364-373.

Kofina, A. N., & Koutsoukos, P. G. (2005). Spontaneous Precipitation of Struvite from Synthetic Wastewater Solutions. *Crystal Growth & Design, 5*(2), 489-496. doi:10.1021/cg049803e

Koutsopoulos, S. (2002). Synthesis and characterization of hydroxyapatite crystals: A review study on the analytical methods. *Journal of Biomedical Materials Research, 62*(4), 600-612. doi:10.1002/jbm.10280

Koutsopoulos, S., & Dalas, E. (2000). The effect of acidic amino acids on hydroxyapatite crystallization. *Journal of Crystal Growth, 217*(4), 410-415. doi:http://dx.doi.org/10.1016/S0022-0248(00)00502-9

Koutsoukos, P., Amjad, Z., Tomson, M. B., & Nancollas, G. H. (1980). Crystallization of calcium phosphates. A constant composition study. *Journal of the American Chemical Society, 102*(5), 1553-1557. doi:10.1021/ja00525a015

Kubota, N., Doki, N., Yokota, M., & Sato, A. (2001). Seeding policy in batch cooling crystallization. *Powder Technology, 121*(1), 31-38. doi:http://dx.doi.org/10.1016/S0032-5910(01)00371-0

Kumar, R., & Pal, P. (2015). Assessing the feasibility of N and P recovery by struvite precipitation from nutrient-rich wastewater: a review. *Environmental Science and Pollution Research, 22*(22), 17453-17464. doi:10.1007/s11356-015-5450-2

Kumar, S., Gupta, R., Lee, Y. Y., & Gupta, R. B. (2010). Cellulose pretreatment in subcritical water: effect of temperature on molecular structure and enzymatic reactivity. *Bioresour Technol, 101*(4), 1337-1347. doi:10.1016/j.biortech.2009.09.035

Kumar, S., Hablot, E., Moscoso, J. L. G., Obeid, W., Hatcher, P. G., DuQuette, B. M., . . . Balan, V. (2014). Polyurethanes preparation using proteins obtained from microalgae. *Journal of Materials Science, 49*(22), 7824-7833. doi:10.1007/s10853-014-8493-8

Küpper, H., Küpper, F., & Spiller, M. (1996). Environmental relevance of heavy metal-substituted chlorophylls using the example of water plants. *Journal of Experimental Botany, 47*(2), 259-266. doi:10.1093/jxb/47.2.259

Lagier, R., & Baud, C. A. (2003). Magnesium Whitlockite, a Calcium Phosphate Crystal of Special Interest in Pathology. *Pathology - Research and Practice, 199*(5), 329-335. doi:http://dx.doi.org/10.1078/0344-0338-00425

Lang, I., Hodac, L., Friedl, T., & Feussner, I. (2011). Fatty acid profiles and their distribution patterns in microalgae: a comprehensive analysis of more than 2000 strains from the SAG culture collection. *BMC Plant Biology, 11*(1), 1-16. doi:10.1186/1471-2229-11-124

Langholtz, M., Stokes, B., & Eaton, L. (2016). 2016 Billion-Ton Report: Advancing Domestic Resources for a Thriving Bioeconomy, Volume 1: Economic Availability of Feedstocks: Oak Ridge National Laboratory Oak Ridge, TN.

Lapuerta, M., Rodríguez-Fernández, J., & de Mora, E. F. (2009). Correlation for the estimation of the cetane number of biodiesel fuels and implications on the iodine

number. *Energy Policy, 37*(11), 4337-4344. doi:https://doi.org/10.1016/j.enpol.2009.05.049

Lardon, L., Hélias, A., Sialve, B., Steyer, J.-P., & Bernard, O. (2009). Life-Cycle Assessment of Biodiesel Production from Microalgae. *Environmental Science & Technology, 43*(17), 6475-6481. doi:10.1021/es900705j

Laurens, L. M. L., Markham, J., Templeton, D. W., Christensen, E. D., Van Wychen, S., Vadelius, E. W., . . . Pienkos, P. T. (2017). Development of algae biorefinery concepts for biofuels and bioproducts; a perspective on process-compatible products and their impact on cost-reduction. *Energy & Environmental Science, 10*(8), 1716-1738. doi:10.1039/C7EE01306J

Laurens, L. M. L., & Wolfrum, E. J. (2011). Feasibility of Spectroscopic Characterization of Algal Lipids: Chemometric Correlation of NIR and FTIR Spectra with Exogenous Lipids in Algal Biomass. *BioEnergy Research, 4*(1), 22-35. doi:DOI 10.1007/s12155-010-9098-y

Lee, J.-Y., Yoo, C., Jun, S.-Y., Ahn, C.-Y., & Oh, H.-M. (2010). Comparison of several methods for effective lipid extraction from microalgae. *Bioresour Technol, 101*(1, Supplement), S75-S77. doi:http://dx.doi.org/10.1016/j.biortech.2009.03.058

Lee, S. Y., Cho, J. M., Chang, Y. K., & Oh, Y.-K. (2017). Cell disruption and lipid extraction for microalgal biorefineries: A review. *Bioresour Technol, 244*(Part 2), 1317-1328. doi:https://doi.org/10.1016/j.biortech.2017.06.038

Levine, R. B., Pinnarat, T., & Savage, P. E. (2010). Biodiesel Production from Wet Algal Biomass through in Situ Lipid Hydrolysis and Supercritical Transesterification. *Energy & Fuels, 24*(9), 5235-5243. doi:10.1021/ef1008314

Li, Y., Horsman, M., Wang, B., Wu, N., & Lan, C. Q. (2008). Effects of nitrogen sources on cell growth and lipid accumulation of green alga Neochloris oleoabundans. *Applied Microbiology and Biotechnology, 81*(4), 629-636.

Liu, B., Giannis, A., Zhang, J., Chang, V. W. C., & Wang, J.-Y. (2013). Characterization of induced struvite formation from source-separated urine using seawater and brine as magnesium sources. *Chemosphere, 93*(11), 2738-2747. doi:http://dx.doi.org/10.1016/j.chemosphere.2013.09.025

Liu, C., Huang, Y., Shen, W., & Cui, J. (2001). Kinetics of hydroxyapatite precipitation at pH 10 to 11. *Biomaterials, 22*(4), 301-306. doi:http://dx.doi.org/10.1016/S0142-9612(00)00166-6

Liu, J., Ye, X., Wang, H., Zhu, M., Wang, B., & Yan, H. (2003). The influence of pH and temperature on the morphology of hydroxyapatite synthesized by hydrothermal method. *Ceramics International, 29*(6), 629-633. doi:http://dx.doi.org/10.1016/S0272-8842(02)00210-9

López Barreiro, D., Bauer, M., Hornung, U., Posten, C., Kruse, A., & Prins, W. (2015). Cultivation of microalgae with recovered nutrients after hydrothermal liquefaction. *Algal Research, 9*, 99-106. doi:http://dx.doi.org/10.1016/j.algal.2015.03.007

López Barreiro, D., Prins, W., Ronsse, F., & Brilman, W. (2013). Hydrothermal liquefaction (HTL) of microalgae for biofuel production: State of the art review and future prospects. *Biomass and Bioenergy, 53*(Supplement C), 113-127. doi:https://doi.org/10.1016/j.biombioe.2012.12.029

Lourenço, S. O., Barbarino, E., Lavín, P. L., Lanfer Marquez, U. M., & Aidar, E. (2004). Distribution of intracellular nitrogen in marine microalgae: Calculation of new nitrogen-to-protein conversion factors. *European Journal of Phycology, 39*(1), 17-32. doi:10.1080/0967026032000157156

Lourenço, S. O., Barbarino, E., Marquez, U. M. L., & Aidar, E. (1998). DISTRIBUTION OF INTRACELLULAR NITROGEN IN MARINE MICROALGAE: BASIS FOR THE CALCULATION OF SPECIFIC NITROGEN-TO-PROTEIN CONVERSION FACTORS. *Journal of Phycology, 34*(5), 798-811. doi:10.1046/j.1529-8817.1998.340798.x

Lovón-Quintana, J. J., Rodriguez-Guerrero, J. K., & Valença, P. G. (2017). Carbonate hydroxyapatite as a catalyst for ethanol conversion to hydrocarbon fuels. *Applied Catalysis A: General, 542*, 136-145. doi:https://doi.org/10.1016/j.apcata.2017.05.020

Lowry, O. H., Rosebrough, N. J., Farr, A. L., & Randall, R. J. (1951). Protein measurement with the Folin phenol reagent. *J biol Chem, 193*(1), 265-275.

Makareviciene, V., Skorupskaite, V., & Andruleviciute, V. (2013). Biodiesel fuel from microalgae-promising alternative fuel for the future: a review. *Reviews in Environmental Science and Bio/Technology, 12*(2), 119-130.

Marcos, J., Renau, N., Valverde, O., Aznar-Laín, G., Gracia-Rubio, I., Gonzalez-Sepulveda, M., . . . Pozo, O. J. (2016). Targeting tryptophan and tyrosine metabolism by liquid chromatography tandem mass spectrometry. *Journal of Chromatography A, 1434*, 91-101. doi:http://dx.doi.org/10.1016/j.chroma.2016.01.023

Markou, G., Vandamme, D., & Muylaert, K. (2014). Microalgal and cyanobacterial cultivation: The supply of nutrients. *Water Research, 65*, 186-202. doi:http://dx.doi.org/10.1016/j.watres.2014.07.025

Martinez-Guerra, E., Gude, V. G., Mondala, A., Holmes, W., & Hernandez, R. (2014). Extractive-transesterification of algal lipids under microwave irradiation with hexane as solvent. *Bioresour Technol, 156*, 240-247.

Mata, T. M., Martins, A. A., & Caetano, N. S. (2010). Microalgae for biodiesel production and other applications: A review. *Renewable and Sustainable Energy Reviews, 14*(1), 217-232. doi:http://dx.doi.org/10.1016/j.rser.2009.07.020

Mayfield, S. P. (2015). *Consortium for Algal Biofuel Commercialization (CAB-COMM) Final Report*. Retrieved from

Mendes, R. L., Fernandes, H. L., Coelho, J., Reis, E. C., Cabral, J. M., Novais, J. M., & Palavra, A. F. (1995). Supercritical CO2 extraction of carotenoids and other lipids from Chlorella vulgaris. *Food chemistry, 53*(1), 99-103.

Mendoza, A., Vicente, G., Bautista, L. F., & Morales, V. (2015). Opportunities for Nannochloropsis gaditana biomass through the isolation of its components and biodiesel production *Green Processing and Synthesis* (Vol. 4, pp. 97).

Meng, Y., Yao, C., Xue, S., & Yang, H. (2014). Application of Fourier transform infrared (FT-IR) spectroscopy in determination of microalgal compositions. *Bioresour Technol, 151*(0), 347-354. doi:10.1016/j.biortech.2013.10.064

Moed, N. M., Lee, D.-J., & Chang, J.-S. (2015). Struvite as alternative nutrient source for cultivation of microalgae Chlorella vulgaris. *Journal of the Taiwan Institute of Chemical Engineers, 56*, 73-76. doi:http://dx.doi.org/10.1016/j.jtice.2015.04.027

Mori, K., Hara, T., Mizugaki, T., Ebitani, K., & Kaneda, K. (2003). Hydroxyapatite-Bound Cationic Ruthenium Complexes as Novel Heterogeneous Lewis Acid Catalysts for Diels−Alder and Aldol Reactions. *Journal of the American Chemical Society, 125*(38), 11460-11461. doi:10.1021/ja0302533

Mori, K., Hara, T., Mizugaki, T., Ebitani, K., & Kaneda, K. (2004). Hydroxyapatite-Supported Palladium Nanoclusters: A Highly Active Heterogeneous Catalyst for Selective Oxidation of Alcohols by Use of Molecular Oxygen. *Journal of the American Chemical Society, 126*(34), 10657-10666. doi:10.1021/ja0488683

Mossaad, C., Starr, M., Patil, S., & Riman, R. E. (2010). Thermodynamic Modeling of Hydroxyapatite Crystallization with Biomimetic Precursor Design Considerations. *Chemistry of Materials, 22*(1), 36-46. doi:10.1021/cm900183v

Münch, E. V., & Barr, K. (2001). Controlled struvite crystallisation for removing phosphorus from anaerobic digester sidestreams. *Water Research, 35*(1), 151-159. doi:http://dx.doi.org/10.1016/S0043-1354(00)00236-0

Mutanda, T., Ramesh, D., Karthikeyan, S., Kumari, S., Anandraj, A., & Bux, F. (2011). Bioprospecting for hyper-lipid producing microalgal strains for sustainable biofuel production. *Bioresour Technol, 102*(1), 57-70. doi:http://dx.doi.org/10.1016/j.biortech.2010.06.077

Nakai, S., Inoue, Y., & Hosomi, M. (2001). Algal growth inhibition effects and inducement modes by plant-producing phenols. *Water Research, 35*(7), 1855-1859.

Nancollas, G. H., & Mohan, M. S. (1970). The growth of hydroxyapatite crystals. *Archives of Oral Biology, 15*(8), 731-745. doi:http://dx.doi.org/10.1016/0003-9969(70)90037-3

Nenkova, S., Vasileva, T., & Stanulov, K. (2008). Production of phenol compounds by alkaline treatment of technical hydrolysis lignin and wood biomass. *Chemistry of Natural Compounds, 44*(2), 182-185.

Nguyen, R. T., Harvey, H. R., Zang, X., van Heemst, J. D. H., Hetényi, M., & Hatcher, P. G. (2003). Preservation of algaenan and proteinaceous material during the oxic decay of Botryococcus braunii as revealed by pyrolysis-gas chromatography/mass spectrometry and 13C NMR spectroscopy. *Organic Geochemistry, 34*(4), 483-497. doi:10.1016/s0146-6380(02)00261-9

Obeid, W., Salmon, E., & Hatcher, P. G. (2014). The effect of different isolation procedures on algaenan molecular structure in Scenedesmus green algae. *Organic Geochemistry, 76*, 259-269. doi:http://dx.doi.org/10.1016/j.orggeochem.2014.09.004

Obeid, W., Salmon, E., Lewan, M. D., & Hatcher, P. G. (2015). Hydrous pyrolysis of Scenedesmus algae and algaenan-like residue. *Organic Geochemistry, 85*, 89-101. doi:http://dx.doi.org/10.1016/j.orggeochem.2015.04.001

Oladoja, N. A., Ololade, I. A., Adesina, A. O., Adelagun, R. O. A., & Sani, Y. M. (2013). Appraisal of gastropod shell as calcium ion source for phosphate removal and recovery in calcium phosphate minerals crystallization procedure. *Chemical Engineering Research and Design, 91*(5), 810-818. doi:http://dx.doi.org/10.1016/j.cherd.2012.09.017

Palazzo, B., Walsh, D., Iafisco, M., Foresti, E., Bertinetti, L., Martra, G., . . . Roveri, N. (2009). Amino acid synergetic effect on structure, morphology and surface properties of biomimetic apatite nanocrystals. *Acta Biomaterialia, 5*(4), 1241-1252. doi:http://dx.doi.org/10.1016/j.actbio.2008.10.024

Pate, R., Klise, G., & Wu, B. (2011). Resource demand implications for US algae biofuels production scale-up. *Applied Energy, 88*(10), 3377-3388. doi:http://dx.doi.org/10.1016/j.apenergy.2011.04.023

Patel, B., Guo, M., Izadpanah, A., Shah, N., & Hellgardt, K. (2016). A review on hydrothermal pre-treatment technologies and environmental profiles of algal biomass processing. *Bioresour Technol, 199*, 288-299. doi:http://dx.doi.org/10.1016/j.biortech.2015.09.064

Patil, P. D., Gude, V. G., Mannarswamy, A., Deng, S., Cooke, P., Munson-McGee, S., . . . Nirmalakhandan, N. (2011). Optimization of direct conversion of wet algae to biodiesel under supercritical methanol conditions. *Bioresour Technol, 102*(1), 118-122.

Peterson, A. A., Vogel, F., Lachance, R. P., Fröling, M., Antal Jr, M. J., & Tester, J. W. (2008). Thermochemical biofuel production in hydrothermal media: a review of sub-and supercritical water technologies. *Energy & Environmental Science, 1*(1), 32-65.

Pienkos, P. T. (2016). *Development of a Novel Biorefinery Concept for Acceleration of Algal Biofuel Commercialization.* Paper presented at the 38th Symposium on Biotechnology for Fuels and Chemicals.

Prabhu, M., & Mutnuri, S. (2014). Cow urine as a potential source for struvite production. *International Journal of Recycling of Organic Waste in Agriculture, 3*(1), 49. doi:10.1007/s40093-014-0049-z

Qi, C., Zhu, Y.-J., Lu, B.-Q., Wu, J., & Chen, F. (2015). Amorphous magnesium phosphate flower-like hierarchical nanostructures: microwave-assisted rapid synthesis using fructose 1,6-bisphosphate trisodium salt as an organic phosphorus source and application in protein adsorption. *RSC Advances, 5*(19), 14906-14915. doi:10.1039/C4RA15842C

Qi, M.-L., He, K., Huang, Z.-N., Shahbazian-Yassar, R., Xiao, G.-Y., Lu, Y.-P., & Shokuhfar, T. (2017). Hydroxyapatite Fibers: A Review of Synthesis Methods. *JOM, 69*(8), 1354-1360. doi:10.1007/s11837-017-2427-2

Quinn, J. C., & Davis, R. (2015). The potentials and challenges of algae based biofuels: a review of the techno-economic, life cycle, and resource assessment modeling. *Bioresour Technol, 184*, 444-452. doi:10.1016/j.biortech.2014.10.075

Quitain, A. T., Sasaki, M., & Goto, M. (2014). *Biopolymer degradation in sub-and supercritical water for biomass waste recycling*: Elsevier: Amsterdam.

Rahman, M. M., Liu, Y., Kwag, J.-H., & Ra, C. (2011). Recovery of struvite from animal wastewater and its nutrient leaching loss in soil. *Journal of Hazardous Materials, 186*(2–3), 2026-2030. doi:http://dx.doi.org/10.1016/j.jhazmat.2010.12.103

Rahman, M. M., Salleh, M. A. M., Rashid, U., Ahsan, A., Hossain, M. M., & Ra, C. S. (2014). Production of slow release crystal fertilizer from wastewaters through struvite crystallization – A review. *Arabian Journal of Chemistry, 7*(1), 139-155. doi:http://dx.doi.org/10.1016/j.arabjc.2013.10.007

Ramesh, D. (2013). Lipid identification and extraction techniques. *Biotechnological Applications of Microalgae: Biodiesel and Value-added Products*, 89-97.

Ranjith Kumar, R., Hanumantha Rao, P., & Arumugam, M. (2015). Lipid Extraction Methods from Microalgae: A Comprehensive Review. *Frontiers in Energy Research, 2*(61). doi:10.3389/fenrg.2014.00061

Rawat, I., Ranjith Kumar, R., Mutanda, T., & Bux, F. (2013). Biodiesel from microalgae: A critical evaluation from laboratory to large scale production. *Applied Energy, 103*, 444-467. doi:http://dx.doi.org/10.1016/j.apenergy.2012.10.004

Ren, F., Leng, Y., Ding, Y., & Wang, K. (2013). Hydrothermal growth of biomimetic carbonated apatite nanoparticles with tunable size, morphology and ultrastructure. *CrystEngComm, 15*(11), 2137-2146. doi:10.1039/C3CE26884E

Ren, X., Zhao, X., Turcotte, F., Deschênes, J.-S., Tremblay, R., & Jolicoeur, M. (2017). Current lipid extraction methods are significantly enhanced adding a water treatment step in Chlorella protothecoides. *Microbial Cell Factories, 16*, 26. doi:10.1186/s12934-017-0633-9

Roberts, G. W., Sturm, B. S., Hamdeh, U., Stanton, G. E., Rocha, A., Kinsella, T. L., . . . Stagg-Williams, S. M. (2015). Promoting catalysis and high-value product streams by in situ hydroxyapatite crystallization during hydrothermal liquefaction of microalgae cultivated with reclaimed nutrients. *Green Chemistry, 17*(4), 2560-2569.

Rodolfi, L., Chini Zittelli, G., Bassi, N., Padovani, G., Biondi, N., Bonini, G., & Tredici, M. R. (2009). Microalgae for oil: strain selection, induction of lipid synthesis and outdoor mass cultivation in a low-cost photobioreactor. *Biotechnol Bioeng, 102*(1), 100-112. doi:10.1002/bit.22033

Rodríguez-Meizoso, I., Jaime, L., Santoyo, S., Señoráns, F., Cifuentes, A., & Ibáñez, E. (2010). Subcritical water extraction and characterization of bioactive compounds

from Haematococcus pluvialis microalga. *Journal of pharmaceutical and biomedical analysis, 51*(2), 456-463.

Ross, A. B., Biller, P., Kubacki, M. L., Li, H., Lea-Langton, A., & Jones, J. M. (2010). Hydrothermal processing of microalgae using alkali and organic acids. *Fuel, 89*(9), 2234-2243. doi:http://dx.doi.org/10.1016/j.fuel.2010.01.025

Ross, A. B., Jones, J. M., Kubacki, M. L., & Bridgeman, T. (2008). Classification of macroalgae as fuel and its thermochemical behaviour. *Bioresour Technol, 99*(14), 6494-6504. doi:10.1016/j.biortech.2007.11.036

Ruhl, I. D., Salmon, E., & Hatcher, P. G. (2011). Early diagenesis of Botryococcus braunii race A as determined by high resolution magic angle spinning (HRMAS) NMR. *Organic Geochemistry, 42*(1), 1-14. doi:DOI 10.1016/j.orggeochem.2010.09.004

Sadat-Shojai, M. (2009). Preparation of hydroxyapatite nanoparticles: Comparison between hydrothermal and Solvo-Treatment processes and colloidal stability of produced nanoparticles in a dilute experimental dental adhesive. *Journal of the Iranian Chemical Society, 6*(2), 386-392. doi:10.1007/bf03245848

Sadat-Shojai, M., Khorasani, M.-T., Dinpanah-Khoshdargi, E., & Jamshidi, A. (2013). Synthesis methods for nanosized hydroxyapatite with diverse structures. *Acta Biomaterialia, 9*(8), 7591-7621. doi:http://dx.doi.org/10.1016/j.actbio.2013.04.012

Sadat-Shojai, M., Khorasani, M.-T., & Jamshidi, A. (2012). Hydrothermal processing of hydroxyapatite nanoparticles—A Taguchi experimental design approach. *Journal of Crystal Growth, 361*, 73-84. doi:http://dx.doi.org/10.1016/j.jcrysgro.2012.09.010

Sanchez-Silva, L., López-González, D., Garcia-Minguillan, A., & Valverde, J. (2013). Pyrolysis, combustion and gasification characteristics of Nannochloropsis gaditana microalgae. *Bioresour Technol, 130*, 321-331.

Sasai, R., Matsumoto, Y., & Itakura, T. (2011). Continuous-flow detoxification treatment of boron-containing wastewater under hydrothermal conditions. *Nippon Seramikkusu Kyokai Gakujutsu Ronbunshi/Journal of the Ceramic Society of Japan, 119*(1388), 277-281.

Schindler, D. W. (2006). Recent advances in the understanding and management of eutrophication. *Limnology and Oceanography, 51*(1), 356-363.

Sebti, S. d., Tahir, R., Nazih, R., & Boulaajaj, S. d. (2001). Comparison of different Lewis acid supported on hydroxyapatite as new catalysts of Friedel–Crafts alkylation. *Applied Catalysis A: General, 218*(1–2), 25-30. doi:http://dx.doi.org/10.1016/S0926-860X(01)00599-3

Sebti, S. d., Tahir, R., Nazih, R., Saber, A., & Boulaajaj, S. d. (2002). Hydroxyapatite as a new solid support for the Knoevenagel reaction in heterogeneous media without solvent. *Applied Catalysis A: General, 228*(1–2), 155-159. doi:http://dx.doi.org/10.1016/S0926-860X(01)00961-9

Sereewatthanawut, I., Prapintip, S., Watchiraruji, K., Goto, M., Sasaki, M., & Shotipruk, A. (2008). Extraction of protein and amino acids from deoiled rice bran by subcritical water hydrolysis. *Bioresour Technol, 99*(3), 555-561.

Sforza, E., Cipriani, R., Morosinotto, T., Bertucco, A., & Giacometti, G. M. (2012). Excess CO2 supply inhibits mixotrophic growth of Chlorella protothecoides and Nannochloropsis salina. *Bioresour Technol, 104*, 523-529. doi:http://dx.doi.org/10.1016/j.biortech.2011.10.025

Sheehan, J. D., & Savage, P. E. (2017). Modeling the effects of microalga biochemical content on the kinetics and biocrude yields from hydrothermal liquefaction. *Bioresour Technol, 239*(Supplement C), 144-150. doi:https://doi.org/10.1016/j.biortech.2017.05.013

Shen, D., Horiuchi, N., Nozaki, S., Miyashin, M., Yamashita, K., & Nagai, A. (2017). Synthesis and enhanced bone regeneration of carbonate substituted octacalcium phosphate. *Bio-medical materials and engineering, 28*(1), 9-21.

Shu, C., Yanwei, W., Hong, L., Zhengzheng, P., & Kangde, Y. (2005). Synthesis of carbonated hydroxyapatite nanofibers by mechanochemical methods. *Ceramics International, 31*(1), 135-138. doi:http://dx.doi.org/10.1016/j.ceramint.2004.04.012

Shurtz, B. K., Wood, B., & Quinn, J. C. (2017). Nutrient resource requirements for large-scale microalgae biofuel production: Multi-pathway evaluation. *Sustainable Energy Technologies and Assessments, 19*, 51-58. doi:https://doi.org/10.1016/j.seta.2016.11.003

Silva, C., Soliman, E., Cameron, G., Fabiano, L. A., Seider, W. D., Dunlop, E. H., & Coaldrake, A. K. (2013). Commercial-scale biodiesel production from algae. *Industrial & Engineering Chemistry Research, 53*(13), 5311-5324.

Simionato, D., Block, M. A., La Rocca, N., Jouhet, J., Maréchal, E., Finazzi, G., & Morosinotto, T. (2013). The Response of Nannochloropsis gaditana to Nitrogen Starvation Includes De Novo Biosynthesis of Triacylglycerols, a Decrease of Chloroplast Galactolipids, and Reorganization of the Photosynthetic Apparatus. *Eukaryotic Cell, 12*(5), 665-676. doi:10.1128/EC.00363-12

Singh, R., & Sharma, S. (2012). Development of suitable photobioreactor for algae production–A review. *Renewable and Sustainable Energy Reviews, 16*(4), 2347-2353.

Slade, R., & Bauen, A. (2013). Micro-algae cultivation for biofuels: Cost, energy balance, environmental impacts and future prospects. *Biomass and Bioenergy, 53*, 29-38. doi:http://dx.doi.org/10.1016/j.biombioe.2012.12.019

Slocombe, S. P., & Benemann, J. R. (2016). *Microalgal Production for Biomass and High-value Products*: CRC Press.

Song, Y. W., Shan, D. Y., & Han, E. H. (2008). Electrodeposition of hydroxyapatite coating on AZ91D magnesium alloy for biomaterial application. *Materials Letters, 62*(17–18), 3276-3279. doi:http://dx.doi.org/10.1016/j.matlet.2008.02.048

Sopyan, I., Mel, M., Ramesh, S., & Khalid, K. A. (2007). Porous hydroxyapatite for artificial bone applications. *Science and Technology of Advanced Materials, 8*(1–2), 116-123. doi:https://doi.org/10.1016/j.stam.2006.11.017

Stansell, G. R., Gray, V. M., & Sym, S. D. (2012). Microalgal fatty acid composition: implications for biodiesel quality. *Journal of Applied Phycology, 24*(4), 791-801.

Steriti, A., Rossi, R., Concas, A., & Cao, G. (2014). A novel cell disruption technique to enhance lipid extraction from microalgae. *Bioresour Technol, 164*(Supplement C), 70-77. doi:https://doi.org/10.1016/j.biortech.2014.04.056

Su, Y., Song, K., Zhang, P., Su, Y., Cheng, J., & Chen, X. (2017). Progress of microalgae biofuel's commercialization. *Renewable and Sustainable Energy Reviews, 74*, 402-411. doi:https://doi.org/10.1016/j.rser.2016.12.078

Suganya, T., & Renganathan, S. (2012). Optimization and kinetic studies on algal oil extraction from marine macroalgae Ulva lactuca. *Bioresour Technol, 107*(Supplement C), 319-326. doi:https://doi.org/10.1016/j.biortech.2011.12.045

Sukenik, A., Zmora, O., & Carmeli, Y. (1993). Biochemical quality of marine unicellular algae with special emphasis on lipid composition. II. Nannochloropsis sp. *Aquaculture, 117*(3), 313-326. doi:http://dx.doi.org/10.1016/0044-8486(93)90328-V

Sunphorka, S., Chavasiri, W., Oshima, Y., & Ngamprasertsith, S. (2012). Kinetic studies on rice bran protein hydrolysis in subcritical water. *Journal of Supercritical Fluids, 65*(0), 54-60. doi:DOI 10.1016/j.supflu.2012.02.017

Sunphorka, S., Chavasiri, W., Oshima, Y., & Ngamprasertsith, S. (2012). Kinetic studies on rice bran protein hydrolysis in subcritical water. *The Journal of Supercritical Fluids, 65*, 54-60. doi:http://dx.doi.org/10.1016/j.supflu.2012.02.017

Suzuki, K., Tanaka, Y., Kuroda, K., Hanajima, D., Fukumoto, Y., Yasuda, T., & Waki, M. (2007). Removal and recovery of phosphorous from swine wastewater by demonstration crystallization reactor and struvite accumulation device. *Bioresour Technol, 98*(8), 1573-1578. doi:http://dx.doi.org/10.1016/j.biortech.2006.06.008

Szcześ, A., Hołysz, L., & Chibowski, E. Synthesis of hydroxyapatite for biomedical applications. *Advances in Colloid and Interface Science*. doi:https://doi.org/10.1016/j.cis.2017.04.007

Talbot, C., Garcia-Moscoso, J., Drake, H., Stuart, B. J., & Kumar, S. (2016). Cultivation of microalgae using flash hydrolysis nutrient recycle. *Algal Research, 18*, 191-197. doi:http://dx.doi.org/10.1016/j.algal.2016.06.021

Tekin, K., Karagöz, S., & Bektaş, S. (2014). A review of hydrothermal biomass processing. *Renewable and Sustainable Energy Reviews, 40*(Supplement C), 673-687. doi:https://doi.org/10.1016/j.rser.2014.07.216

Templeton, D. W., & Laurens, L. M. L. (2015). Nitrogen-to-protein conversion factors revisited for applications of microalgal biomass conversion to food, feed and fuel. *Algal Research, 11*, 359-367. doi:http://dx.doi.org/10.1016/j.algal.2015.07.013

Teymouri, A., Kumar, S., Barbera, E., Sforza, E., Bertucco, A., & Morosinotto, T. (2017). Integration of biofuels intermediates production and nutrients recycling in the processing of a marine algae. *AIChE Journal, 63*(5), 1494-1502. doi:10.1002/aic.15537

Teymouri, A., Stuart, B. J., & Kumar, S. (2017). Effect of Reaction Time on Phosphate Mineralization from Microalgae Hydrolysate. *ACS Sustainable Chemistry & Engineering*. doi:10.1021/acssuschemeng.7b02951

Teymouri, A., Stuart, B. J., & Kumar, S. (2018). Hydroxyapatite and dittmarite precipitation from algae hydrolysate. *Algal Research, 29*, 202-211. doi:https://doi.org/10.1016/j.algal.2017.11.030

Theophanides, T. M. (2012). *Infrared Spectroscopy-Materials Science, Engineering and Technology* (T. Theophanides Ed.): InTech.

Thomas, W. H., & Krauss, R. W. (1955). Nitrogen Metabolism in Scenedesmus as Affected by Environmental Changes. *Plant physiology, 30*(2), 113.

Tibbetts, S. M., Milley, J. E., & Lall, S. P. (2014). Chemical composition and nutritional properties of freshwater and marine microalgal biomass cultured in photobioreactors. *Journal of Applied Phycology, 27*(3), 1109-1119. doi:10.1007/s10811-014-0428-x

TOMSON, M. B., & NANCOLLAS, G. H. (1978). Mineralization Kinetics: A Constant Composition Approach. *Science, 200*(4345), 1059-1060. doi:10.1126/science.200.4345.1059

Tong, D., Hu, C., Jiang, K., & Li, Y. (2011). Cetane Number Prediction of Biodiesel from the Composition of the Fatty Acid Methyl Esters. *Journal of the American Oil Chemists' Society, 88*(3), 415-423. doi:10.1007/s11746-010-1672-0

Toor, S. S., Reddy, H., Deng, S., Hoffmann, J., Spangsmark, D., Madsen, L. B., . . . Rosendahl, L. A. (2013). Hydrothermal liquefaction of Spirulina and Nannochloropsis salina under subcritical and supercritical water conditions. *Bioresour Technol, 131*, 413-419. doi:http://dx.doi.org/10.1016/j.biortech.2012.12.144

Toor, S. S., Rosendahl, L., & Rudolf, A. (2011). Hydrothermal liquefaction of biomass: A review of subcritical water technologies. *Energy, 36*(5), 2328-2342. doi:http://dx.doi.org/10.1016/j.energy.2011.03.013

Tsuru, K., Ruslin, Maruta, M., Matsuya, S., & Ishikawa, K. (2015). Effects of the method of apatite seed crystals addition on setting reaction of alpha-tricalcium phosphate based apatite cement. *J Mater Sci Mater Med, 26*(10), 244. doi:10.1007/s10856-015-5570-8

Tunay, O., Kabdasli, I., Orhon, D., & Kolcak, S. (1997). Ammonia removal by magnesium ammonium phosphate precipitation in industrial wastewaters. *Water Science and Technology, 36*(2-3), 225-228. doi:Doi 10.1016/S0273-1223(97)00391-0

Turker, M., & Celen, I. (2007). Removal of ammonia as struvite from anaerobic digester effluents and recycling of magnesium and phosphate. *Bioresour Technol*, *98*(8), 1529-1534. doi:10.1016/j.biortech.2006.06.026

Twidell, J., & Weir, T. (2015). *Renewable energy resources*: Routledge.

U.S. energy consumption by energy source. (2017). April 2017. Retrieved from https://www.eia.gov/energyexplained/?page=us_energy_home

Utagawa, T. (2004). Production of arginine by fermentation. *J Nutr*, *134*(10 Suppl), 2854S-2857S; discussion 2895S.

Van Wychen, S., & Laurens, L. M. L. (2013). *Determination of Total Solids and Ash in Algal Biomass: Laboratory Analytical Procedure (LAP)* (NREL/TP-5100-60956 United States 10.2172/1118077 NREL English). Retrieved from http://www.osti.gov/scitech/servlets/purl/1118077

Venteris, E. R., Skaggs, R. L., Wigmosta, M. S., & Coleman, A. M. (2014). A national-scale comparison of resource and nutrient demands for algae-based biofuel production by lipid extraction and hydrothermal liquefaction. *Biomass & Bioenergy*, *64*, 276-290. doi:10.1016/j.biombioe.2014.02.001

Vonshak, A. (1990). Recent advances in microalgal biotechnology. *Biotechnol Adv*, *8*(4), 709-727. doi:http://dx.doi.org/10.1016/0734-9750(90)91993-Q

Wang, H. (2004). *Hydroxyapatite degradation and biocompatibility*. The Ohio State University. Retrieved from http://rave.ohiolink.edu/etdc/view?acc_num=osu1087238429

Wang, J., Burken, J. G., & Zhang, X. (2006). Effect of seeding materials and mixing strength on struvite precipitation. *Water Environ Res*, *78*(2), 125-132. doi:10.2175/106143005X89580

Wang, K., Brown, R. C., Homsy, S., Martinez, L., & Sidhu, S. S. (2013). Fast pyrolysis of microalgae remnants in a fluidized bed reactor for bio-oil and biochar production. *Bioresour Technol*, *127*, 494-499. doi:10.1016/j.biortech.2012.08.016

Wei, Q., Li, S., Han, C., Li, W., Cheng, L., Hao, L., & Shi, Y. (2015). Selective laser melting of stainless-steel/nano-hydroxyapatite composites for medical applications: Microstructure, element distribution, crack and mechanical properties. *Journal of Materials Processing Technology*, *222*, 444-453.

Wei, R., Zhang, L., Cang, D., Li, J., Li, X., & Xu, C. C. (2017). Current status and potential of biomass utilization in ferrous metallurgical industry. *Renewable and Sustainable Energy Reviews*, *68*(Part 1), 511-524. doi:https://doi.org/10.1016/j.rser.2016.10.013

Woo, K. L., & Kim, J. I. (1999). New hydrolysis method for extremely small amount of lipids and capillary gas chromatographic analysis as N(O)-tert.-butyldimethylsilyl fatty acid derivatives compared with methyl ester derivatives. *Journal of Chromatography A*, *862*(2), 199-208. doi:Doi 10.1016/S0021-9673(99)00934-6

Yan, L., Li, Y. D., Deng, Z. X., Zhuang, J., & Sun, X. M. (2001). Surfactant-assisted hydrothermal synthesis of hydroxyapatite nanorods. *International Journal of Inorganic Materials, 3*(7), 633-637. doi:Doi 10.1016/S1466-6049(01)00164-7

Yetilmezsoy, K., & Sapci-Zengin, Z. (2009). Recovery of ammonium nitrogen from the effluent of UASB treating poultry manure wastewater by MAP precipitation as a slow release fertilizer. *J Hazard Mater, 166*(1), 260-269. doi:10.1016/j.jhazmat.2008.11.025

Yu, G., Zhang, Y. H., Schideman, L., Funk, T., & Wang, Z. C. (2011). Distributions of carbon and nitrogen in the products from hydrothermal liquefaction of low-lipid microalgae. *Energy & Environmental Science, 4*(11), 4587-4595. doi:10.1039/c1ee01541a

Yu, Y., Wu, R., & Clark, M. (2010). Phosphate removal by hydrothermally modified fumed silica and pulverized oyster shell. *Journal of Colloid and Interface Science, 350*(2), 538-543. doi:http://dx.doi.org/10.1016/j.jcis.2010.06.033

Yun, J.-H., Smith, V. H., & Pate, R. C. (2015). Managing nutrients and system operations for biofuel production from freshwater macroalgae. *Algal Research, 11*, 13-21. doi:http://dx.doi.org/10.1016/j.algal.2015.05.016

Zang, G. L., Sheng, G. P., Li, W. W., Tong, Z. H., Zeng, R. J., Shi, C., & Yu, H. Q. (2012). Nutrient removal and energy production in a urine treatment process using magnesium ammonium phosphate precipitation and a microbial fuel cell technique. *Phys Chem Chem Phys, 14*(6), 1978-1984. doi:10.1039/c2cp23402e

Zang, X., Nguyen, R. T., Harvey, H. R., Knicker, H., & Hatcher, P. G. (2001). Preservation of proteinaceous material during the degradation of the green alga Botryococcus braunii: A solid-state 2D 15N 13C NMR spectroscopy study. *Geochimica et Cosmochimica Acta, 65*(19), 3299-3305. doi:10.1016/s0016-7037(01)00679-2

Zhang, T. Y., Hu, H. Y., Wu, Y. H., Zhuang, L. L., Xu, X. Q., Wang, X. X., & Dao, G. H. (2016). Promising solutions to solve the bottlenecks in the large-scale cultivation of microalgae for biomass/bioenergy production. *Renewable & Sustainable Energy Reviews, 60*, 1602-1614. doi:10.1016/j.rser.2016.02.008

APPENDIX A

Supplementary information for chapter 2 (Kinetics of Peptides and Arginine Production from Microalgae (*Scenedesmus* sp.) by Flash Hydrolysis)

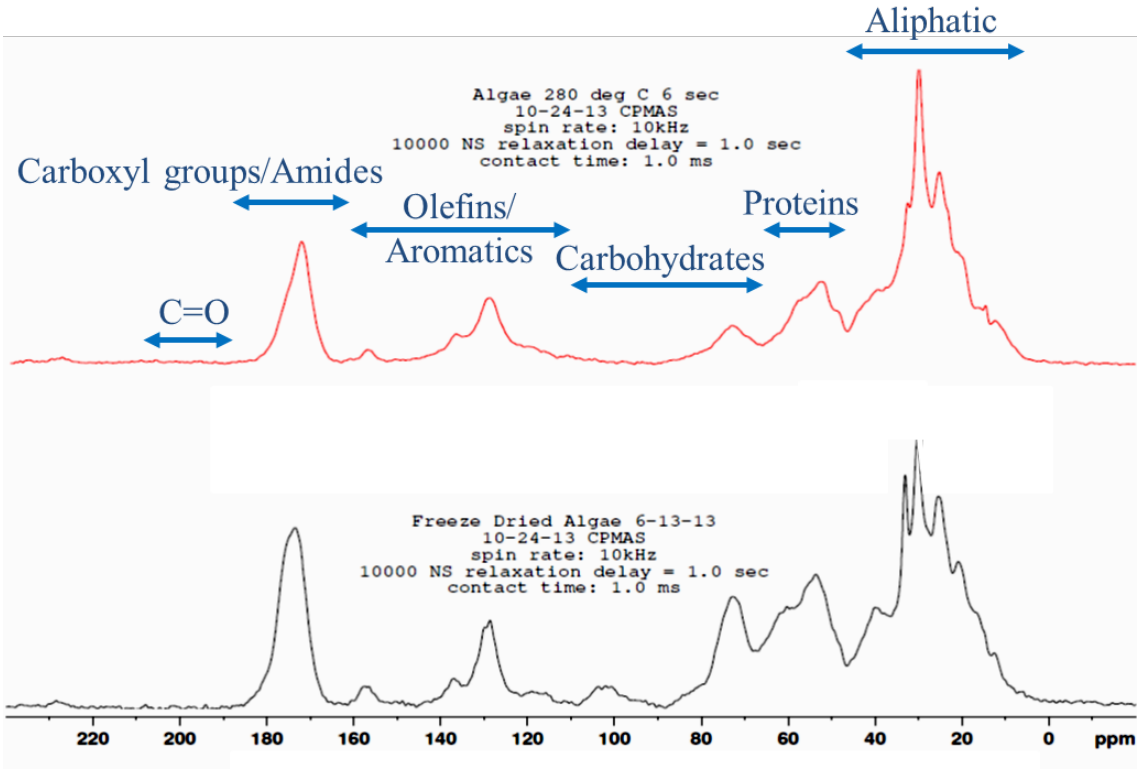

Figure 44. NMR spectra of the *Scenedesmus* sp. microalgae and the biofuels intermediate from run 4 (280 ºC, 6 s).

APPENDIX B

Recycling minerals in microalgae cultivation through a combined flash hydrolysis-precipitation process

This was a collaborative study with the University of Padova, Italy. Dittmarite that was precipitated through the integrated FH-AP pathway as explained in the chapter 4 of this dissertation, was used as a nutrient source for algal cultivation. The content of this study was published in the *ACS Sustainable Chemistry and Engineering* journal with the following address:

- Barbera, E.; **Teymouri, A.**; Bertucco, A.; Stuart, B. J.; Kumar, S., Recycling Minerals in Microalgae Cultivation through a Combined Flash Hydrolysis-Precipitation Process. *ACS Sustainable Chemistry & Engineering* 2017, 5 (1), 929-935.

The high demand of nutrients is one of the major limitations to a sustainable large-scale production of microalgae-derived biofuels. This issue is particularly critical for phosphorus, whose natural reserves will soon be depleted. This work aims at testing the possibility of recycling phosphorus from the microalgal biomass in the form of magnesium ammonium phosphate (MAP, or struvite), a stable fertilizer suitable for transportation and long-term storage purposes, obtained through flash hydrolysis (FH) of microalgae followed by precipitation of the extracted minerals. To this goal, microalgae growth experiments were carried out with *Scenedesmus* sp., in batch and continuous lab-scale photobioreactors, using struvite recovered from the proposed process, thus replacing traditional phosphate fertilizers in the cultivation medium. Results showed that the growth rate and productivity obtained with the recycled minerals as phosphorus

source equal those achieved in the standard medium, suggesting that the proposed process could be a viable and a relatively simple way to increase the sustainability of microalgal production at large-scale.

APPENDIX C

Life Cycle Impacts and Techno-economic Implications of Flash Hydrolysis in Algae Processing

This was a collaborative study with the Montana State University Northern. The main objective of this work was to evaluate the environmental performance and economic underpinnings of using FH in processing algae for biofuels production. In this study, FH was offered as an alternative algae conversion pathway to fuel. FH partitioned microalgae in an aqueous protein-rich phase and a solid lipid-rich biofuels intermediates phase. The aqueous phase underwent HTM or AP process to recover maximum macronutrients as valuable co-products (as discussed in chapter 4 of this dissertation) while the solid phase was upgraded to transportation biofuel. In this work, the production of three algae-based fuel products (renewable diesel II (RDII), renewable gasoline (RG), and hydroprocessed renewable jet fuel (HRJ)) were compared using FH as the central thermochemical process, HTM/AP as co-product generation processes in the recovery of macronutrients, and HTL as a method of producing biocrude, the raw material for drop-in transportation fuel. The content of this study was submitted for publication in the *ACS Sustainable Chemistry and Engineering* journal as the following:

- Bessette, A.; **Teymouri, A.**; Martin M.; Stuart, B.; Resurreccion, E.; Kumar, S., Life Cycle Impacts and Techno-economic Implications of Flash Hydrolysis in Algae Processing. *ACS Sustainable Chemistry & Engineering* 2017, Manuscript ID: sc-2017-039122; under review.

APPENDIX D

1. Analytical method for orthophosphate measurement using UV–visible spectrophotometer

This is the method that was used for the phosphate analysis in the chapters 4 and 5 of this dissertation. This method has been previously modified to be applied to a sample of 2.5 ml (Bettin, 2013). The reagent mixture was prepared fresh every time before analysis, since it would become unstable in 3–4 hours. The reagent consists of four components including:

1. Ammonium molybdate (10 ml)
2. Potassium antimonyl tartrate (5 ml)
3. Ascorbic acid (10 ml)
4. Sulfuric acid 5N (25 ml)

Among all four components, only ascorbic acid must be stored in the refrigerator and is stable only for few days. The other solutions can be stored for months. Stock solutions were prepared as the following (same numbering as above):

1. 7.5 g of ammonium molybdate tetrahydrate was added to a 250 ml DI water
2. 0.34 g of potassium antimonyl tartrate was dissolved in 250 ml DI water
3. 1.35 g of ascorbic acid was mixed with 25 ml of DI water.
4. 35 ml of 96% concentrated sulfuric acid was diluted in 250 ml of DI water

After reagent was prepared, 0.25 ml was pipetted into each sample. The reaction between phosphate ion and molybdenum produced a blue color, which the absorbance was measured at a wavelength of 705 nm using UV–visible spectrophotometer

(Varian, Cary 50 Conc) after 5 min. Prior to the actual sample analyses, multiple known concentrations of phosphate (prepared from a 1000 ppm potassium phosphate stock solution) were analyzed to plot the calibration curve. The phosphate concentration of a sample was then calculated through the equation associated with the calibration curve.

2. Analysis of cation (magnesium) using Ion Chromatography Method (AAA-Direct DIONEX ICS-5000)

The Thermo Scientific Dionex^{TM} ICS-5000^{+} Ian Chromatography system offers a full range of analytical measurements for amino acids, carbohydrates, anions, and cations. In this study the Dionex IonPacTM CS16 analytical column equipped with a guard column was used to evaluate the initial concentration of magnesium cation in the microalgae hydrolysate before performing the atmospheric precipitation (AP) process in chapter 4 of this dissertation. The overall process can be described as the following:

1. Make the eluent

2. Fill the 2-liter plastic bottles with the eluent and purge the bottles with pure nitrogen gas. This will help the eluent to stay fresh for a longer period of time.

3. Connect the guard column (Dionex IonPac^{TM} CG16 RFIC^{TM}, 3×50 mm) and analytical column (Dionex IonPac^{TM} CG16 RFIC^{TM}, 3×250 mm) in the appropriate direction. Please make sure the black arrow sign on the column and guard are in the same direction as the flow. The guard column should always be installed before the analytical column to protect it against contamination.

4. Flush the system with the eluent for 30 min (to the waste). Do not forget to bypass the suppressor (Dionex^{TM} CERS^{TM} 500, 2 mm, P/N: 082543).

5. Connect the suppressor, start the pump with a low flow rate such as 0.1 ml/min, and turn on the acquisition. It is always suggested to prime the pump for 10 mins before starting the actual run.

6. Ramp the flow to 0.36 ml/min (stepwise) and let the instrument to stabilize for couple of hours (preferably overnight) to reach a straight baseline (background conductivity $\leq 3\mu S$).

7. Prepare and load your samples into the auto sampler including 5–7 dilutions of standard solution for the calibration curve. The volume of each sample/standard must be exactly 5 ml.

8. Create your sample table in the program, turn off the acquisition, and start your batch. Turning off the acquisition is a mandatory step, otherwise an error massage will pop up and the run will not proceed. It is suggested to create the sample table from one of the previous successful runs by simply, saving the file as a new file in the new location following by the appropriate modifications in the sample table.

Eluent stock solution preparation:

A 1.0 N methanesulfonic acid (MSA) stock solution can be prepared as follows:

- Weight out 96.10 g of MSA (P/N: 033478)
- Carefully add it to a 1-liter volumetric flask containing about 500 ml of DI water.
- While mixing thoroughly, dilute to the mark.

After preparation of the 1.0 N MSA stock solution, pipet 30 ml of the concentrate stock solution into a 1-liter volumetric flask and dilute it to 1 liter using milli-Q water. This eluent is appropriate concentration to be poured into the IC plastic eluent containers located on the top of the equipment.

Please check the following links for more information regarding provided method:

- Manuals for the guard and analytical columns: https://www.thermofisher.com/order/catalog/product/057574
- Manual for operating the Dionex Ion Chromatography system: https://tools.thermofisher.com/content/sfs/manuals/Man-065446-IC-ICS-5000+-Operators-Manual.pdf
- Manual for the Dionex ERS 500 suppressor https://tools.thermofisher.com/content/sfs/manuals/Man-031956-IC-Dionex-ERS-Suppressor-Man031956-EN.pdf

VITA

EDUCATION

Doctor of Philosophy, Environmental Engineering December 2017

Old Dominion University, Norfolk, VA

Cumulative GPA: 4.0/4.0

Dissertation: *Holistic Approach in Microalgae Conversion to Bioproducts and Biofuels through Flash Hydrolysis*

Master of Science, Chemical Engineering May 2008

Islamic Azad University, Shahroud, Iran

Thesis: *Modeling and Simulation of Unsteady-state Mass Balance of PBDEs Combustion in Incinerators*

Bachelor of Science, Chemical Engineering May 2004

Islamic Azad University, Gachsaran, Iran

Thesis: *The Absorption of Nitrogen Dioxide in a Variety of Conditions on Solid Material*

HONORS & AWARDS

- Young Researcher Award, First Place in the Engineering and Analysis Division Poster Session at Algae Biomass Summit, October 29 - November 1, 2017, Salt Lake City, UT.
- An honorable mentioned in the U.S. Environmental Protection Agency's P3 (People, Prosperity and the Planet) sustainability competition in Washington D.C. as a member of Old Dominion University's team, 2014.
- The Honor Society of Phi Kappa Phi, Member, 2017 (membership is by invitation for the top 10 graduate students)
- Mary Rosenthal Memorial Student Travel Grant, Algae Foundation for Algae Biomass Summit, October 29 - November 1, 2017, Salt Lake City, UT.
- Graduate Student Research Travel Award, Division of Student Engagement & Enrollment Services, Old Dominion University, November 2015

JOURNAL PUBLICATIONS (Ph.D.)

1. Teymouri, A.; Adams, K.; Dong, T.; Stuart, B.; Kumar, S., Evaluation of Lipid

Extractability after Flash Hydrolysis of Algae. *Fuel Journal* 2017, manuscript id: JFUE-D-17-04622.

2. Bessette, A.; Teymouri, A.; Martin M.; Stuart, B.; Resurreccion, E.; Kumar, S., Life Cycle Impacts and Techno-economic Implications of Flash Hydrolysis in Algae Processing. *ACS Sustainable Chemistry & Engineering* 2017, Manuscript ID: sc-2017-039122; under review.
3. Teymouri, A., Stuart, B. J., & Kumar, S. (2017). Effect of Reaction Time on Phosphate Mineralization from Microalgae Hydrolysate. ACS Sustainable Chemistry & Engineering. doi:10.1021/acssuschemeng.7b02951
4. Teymouri, A., Stuart, B. J., & Kumar, S. (2018). Hydroxyapatite and dittmarite precipitation from algae hydrolysate. Algal Research, 29, 202-211. doi: https://doi.org/10.1016/j.algal.2017.11.030
5. Teymouri, A.; Kumar, S.; Barbera, E.; Sforza, E.; Bertucco, A.; Morosinotto, T., Integration of Biofuels Intermediates Production and Nutrients Recycling in the Processing of a Marine Algae. *AIChE Journal* 2017, 63 (5), 1494-1502.
6. Barbera, E.; Teymouri, A.; Bertucco, A.; Stuart, B. J.; Kumar, S., Recycling Minerals in Microalgae Cultivation through a Combined Flash Hydrolysis-Precipitation Process. *ACS Sustainable Chemistry & Engineering* 2017, 5 (1), 929-935.
7. Garcia-Moscoso, J. L.; Teymouri, A.; Kumar, S., Kinetics of Peptides and Arginine Production from Microalgae (Scenedesmus sp.) by Flash Hydrolysis. *Industrial & Engineering Chemistry Research* 2015, 54 (7), 2048-2058.

JOURNAL PUBLICATIONS (M.S.)

8. Mousavi, M.; Teymouri, A.; Ghaffarian, V., Transient Mass Transfer Modeling and Simulation of Polybrominated Diphenyl Ethers Combustion in Incinerators. *International Journal of Environmental Science and Technology* 2009, 6 (3), 499-508.

PATENTS

- Kumar, S.; Stuart, B.; Teymouri, A., An Integrated Method for Biofuels, Slow-Release Fertilizer, and Biomaterials Production from Different Types of Algae/Cyanobacteria. U.S. patent application# 15602707 filed on 05/23/2017.